UNIVERSIDADE ESTADUAL PAULISTA
"JÚLIO DE MESQUITA FILHO"
Câmpus de São José do Rio Preto

Jéssica Thaís do Prado Silva

Exploring tannic acid-whey protein isolate microgels as Pickering stabilizers:

From microscale studies to conventional homogenization techniques

São José do Rio Preto

2021

Jéssica Thaís do Prado Silva

Exploring tannic acid-whey protein isolate microgels as Pickering stabilizers:

From microscale studies to conventional homogenization techniques

Tese apresentada como parte dos requisitos para obtenção do título de Doutor em Engenharia e Ciência de Alimentos, junto ao Programa de Pós-Graduação em Engenharia e Ciência de Alimentos, do Instituto de Biociências, Letras e Ciências Exatas da Universidade Estadual Paulista “Júlio de Mesquita Filho”, Câmpus de São José do Rio Preto.

Financiadora: CAPES

Orientadora: Profª. Drª. Vânia Regina Nicoletti
Coorientador: Dr. Odilio Benedito Garrido de Assis
Coorientadora: Profª. Drª. Karin Schroën

São José do Rio Preto
2021

S586e

Silva, Jessica Thaís do Prado

Exploring tannic acid-whey protein isolate microgels as Pickering stabilizers : from microscale studies to conventional homogenization techniques / Jessica Thaís do Prado Silva. -- São José do Rio Preto, 2021

147 f. : il., tabs., fotos

Tese (doutorado) - Universidade Estadual Paulista (Unesp), Instituto de Biociências Letras e Ciências Exatas, São José do Rio Preto

Orientadora: Vânia Regina Nicoletti

Coorientador: Odilio Benedito Garrido Assis

1. Tecnologia de alimentos. 2. Leite Proteínas. 3. Nanopartículas. 4. Microfluídica. 5. Estabilidade. I. Título.

Sistema de geração automática de fichas catalográficas da Unesp. Biblioteca do Instituto de Biociências, Letras e Ciências Exatas, São José do Rio Preto. Dados fornecidos pelo autor(a).

Essa ficha não pode ser modificada.

Jéssica Thaís do Prado Silva

Exploring tannic acid-whey protein isolate microgels as Pickering stabilizers:

From microscale studies to conventional homogenization techniques

Tese apresentada como parte dos requisitos para obtenção do título de Doutor em Engenharia e Ciência de Alimentos, junto ao Programa de Pós-Graduação em Engenharia e Ciência de Alimentos, do Instituto de Biociências, Letras e Ciências Exatas da Universidade Estadual Paulista “Júlio de Mesquita Filho”, Câmpus de São José do Rio Preto.

Financiadora: CAPES

Comissão Examinadora/Examining Board

Profª. Drª. Vânia Regina Nicoletti
UNESP – Câmpus de São José do Rio Preto
Orientadora

Profª. Drª. Samantha Cristina de Pinho
Universidade de São Paulo

Prof. Dr. Eduardo Basílio De Oliveira
Universidade Federal De Viçosa

Drª. Talita Aline Comunian
Technische Universität Berlin

Prof. Dr. Odinei Hess Gonçalves
Universidade Tecnológica Federal do Paraná

São José do Rio Preto
23 de agosto de 2021

To my parents, José Antônio and Inês, who abdicated so many things to give me high quality education.

AKNOWLEDGMENTS

I thank God, for guiding me through this challenging journey and for gifting me strength during difficult times.

I thank my partner, Julio, for his support and for always be waiting for me at the end of a tiring day with warm food and nice talks. I also thank his efforts on trying to understand Pickering systems to discuss my results with me.

I thank Luna for her adorable companion during my writing times and for taking me for a walk twice a day.

I thank my supervisor, Vânia, for all the sheared knowledge, for believing in my work and for the conceptualization of this thesis.

I thank my co-supervisor, Odilio, for hosting me on his lab to perform analysis and for the fruitful discussion about our results. I also thank EMBRAPA for providing the general facilities.

I thank my Dutch supervisors, Karin and Jolet, for being so patient while teaching me new techniques on their lab. I really appreciated all our meetings accompanied by a nice cup of tea and shared tips about The Netherlands. I also thank Annabel, for helping me with experiments and for being a great student.

I thank the Food Process Engineering group from Wageningen University for hosting me during my one-year internship, especially the technicians Maurice, Jos, and Wouter for their valuable support.

I thank my colleagues from the Physical Measurement lab, for all the good moments spent during lab work and the pleasant breaks for coffee or açaí.

I thank my dearest friends, Larissa, Mariana, Elisa, and Flávia for their companion during this journey, for the good laughs, for the shared tears, and for being my family while I was away from home.

This study was financed in part by the Coordenação de Aperfeiçoamento de Pessoal de Nível Superior - Brasil (CAPES) - Finance Code 001, through the Program CAPES-PrInt-Unesp, process number 88887.194785/2018-00, Mobility number 88887.374187/2019-00.

“I’ve done my best, and I begin to understand what is meant by ‘the joy of strife’. Next to trying and winning, the best thing is trying and failing.”

Lucy M. Montgomery (2019, p. 311)

RESUMO

Emulsões de Pickering têm recebido crescente atenção devido à sua alta estabilidade contra coalescência. Contrastando com emulsificantes convencionais, partículas sólidas adsorvem irreversivelmente na interface óleo-água. O conhecimento fundamental sobre estabilização de Pickering se concentra no comportamento de adsorção de partículas de origem inorgânica, de modo que mais entendimento a respeito de emulsões de Pickering de grau alimentício se faz necessário a fim de explorar a aplicação desse sistema vantajoso em alimentos. Em vista disso, nós propomos microgéis de proteínas do soro de leite (WPI) obtidas a partir da reticulação com ácido tânico como uma nova partícula de grau alimentício a ser utilizada para estabilizar emulsões de Pickering. Nossos resultados mostram que a etapa de reticulação pôde ajustar as propriedades físicas dos microgéis de WPI, conferindo-lhes menos polidispersidade, menor tamanho de partícula e maior ângulo de contato, o que refletiu em emulsões de Pickering mais estáveis. Em seguida, exploramos o comportamento de adsorção dos microgéis de WPI reticulados com ácido tânico por meio de experimentos de Langmuir trough. Monocamadas formadas pelos microgéis e WPI nativo foram comparadas, fornecendo entendimentos sobre a atividade de superfície dos microgéis e a respectiva elasticidade da monocamada. Esses entendimentos foram combinados com a estabilidade física de emulsões de Pickering produzidas por dispositivos de microfluídica, o que permitiu determinar os principais parâmetros para a produção de gotas de emulsão estáveis utilizando esses microgéis. Tendo em mente a composição complexa de produtos alimentícios, a influência de surfactantes de baixa massa molar nas propriedades físicas de emulsões de Pickering também foi avaliada. Microgéis de WPI reticulados por ácido tânico demonstraram ser melhores estabilizantes que o WPI nativo, principalmente pela supressão de coalescência causada pela floculação em ponte. Ao contrário de partículas de Pickering convencionais, onde somente a força de cisalhamento aplicada é relevante para a adsorção de partículas na interface, observamos que um determinado intervalo de tempo é requerido pelos microgéis para promover a cobertura completa das gotas, devido à sua atividade superficial. A presença de surfactantes de baixa massa molar não comprometeu a estabilidade física de emulsões de Pickering ou removeu quantidade considerável de microgéis da interface ao longo do tempo. Sendo assim,

nós oferecemos uma nova partícula de origem biológica com oportunidade de ser aplicada como estabilizante de Pickering em sistemas alimentícios.

Palavras-chave: Microgéis de WPI. Comportamento de adsorção. Microfluídica. Floculação. Estabilização sinergística.

ABSTRACT

Pickering emulsions have received increased attention due to their high stability against coalescence. Contrasting to conventional stabilizers, solid particles adsorb irreversibly at the oil-water interface. The fundamental knowledge about Pickering stabilization is concentrated on the adsorption behaviour of particles from inorganic origin. More understanding about food-grade Pickering emulsions is needed in order to explore the application of such advantageous system into foodstuff. In view of that, we propose whey protein (WPI) microgels obtained from crosslinking with tannic acid as a novel food-grade particle for stabilizing Pickering emulsions. Our results showed that the crosslinking step was able to tune physical properties of WPI microgels, conferring to them small polydispersity, smaller particle size and increased contact angle, which reflected to more stable Pickering emulsions. Later, we explored the adsorption behaviour of tannic acid-crosslinked WPI microgels by means of Langmuir trough experiments. Monolayers formed by microgels and native WPI were compared, giving insights about the surface activity of microgel particles and the elasticity of the formed monolayer. Those understandings were combined with the physical stability of Pickering emulsions produced through a microfluidic device, enabling to determine the main parameters for producing stable droplets using those microgels. Keeping in mind the complex composition of foodstuff, the influence of low molecular weight surfactant on the physical properties of Pickering emulsions was also addressed. Tannic acid-crosslinked WPI microgels showed to be a better stabilizer than native WPI mainly by supressing droplet coalescence by bridging flocculation. Due to their surface-active character, enough adsorption time is required to promote completely coverage of emulsion's droplets, as opposed to conventional Pickering particles, in which only the shear force plays a role on particle adsorption. The presence of low molecular weight surfactants did not impair the physical stability of Pickering emulsions nor desorbed considerable amounts of microgels from the interface over time. Thus, we offered here a new food-grade particle as opportunity to be applied as Pickering stabilizer into food systems.

Keywords: WPI microgels. Adsorption behaviour. Microfluidics. Bridging flocculation. Synergistic stabilization.

LIST OF FIGURES

LIST OF TABLES

SUMMARY

1 INTRODUCTION

Pickering emulsions (PICKERING, 1907) or particle-stabilized emulsions are well known for their high stability against coalescence. In these systems, particles with partial wettability are able to place themselves at the oil-water interface, giving rise to a rigid physical barrier that protects neighbouring droplets from merging upon collision. Besides the high stability, Pickering emulsions present an asset for application in the food industry due to their surfactant-free character, enabling the design of clean label products that have been increasingly demanded by consumers around the world (BERTON-CARABIN; SCHROËN, 2019; CHEVALIER; BOLZINGER, 2013).

Considerable knowledge has been collected about the interaction of stabilizing particles from inorganic sources at the oil-water interface and its impact on emulsion's stability (YANG et al., 2017). However, the production of suitable Pickering stabilizer particles using food components as starting materials remains a challenge, mainly because food materials possess a very complex composition, which lead to the obtention of heterogeneous particles (i.e., high polydispersity, rugous surface, non-homogeneous shape) (SAN-MIGUEL; BEHRENS, 2012; ZANINI et al., 2017). In addition, particles made from food materials are often accompanied by surface-active molecules that can adsorb at the interface, thus leading to synergistic or competitive interactions with the particles and moving the system away from a classic Pickering stabilization (BERTON-CARABIN; SCHROËN, 2015). Both reasons make it very difficult for scientists to connect emulsion characteristics with particle attributes but, in spite of this, some food materials have already been explored for producing Pickering particles, such as starch (MAREFATI et al., 2015), cellulose (HU et al., 2016b), chitosan (RIBEIRO et al., 2020), soy protein isolate (BENETTI; SILVA; NICOLETTI, 2019), zein (WANG et al., 2020a), fat (SCHRÖDER et al., 2019), and gelatin (TAN et al., 2014). Nonetheless, the explanation about mechanisms involved in the formation of such emulsions remains supported by the knowledge on adsorption of inorganic particles.

With the increasing interest on Pickering emulsions by the scientific community, a new class of stabilizing particles has emerged. The so-called microgel particles are composed by soft swollen polymer networks that differ considerably from hard particles in their interfacial functionality. Microgels can deform upon adsorption, assuming a fried-egg like structure that is able to cover a larger interfacial area than hard Pickering

particles, conferring even higher desorption energy (DICKINSON, 2017). Among food materials, whey protein is regarded as a widely available and accepted protein source that can be successfully used as starting material for microgel's production. The high surface activity of protein molecules is an asset to produce microgel particles because they combine the high desorption energy of Pickering particles with the ability of protein molecules to adsorb at any interface (LI et al., 2018; MURRAY, 2019). Thus, protein microgels represent an interesting option to be applied as stabilizer particles in food-grade Pickering emulsions.

Additionally, the physical properties of microgel particles can be tuned in order to improve even more their ability as Pickering stabilizer. The crosslinking reaction is claimed as a method to modify physical and mechanical properties of materials, such as chemical and thermal stability, structural rigidity, and permeability (Gonsalves, Araújo, Soares, Goulart, & Abreu, 2011). In proteins, the crosslinking is mostly performed by reactions with aldehydes, mainly glutaraldehyde and formaldehyde. However, these substances have toxic potential and are not allowed for use in food (Azeredo & Waldron, 2016), making necessary to search for alternative reactants.

In this thesis, we propose the use of whey protein microgels crosslinked by organic acids as an alternative for Pickering emulsions stabilizer. Firstly, the microgel particles were produced, characterized regarding their physical properties, and evaluated as stabilizer of emulsions containing roasted coffee oil as disperse phase. Later, an extensive investigation about the interfacial behaviour of whey protein microgels prepared by crosslinking with tannic acid was implemented. Subsequently, emulsions stabilized by these microgels were produced using a microfluidic device, which enabled to determine the main parameters that affect the physical stability of these emulsions. Finally, the influence of the presence of low molecular weight molecules in Pickering emulsions stabilized by the microgel particles was investigated.

2 OBJECTIVES AND THESIS ORGANIZATION

2.1 General objective

The general objective of the present thesis was to produce novel whey protein microgels by crosslinking with organic acids and investigate their role as Pickering stabilizers.

2.2 Specifics objectives

i. Produce WPI microgels by crosslinking with tannic acid or citric acid;
ii. Characterize the produced microgels regarding to size distribution, zeta potential, morphology, and contact angle;
iii. Investigate the ability of tannic acid- and citric acid-crosslinked WPI microgels in stabilizing Pickering emulsions containing roasted coffee oil as disperse phase;
iv. Implement a purification methodology to remove possible non-reacted molecules from the microgel dispersion;
v. Study the adsorption behaviour of tannic acid-crosslinked WPI microgels at the air-water interface;
vi. Investigate the factors that affect the coalescence of microgel-stabilized emulsions through experiments on microfluidic device and compare them with conventional emulsions (stabilized only by native WPI);
vii. Verify the effects of low molecular weight surfactants added either before or after homogenisation on physical characteristics of Pickering emulsions stabilized by tannic acid-crosslinked WPI microgels;
viii. Explore the ability of tannic acid-crosslinked WPI microgels in stabilizing Pickering emulsions through different homogenization techniques.

2.3 Thesis organization

This thesis is divided into 9 chapters. In Chapter 1, a general introduction to the main topics covered in this thesis is provided, followed by the general and specific objectives that we aimed to achieve by carrying out this research (Chapter 2).

Chapter 3 is composed by a literature review that describes the basic concepts applied and discussed throughout the thesis.

Chapter 4 presents the production and characterization of WPI microgels crosslinked by organic acids. Tannic acid and citric acid were the organic acids selected to modulate WPI microgel properties. Parameters such as size distribution, morphology, and wettability of particles, as well as the physical stability provided by those microgels to Pickering emulsions containing roasted coffee oil, indicated the most suitable organic acid to tune WPI microgels to be applied as Pickering stabilizer.

In chapter 5, tannic acid-crosslinked WPI microgels were further investigated regarding their ability to stabilize interfaces. Firstly, a purification method was proposed in order to remove non-reacted native WPI from the microgel dispersion. Then, the adsorption behaviour of these microgels on model interface was evaluated and linked to their ability of stabilizing emulsions. By using a microfluidic device, the propensity to coalescence of microgel-stabilized emulsions and their conventional counterparts (emulsions stabilized by native WPI) were evaluated at millisecond scale. This enabled to demonstrate the superior stability against coalescence of Pickering emulsions stabilized by crosslinked WPI microgels.

In Chapter 6, an extensive investigation about the composition of tannic acid-crosslinked WPI microgel, as well as the remaining protein fractions of native WPI inside the disperse phase is provided. We demonstrated that, despite our efforts, not all remained non-reacted protein could be removed from the microgel dispersion. In view of that, we investigated the influence of such low molecular weight surfactants on physical properties of Pickering emulsions. Two different homogenization techniques (lower and higher shear) were applied to produce emulsions stabilized by blends of microgels and native WPI, culminating in emulsions with different physical characteristics. This also enabled to verify the impact of shear force on the organization of microgels at the interface and the possible role of native WPI on emulsion formation/interfacial organization.

To conclude, Chapters 7 and 8 present the general discussion and the general conclusions, respectively, while Chapter 9 presents suggestions for future studies.

3 LITERATURE REVIEW

3.1 Pickering emulsions

Pickering emulsions comprises a category of emulsions in which solid particles act as stabilizers (Figure 3.1). They were described for the first time at the beginning of twentieth century by Spencer Umfreville Pickering, who observed the creation of a pellicle over oil globules formed by copper sulphate particles (PICKERING, 1907). More than a hundred years after his discovery, Pickering emulsions are being extensively investigated due to their high physical stability, which is an asset for product design in different fields.

Figure 3.1 – Oil droplets stabilized by conventional emulsifiers and solid particles.

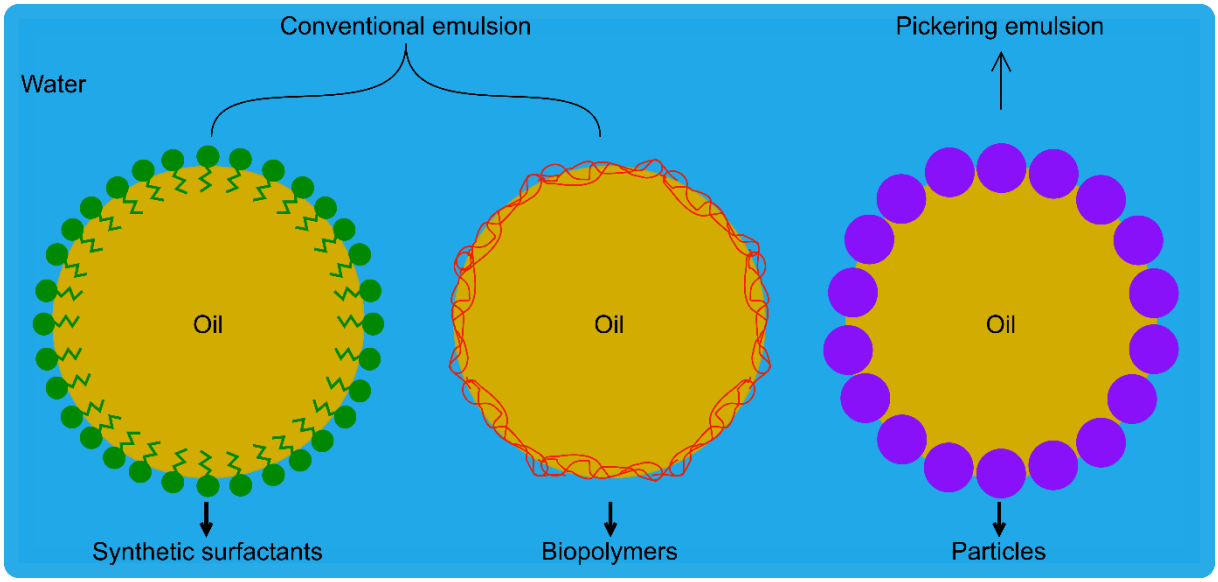

Source: Author's compilation.

Several inorganic materials were applied for producing Pickering particles over the years, namely hydroxyapatite, clay, magnetic nanoparticles (FeO_4), and silica nanoparticles. The latter is responsible for the majority of current understandings about Pickering stabilization (YANG et al., 2017). Their use is justified by the regular spherical shape and well-defined size and hydrophobicity. Besides that, silica particles are largely commercially available in different sizes and tuning their hydrophobicity is also possible (BERTON-CARABIN; SCHROËN, 2015).

In contrast with the remarkable research progresses on inorganic and synthetic materials, there are much less research concerning to the role of biological and food-

grade particles as Pickering stabilizers (XIAO; LI; HUANG, 2016). Fundamental knowledge about the arrangement and adsorption of biological particles at interfaces still needs further investigation. Despite that, some advances were already achieved by food scientists using Pickering emulsions, i.e: encapsulation and protection of sensitive bioactive compounds from degradation (HU et al., 2016a; RIBEIRO et al., 2020), tunning the application of food ingredients (WANG et al., 2016a; ZENG et al., 2017), and also as precursor for producing microcapsules (BENETTI; SILVA; NICOLETTI, 2019; MAREFATI et al., 2015; WHITBY; SCARBOROUGH; NGOTHAI, 2017).

3.1.1 Principles of Pickering stabilization

The stabilization mechanism of Pickering emulsions is based on the formation of a steric barrier provided by the adsorption of solid particles at the droplet interface. Due to capillary forces, particles form a dense single-layer or multi-layer particle film over the oil droplets. This particle film becomes a physical barrier that prevents neighbouring droplets from touching and aggregating each other, preventing coalescence (CHEN et al., 2020). As enumerated by Dickinson (2017), the stability condition of fully covered droplets involves contributions of: (I) adhesion energy effect, that prevents the desorption of individual particle from the interface; (II) steric hindrance effect, whereby proximity to other particles restricts lateral particle movement, (III) capillary pressure effect, that inhibits the rupture of the thin liquid film at the interface and, (IV) interfacial rheological effect, that affects film drainage.

The energy required to spontaneously desorb particles from the interface is extremely large compared to the thermal energy, in such way that particle adsorption is considered as irreversible (GOULD; GARCIA-GARCIA; WOLF, 2016). Unlike surfactants, solid particles theoretically do not influence the interfacial tension between both liquids, but their irreversible adsorption to the interface causes a replacement of part of the bare interface between both liquids, which also decreases the free energy, but through a different pathway (BERTON-CARABIN; SCHROËN, 2015). The desorption energy of Pickering particles is expressed by Equation 1:

$$\Delta E = \pi r^2 \gamma (1 - |\cos\theta|)^2, \quad (1)$$

where r is the particle radius, γ is the interfacial tension between oil and water and θ is the particle three-phase contact angle measured through the water phase, in presence of oil (Figure 3.2).

Figure 3.2 - Schematic representation of a single Pickering particle at a droplet interface and the three-phase contact angle.

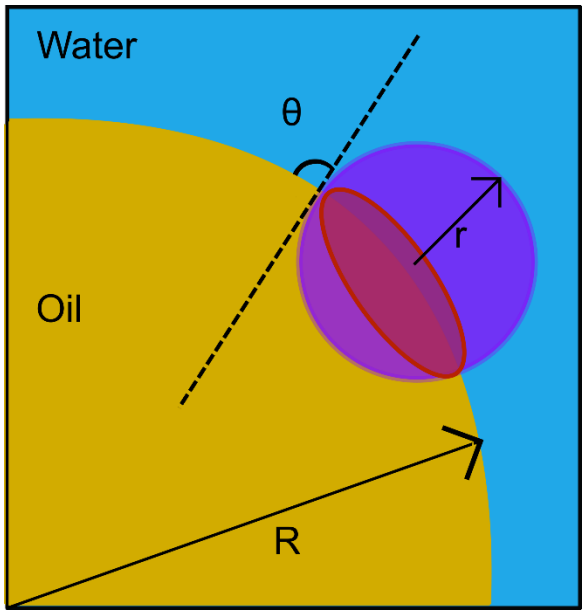

Source: Author's compilation.

The main parameter concerning the ability of a particle to adsorb at interfaces is its partial wettability, which is predicted by the three-phase contact angle (θ). If particles are completely hydrophilic (θ << 90°), they would remain in the aqueous phase. Similarly, if the particle is completely hydrophobic (θ >> 90°), they would remain in the oil phase. However, if particles present partial wettability by the aqueous and the oil phases (15° < θ < 165°), they tend to migrate and to adsorb at the interface, forming a rigid layer over emulsion's droplets. In this way, solid particles may stabilize both O/W and W/O emulsions. The better wetting liquid becomes the continuous phase and the other remains as dispersed phase. Still, to achieve the maximum value of desorption energy, θ should be relatively close to 90°, as predicted by Equation 1 (TAVERNIER et al., 2016; XIAO; LI; HUANG, 2016; YANG et al., 2017).

Additionally, from Equation 1 it can be deduced that the desorption energy depends strongly on particle radius, namely quadratically: increasing the particle size means that more energy is needed to remove it from the interface. However, it can easily be calculated that even for particles in the nano size range ($r \sim 5$ – 10 nm), the

desorption energy (ΔE) is well above tenfold the thermal energy (K_bT, in which K_b is the Boltzman's constant and T the absolute temperature) (LINKE; DRUSCH, 2018). There is no lower limit of particle size for Pickering stabilization, however, it is recommended that particle size remains at least one order of magnitude smaller than the emulsion target droplet size. By following this general rule, particles would be properly located around the droplets, achieving a successful stabilization (HUNTER et al., 2008).

3.1.2 Physical destabilization of Pickering emulsions

Emulsions are metastable systems and, eventually, they undergo through phase separation. Almost all emulsions are prone to physical destabilisation that may occur through different pathways (Figure 3.3) and at different time scales. Specifically for Pickering emulsion, the physical stability is largely related to the characteristics of stabilizing particles (NIROULA et al., 2021).

Figure 3.3 - Destabilization phenomena possibly observed in emulsion systems.

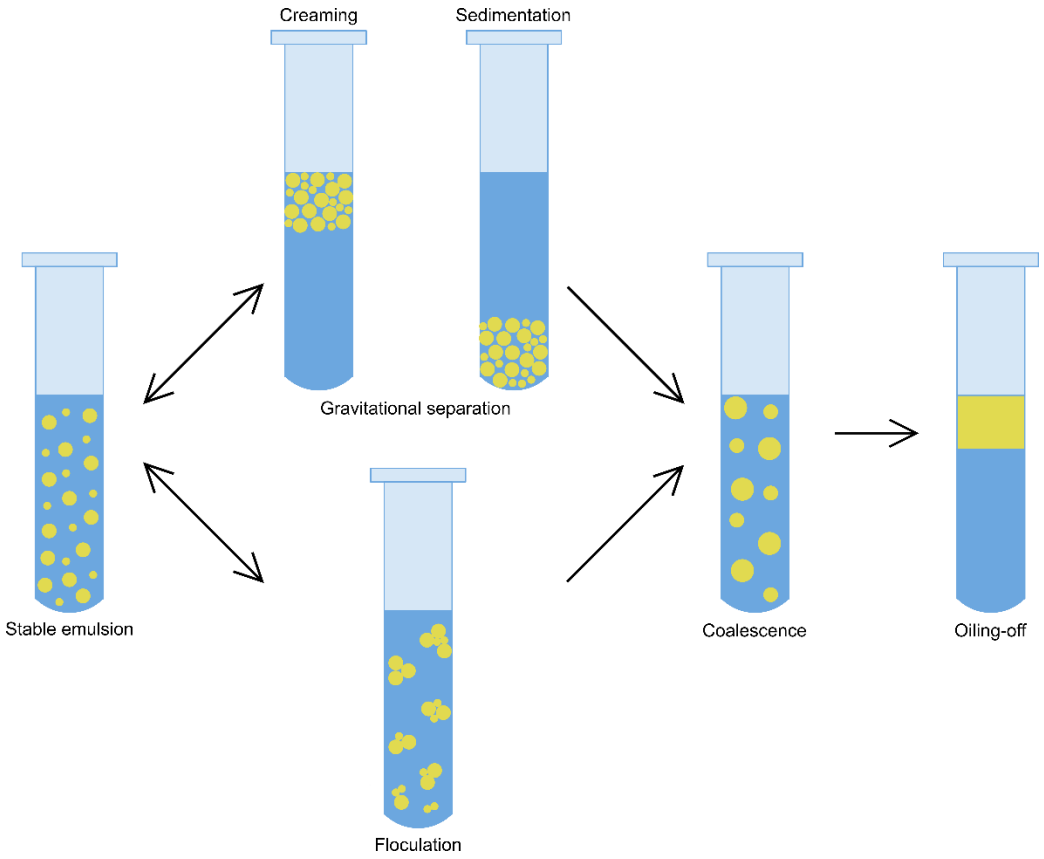

Source: Author's compilation.

In general, the most common physical destabilization in Pickering emulsions is gravitational separation (creaming or sedimentation), that occurs due to the density difference between the continuous and disperse phase. Creaming happens when the disperse phase with lower density compared to the continuous phase moves upward, generating a thick separate layer. Oppositely, sedimentation happens when the disperse phase has higher density than the continuous phase, causing droplets to move downwards. Due to the typically large droplet size of particle-stabilized emulsions, most droplets exhibit rapid gravity-induced phase separation. These phenomena affect emulsions appearance, and decreasing the droplet size and/or increasing the viscosity of continuous phase are usually applied as strategies to avoid such effect (BERTON-CARABIN; SAGIS; SCHROËN, 2018; DICKINSON, 2019; HU et al., 2017).

Another physical destabilization mechanism of emulsions is flocculation, that can happen when attractive forces overcome repulsive forces between emulsion droplets, due to excessive amount of emulsifier in the continuous phase (depletion flocculation) or through low particle concentration (bridging flocculation). In this configuration, droplets aggregate to form a floc, but maintaining their individual size. Nevertheless, the presence of flocs causes an increase on the effective emulsion's droplet size, which may promote gravitational separation. In addition, a fraction of the continuous phase is entrapped by the flocks, reducing the effective disperse phase fraction, hence increasing the emulsions' viscosity (BERTON-CARABIN; SAGIS; SCHROËN, 2018).

In Pickering emulsions, bridging flocculation (Figure 3.4) is a very intriguing phenomenon: at low surface coverage, one single layer of particles is able to stabilise two colliding droplets at the same time. In this configuration, the particle is wetted by two separate disperse phase regions, but still with its major portion lying in the intervening region of bulk continuous phase (DICKINSON, 2017). According to Dickinson (2010), coalescence stability of bridged droplets is attributed to the steric hindrance effect, that prevents particle displacement away from or within the bridging layer. Thus, bridged droplets may impart superior stability to emulsions. On the other hand, bridging flocculation also increases the effective droplet size that may enhance the creaming rate, which can affect emulsion's appearance and emulsion's rheological properties. Therefore, emulsions with bridged droplets may be (or not) desirable, depending on the application (FRENCH et al., 2015).

Figure 3.4 - Scheme of bridging flocculation in particle-stabilized droplets.

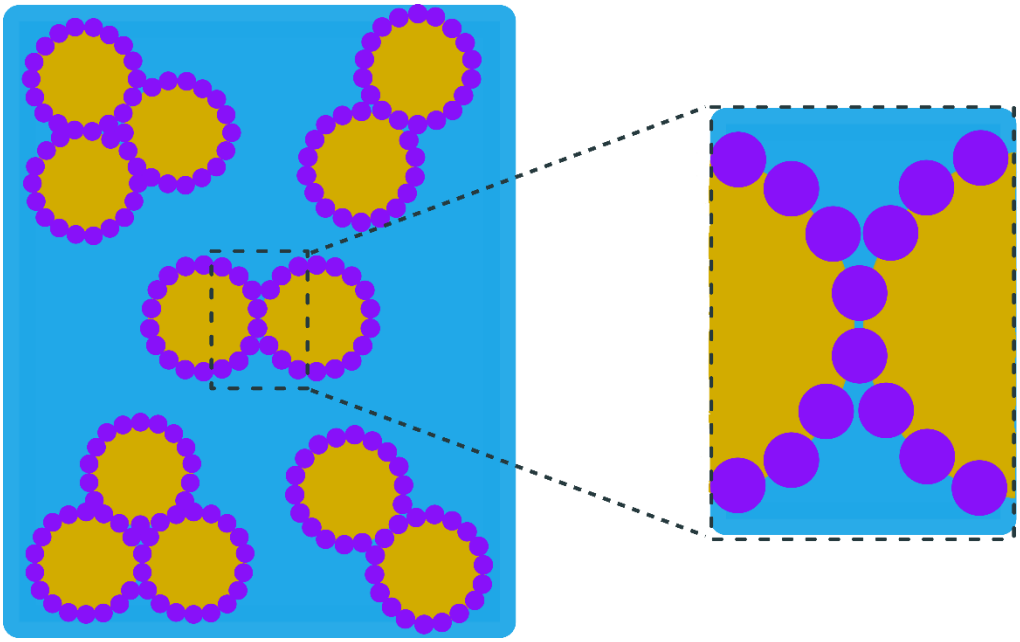

Source: Author's compilation.

Coalescence, in turn, occurs when two or more approaching droplets fuse together to form a single larger droplet. In this case, the interfacial film around connecting droplets needs to rupture so they can merge. However, for Pickering emulsions, as long as the interface is covered enough, the physical barrier created by the particles will not allow interfacial rupture, avoiding droplet coalescence. Coalescence leads to a decrease in the interfacial area, which is thermodynamically favourable, therefore, contrary to creaming and flocculation, coalescence is irreversible (BERTON-CARABIN; SAGIS; SCHROËN, 2018; DICKINSON, 2019).

3.2 Soft particles as stabilizers and the "Mickering emulsion" concept

The role of soft particles as emulsion stabilizer is somehow different from that of hard particles. Mainly because soft particles can stretch at fluid interfaces, being able to spread and cover a larger interfacial area than hard particles, which culminates in increased adsorption energy (Equation 1) (GONZALEZ ORTIZ et al., 2020). Microgels made from crosslinked polymers are the most recognized soft particles for Pickering stabilization. The soft and porous characteristics of microgels leads to emulsions with significantly different properties. Based on this affirmation, Schmidt et

al. (2011) proposed the term “Mickering emulsions” in order to stress similarities and differences to Pickering emulsions stabilized by rigid particles.

Microgel particles are kinetically stable entities held together by covalent bonding, with capacity to trap solvent inside their crosslinked polymer network and occupying an intermediate position between colloidal particles and molecular polymers (DESTRIBATS et al., 2011; DICKINSON, 2017; TANG, 2020). When in aqueous media, microgel particles present a roughly spherical shape. They form a core-shell morphology with a denser core and a loosely cross-linked shell, in which dangling polymers are located at the outermost part. Up to date, microgels made with Poly(N-isopropylacrylamide) (p(NIPAM)) are the most well described in the literature. Since their discovery on 30 years ago, considerable amount of knowledge has been acquired and, nowadays, p(NIPAM) microgels are considered model systems for understanding the overall behaviour of microgels (FERNANDEZ-RODRIGUEZ; MARTÍN-MOLINA; MALDONADO-VALDERRAMA, 2021).

3.2.1 Microgels behaviour at interfaces

For well-defined hard particles, the adsorption at interfaces is mainly ruled by their contact angle, forming a strong physical barrier against coalescence. In contrast, microgel adsorption is ruled by the surface active character of their dangling chains, while their stabilizing capacity is due to the viscoelasticity of the formed interfacial layer (DESTRIBATS et al., 2013; DICKINSON, 2017).

Microgels adsorbed at interfaces stretch as much as possible, sometimes achieving the double of their diameter in bulk (Figure 3.5). This deformation is driven by the reduction of the free energy (interfacial tension), and it is counterbalanced by their intrinsic viscoelasticity, which is directly related to their crosslinking degree. In this scenario, microgels assume a unique structure with a protruding core and a wide shell made of long ramifications that covers the remaining part of the interface, forming a “fried-egg like” structure. This individual conformation gives rise to a hexagonally-packed ordered layer of microgels at the interface (DESHMUKH et al., 2015; FERNANDEZ-RODRIGUEZ; MARTÍN-MOLINA; MALDONADO-VALDERRAMA, 2021).

Figure 3.5 - Scheme of an individual oil droplet stabilized by microgel particles.

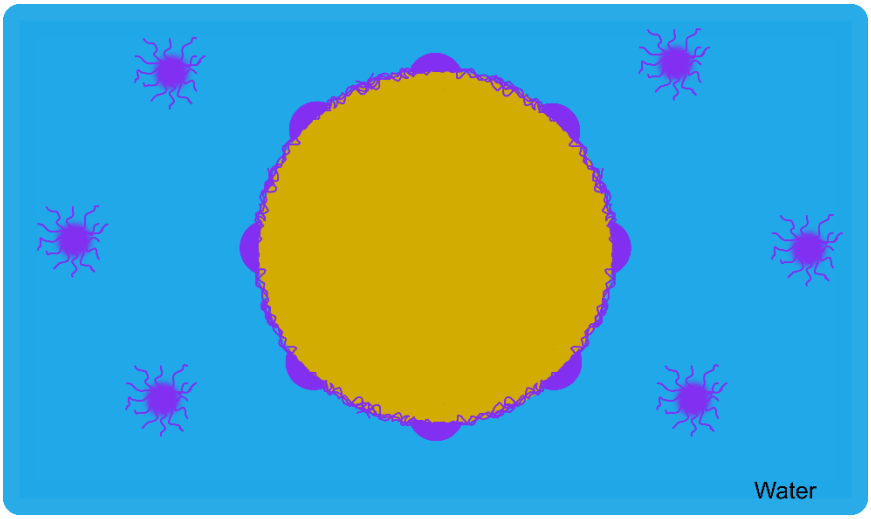

Source: Author's compilation.

The adsorption process at interfaces was shown to be spontaneous for different microgel types – p(NIPAM), soy protein, and β-lactoglobulin (MURPHY; FARKAS; JONES, 2016; TATRY et al., 2019; ZHANG et al., 2020c). In all these cases, the adsorption kinetics was faster for increasing microgel concentration. Both phenomena were attributed to the presence of amphiphilic moieties on the dangling chains of the microgels, which promotes the microgel diffusion to the interface.

In spite of the ability of microgels to act as Pickering stabilizer is already known, some questions remain about the reversibility of their adsorption. This issue was addressed by Tatry et al. (2019), who demonstrated that p(NIPAM) microgels adsorption was in fact irreversible. In addition, they found out that the conformation of microgels at the interface do not evolve over more than 7 hours, unlike for proteins, in which no true equilibrium state can be established due to continuous denaturation at the interface. This observation led the authors to conclude that microgels behave neither as particles nor as proteins, despite sharing the characteristics of these two materials.

The complexity presented by microgel particles makes room for a new and rich field for research. The functionality of such structures can be tuned in many ways in order to achieve the target application: from small changes in the bulk phase to the addition of responsive chemical groups to the microgel composition. The key point for adjusting microgel properties for a given application is closely related to modifying their spreading behaviour at interfaces, which will be discussed next.

3.2.2 Parameters that influence microgel spreading at interfaces

3.2.2.1 Crosslinking density

The crosslinking density of microgels defines their swelling capacity (Figure 3.6) and therefore, their softness. As a consequence, the lower the crosslinking density, the more the microgels flatten at the interface. The entanglement of adjacent microgels forms a two-dimensional elastic network of connected microgels. Thus, highly deformed microgels create a very elastic interfacial network, protecting droplets against coalescence. On the other hand, highly crosslinked microgels give rise to less deformable particles that barely form entanglements, thus failing in stabilizing emulsions (PICARD et al., 2017; REY et al., 2020; TATRY et al., 2021).

Figure 3.6 - Effect of crosslinking degree on microgel configuration.

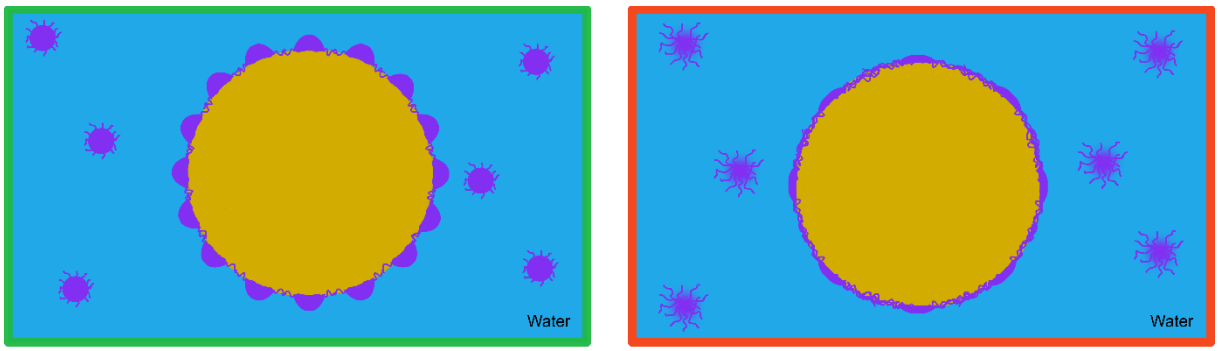

High crosslinking density Low crosslinking density

Source: Author's compilation.

The link between the crosslinking density of p(NIPAM) microgels and emulsion stability was shown by Destribats et al. (2011), who found out that the most crosslinked microgels gave rise to emulsions highly flocculated and polydisperse. Such emulsions remained stable for weeks under quiescent conditions, but they underwent to fast phase separation under low shear (manual shaking and centrifugation). An opposite behaviour was observed for emulsions stabilized by the less crosslinked microgels; besides being highly stable under storage, these emulsions could resist to mechanical disturbances (compression and shear). Thus, the more stable emulsions were those with the highest shell overlapping capacity. Later, this same research group concluded that the amount of energy required for microgel adsorption increased with the increasing microgel crosslinking density (DESTRIBATS et al., 2013).

Interfacial studies corroborate with the observations made by Destribats et al. (2011). Tatry et al. (2019) showed that microgels adsorb spontaneously whatever their crosslinking density. However, the adsorption kinetics is faster for the less crosslinked microgels. Similar results were found by Picard et al. (2017) for microgel adsorption upon compression. In their study, it was observed that less crosslinked microgels are compressed to a higher extent, achieving higher surface pressure values than the more crosslinked ones. This means that the density of the interpenetrated shells at the interface is higher for softer microgels. Thus, the authors concluded that the interfacial elasticity increased as the crosslinking density decrease.

3.2.2.2 Electrostatic interactions

Unlike classical hard Pickering particles, electrostatic interactions do not play a major role on microgel-stabilized emulsions. Usually, electrostatic repulsion and Van der Waals attraction are weak for microgel particles, making their ability to flat at interfaces more important (DESHMUKH et al., 2015). It has been shown that oppositely charged droplets covered by microgels do not coalesce upon collision into a microfluidic device (LIU et al., 2012).

The role of electrostatic interactions on the performance of microgels as stabilizer is related to their physical structure: charged microgels swell more strongly than uncharged ones due to the osmotic pressure of the counterions (Figure 3.7). When in bulk, charged microgels are soft and present a fuzzy surface containing the polymeric dangling chains. In contrast, uncharged microgels are denser and their polymeric dangling chains are denser as well (GEISEL; ISA; RICHTERING, 2014). At fluid interfaces, charged microgels can be compressed further compared to uncharged microgels, due to the differences on swelling ratio. However, it was demonstrated that charges do not affect neither interactions between microgels nor their adsorption. Therefore, the steric contributions of the polymeric dangling chains dominate electrostatic interactions, meaning that the adsorption mechanism of microgels relates more to their polymeric nature rather than to their particle nature (GEISEL; ISA; RICHTERING, 2014; PICARD et al., 2017; SCHMIDT et al., 2011).

Figure 3. 7 - Effect of electrostatic interactions on microgel configuration.

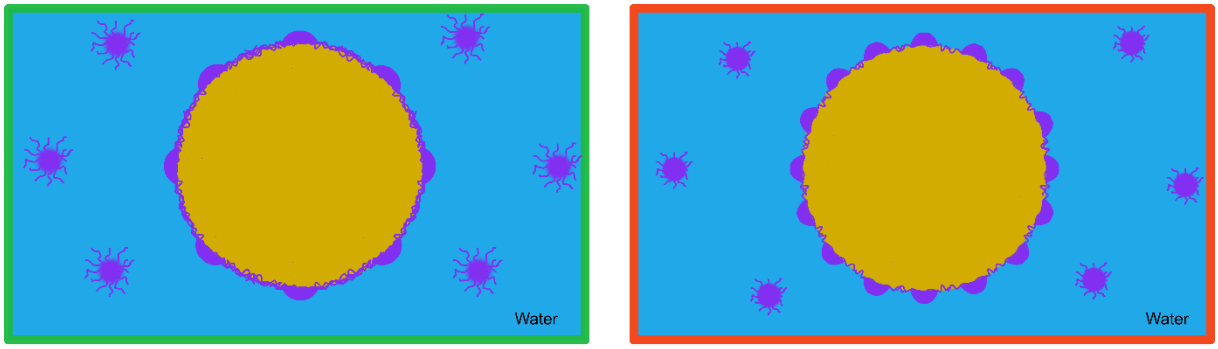

High net charge Low net charge

Source: Author's compilation.

3.2.2.3 Size

Microgels' size is another important parameter for defining their behaviour at the interface (Figure 3.8).

Figure 3.8 - Effect of particle size on microgel configuration at oil-water interface.

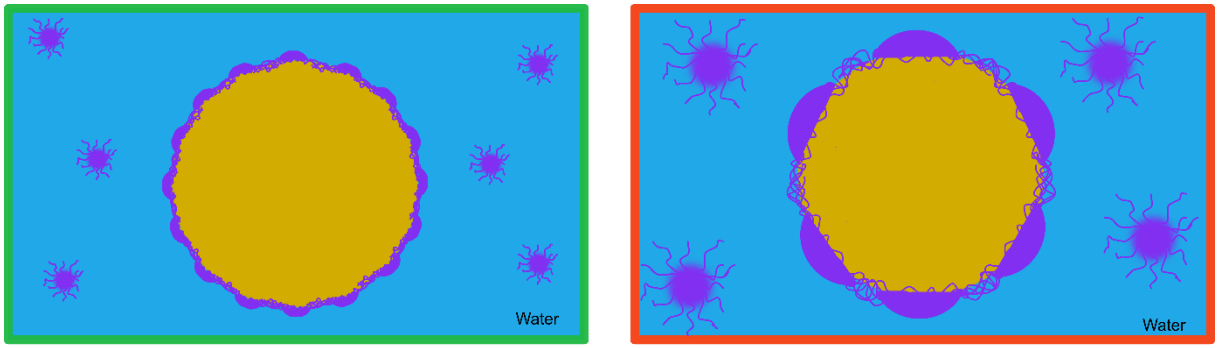

Small microgels Large microgels

Source: Author's compilation.

As the microgel size increases, their internal structure becomes more heterogeneous, with a more pronounced core-shell morphology. Upon adsorption, such microgels form a heterogeneous layer as well, which favours bridging between droplets, leading to flocculated emulsions. In contrast, small microgels cover the interface more uniformly and with a higher density. Additionally, such particles have greater mobility at the interface and are able to better rearrange at the interfacial layer, contributing to increase the droplet resistance against mechanical stress. In this way, smaller microgels give rise to less flocculated emulsions that are also more resistant to applied stresses (DESTRIBATS et al., 2014a). These features were confirmed by

Murphy, Farkas and Jones (2016), who studied the adsorption of β-lactoglobulin microgels of varying sizes at an oil-water interface. They demonstrated that smaller microgels adsorb and deform at the interface faster than larger microgels, resulting in a more elastic interfacial layer, which can provide highly stable emulsions.

3.2.2.4 Emulsification energy

The preparation pathway of Pickering emulsions defines the microgel organization at the interface (Figure 3.9). The mechanical strength of the interfacial layer and consequently the stability of emulsions is directly related to the way in which the microgels adsorb and arrange at the interface (DESHMUKH et al., 2015).

Figure 3.9 - Effect of emulsification energy on microgel configuration at oil-water interface: (A) high shear and (B) low shear.

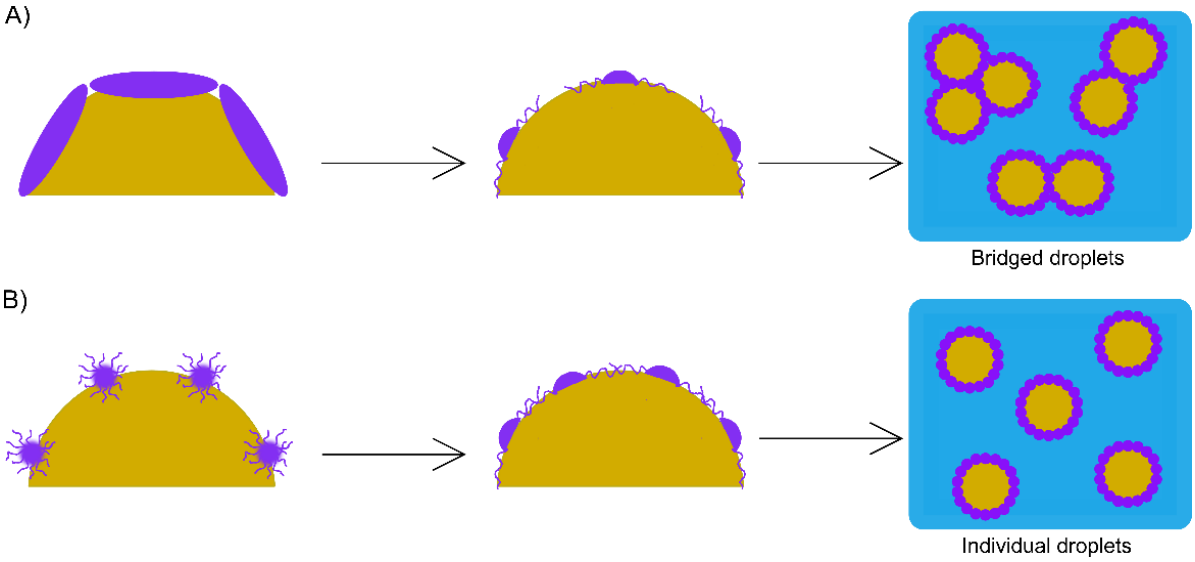

Source: Author's compilation.

In an extensive investigation, Destribats et al. (2013) showed how the emulsification energy can affect the deformation of microgels at the oil/water interface. According to their findings, high emulsification energy allows microgels to assume several possible configurations, enhancing the adsorption of their dangling chains and resulting in strong microgel deformation at the interfacial plane. Moreover, a larger interfacial area is created by applying high emulsification energy and, in such conditions, microgels have enough space to deform laterally, but their density at the interface is low, which may promote the occurrence of bridging flocculation. On the

other hand, using low emulsification energy, the deformation dynamics of microgel particles is too slow compared to droplet's recombination rate and the interfacial area created during homogenization is small. In this way, microgels neither have time nor space to extend. Thus, a highly dense interfacial layer is created, hindering bridging between droplets and consequently avoiding flocculation.

3.3 Microgel particles as alternative for food applications

The increasing trend for clean-label products is pushing food manufacturers to replace synthetic additives for natural ingredients. Indeed, some natural ingredients are already applied as emulsion stabilizer (e.g. lecithin and dairy proteins), but many others are from synthetic origin (e.g. polysorbates and sucrose esters). Thus, massive efforts are being applied to investigate further the potential of natural biobased molecules for stabilizing emulsions (BERTON-CARABIN; SCHROËN, 2019).

Murray et al. (2021) developed a theoretical analysis for the perfect hydrocolloid stabilizer. For their choice, different aspects relevant to food products were considered, such as physical stability, cost, safety, palatability, and potential long-term health implications. Obviously, the conclusion was that even from a pure theoretical viewpoint, no single hydrocolloid stabilizer could satisfy all the functional requirements involved in production, storage, consuming, and digestion of colloidal systems. In practice, the choice of a stabilizer depends on the nature of the food product application, the desired textural properties, and the characteristics of other components in the formulation. Interestingly, the authors finalize their study by suggesting that microgel particles made from conjugated or complexed biopolymers is compatible with the idea of an ideal hydrocolloid. This is because such structure combines the required molecular attributes with the functional advantages of particle-like behaviour, being able to attend many of the requirements exposed above at the same time.

Two main classes of biopolymers may be used for producing food-grade microgel particles: polysaccharides and proteins. Proteins are highly surface-active molecules and thus, protein microgels combine the high desorption energy of Pickering particles with the ability of protein molecules to adsorb at any interface. On the contrary, polysaccharides are generally non-surface active, in such a way that polysaccharide microgels may be complexed with other ingredients to achieve the

same effect. Hence, the high interfacial activity together with high nutritional value of commonly available proteins make them an advantageous material for producing food-grade microgels for stabilizing Pickering emulsions. Since most of these proteins are more compatible with water than oil, the microgels obtained are most suitable (or designed) to stabilize oil-in-water emulsions (CALABRESE et al., 2018; MURRAY, 2019).

A simple heating process can be applied to prepare protein microgels in an efficient way. At temperatures above 80°C and at a determined pH range, protein molecules aggregate, promoting the formation of relatively spherical microgel particles composed of densely packed proteins. This approach has shown excellent results when applied to proteins of different sources, such as soy (BENETTI; SILVA; NICOLETTI, 2019; GUO et al., 2016), egg (LI et al., 2020), sorghum grain (XIAO; LU; HUANG, 2017), pea (ZHANG et al., 2020b), rapeseed (WANG et al., 2020b), and dairy (CHEN; ZHANG, 2019; MURPHY; FARKAS; JONES, 2016; ZHANG et al., 2020a). The latter is an especially attractive option since dairy protein fractions are already included in many food products as stabilizer.

3.3.1 Whey protein isolate microgels

Whey protein isolate (WPI) is a co-product from the cheese making process. It is obtained after removing fat and lactose from whey, thus presenting high protein content (> 90%) – mainly composed of β-lactoglobulin (80%) and α-lactalbumin (15%) (GANJU; GOGATE, 2017). Due to its high composition ratio, β-lactoglobulin tends to dominate the overall properties of WPI, especially in processes in which heat treatment is involved (WALSTRA; WOUTERS; GEURTS, 2006). This protein has a globular configuration with approximately 2 nm-radius and molecular weight of 18.2 kg mol^{-1} (WALSTRA; WOUTERS; GEURTS, 2006).

Globular proteins can only be formed if enough hydrophobic radicals are present into protein's structure. In the case of β-lactoglobulin, the main amino acids in the polypeptide chain are leucin (R= $-CH_2CH(CH_3)CH_3$), glutamic acid (R= $-CH_2CH_2CO_2^-$), lysine (R= $-(CH_2)4NH_3^+$), and alanine (R= $-CH_3$). The hydrophobic radicals are positioned on the inside of the molecule, while the hydrophilic radicals are at the outside. Globular proteins present themselves as monomer and dimers in aqueous solution. When subjected to heating, their chains gain mobility, but they do not unfold

completely. The hydrophobic parts of the molecule are then exposed, being able to interact with other molecules. Initially, small oligomers are formed through disulphide bounds and, after reaching a critical amount, the oligomers associate to each other into primary aggregates, that are relatively monodisperse. The size and structure of such aggregates depend on protein concentration, heating protocol, ionic strength and pH (NICOLAI; BRITTEN; SCHMITT, 2011; WALSTRA; WOUTERS; GEURTS, 2006).

After heating at a narrow pH range (5.7 to 5.9), WPI gives rise to relatively spherical microgel particles that have been shown promising results when applied as Pickering stabilizer. Destribats et al. (2014b) demonstrated that emulsions stabilized by WPI microgels have high stability against coalescence, in which micrometric droplets were stable even after 8 months of storage. The authors claim that such stable emulsion could not be obtained with low molecular weight surface-active compounds alone. They also highlighted that a complex material such as WPI would not generate strictly identical particles. Instead, individual microgels from the same batch can present subtle differences in their characteristics (i.e. protein composition, size, surface charge, and crosslinking degree), and this should be taken into account when formulating emulsions. Zamini et al. (2018) produced high internal phase emulsions (HIPE) stabilized by WPI microgels with different sizes (90 – 350 nm). HIPE droplet sizes decreased when the formulation that resulted in the smallest microgels was used, producing hexagonally structured oil droplets, unlike larger microgels. In addition, small microgel particles presented higher dynamic interfacial tension, which means that larger microgels are more limited with regard to possible interface conformations than smaller microgels.

Different techniques have been applied to modulate the performance of WPI microgels as Pickering stabilizer. Karbasi, Askari and Madalou (2021) showed that acetylation of WPI microgels increased both their hydrophobicity and emulsification activity. Araiza-Calahorra et al. (2020) demonstrated that emulsions stabilized by conjugate microgels made from WPI and dextran via Maillard reaction had decreased pepsin digestibility compared to emulsions stabilized by their non-conjugated counterparts. As discussed earlier, the crosslinking of microgel particles is also able to modulate their spreading behaviour at the interface, and thus, their performance as stabilizer. In fact, crosslinking process is well-applied to proteins in order to improve their mechanical properties (GONSALVES et al., 2011).

Due to the high number of nucleophilic amino acids, proteins are prone to involve in different crosslinking reactions, be them chemical, physical, or enzymatic. The chemical crosslinking of proteins is generally done by reaction with aldehydes, namely glutaraldehyde and formaldehyde. However, these molecules are toxic and not allowed for food purposes. In this way, alternative compounds need to be explored as chemical crosslinker for proteins (AZEREDO; WALDRON, 2016; WEI et al., 2019). The use of organic acids for such application has shown positive results, according to which crosslinked particles presented a denser structure and smaller size compared to the non-crosslinked counterparts (FARJAMI; MADADLOU; LABBA, 2015; MURPHY; FARKAS; JONES, 2017; TAVASSOLI-KAFRANI; GOLI; FATHI, 2017; WANG et al., 2016b).

In that regard, the crosslinking of WPI microgel particles is expected to give rise to a more compact polymeric network, with homogeneous internal structure and small particle size. This can benefit the spreading behaviour of the microgels at the oil-water interface, promoting the formation of a full homogeneous coverage, which may positively reflect on the characteristics of the produced Pickering emulsions.

4 WHEY PROTEIN ISOLATE MICROGEL PROPERTIES TUNED BY CROSSLINKING WITH ORGANIC ACIDS TO ACHIEVE STABILIZATION OF PICKERING EMULSIONS

Jéssica Thaís do Prado Silva [1,2,*], João Vitor Munari Benetti [1], Taís Téo de Barros Alexandrino [3,4], Odilio Benedito Garrido Assis [4], Jolet de Ruiter [2], Karin Schroën [2] and Vânia Regina Nicoletti [1]

[1] Institute of Biosciences, Humanities and Exact Sciences (Ibilce), São Paulo State University, Cristóvão Colombo 2265, São José do Rio Preto 15054-000, SP, Brazil

[2] Food Process Engineering Group, Wageningen University & Research, 6700 AA Wageningen, The Netherlands

[3] Biotechnology Graduate Program (PPG-Biotec), Campus São Carlos (UFSCar), Federal University of São Carlos, Rodovia Washington Luiz km 235, São Carlos 13565-905, SP, Brazil

[4] National Nanotechnology Laboratory for Agriculture (LNNA), Embrapa Instrumentação, XV de Novembro 1452, São Carlos 13560-970, SP, Brazil;

Published in Foods, Volume 10, June 2021, 1296.
https://doi.org/10.3390/foods10061296.

Abstract

Whey protein isolate (WPI) can be used effectively to produce food-grade particles for stabilizing Pickering emulsions. In the present study, crosslinking of WPI microgels using organic acids (tannic and citric acids) is proposed to improve their functionality in emulsions containing roasted coffee oil. It was demonstrated that crosslinking of WPI by organic acids reduces the microgels' size from ≈1850 nm to 185 nm and increases their contact angle compared to conventional WPI microgels, achieving values as high as 60°. This led to the higher physical stability of Pickering emulsions: the higher contact angle and smaller particle size of acid-crosslinked microgels contribute to the formation of a thinner layer of particles on the oil/water (O/W) interface that is located mostly in the water phase, thus forming an effective barrier against droplet coalescence. Particularly, emulsions stabilized by tannic acid-crosslinked WPI microgels presented neither creaming nor sedimentation up to 7 days of storage. The present work demonstrates that the functionality of these crosslinked WPI microgels can be tweaked considerably, which is an asset compared to other foodgrade particles that mostly need to be used as such to comply with the clean-label policy. In addition, the applications of these particles for an emulsion are much more diverse as of the starting material.

Keywords: protein microgels; whey protein isolate; particle properties; tannic acid; citric acid.

1 Introduction

Emulsions stabilized by solid particles (Pickering emulsions) are extensively explored as they offer high stability against coalescence. At the same time, they represent an alternative for avoiding the use of artificial surfactants that, despite obeying government food and health regulations, are less desired from a consumer (clean label) point of view. For these reasons, Pickering emulsions are attractive possible choices for application into foodstuff, whether for designing products that require long shelf life or as a vehicle system for delivery of bioactive compounds [1–3].

Current research is focused on the development of Pickering stabilizers using natural and food-grade polymers, such as polysaccharides (starch, cellulose, and chitosan), lipids (fat crystals), and proteins (casein, soybean protein isolate, and zein) [4–6]. However, developing food-grade Pickering particles is difficult as they must obey strict prerequisites, such as partial wettability and specific size. Particles should be wetted by both continuous and dispersed phases in order to stay anchored at the interface. This property is related to the three-phase contact angle (θ): if $\theta << 90^{\circ}$, particles are highly wetted by water, remaining dispersed at the water phase; if $\theta >> 90^{\circ}$, particles are highly wetted by oil, remaining dispersed at the oil phase. For intermediate θ values, particle adsorption would be optimal with the particles being partially wetted by both phases, which favours embedding in the interface, with very high detachment energy. In addition, large particles could be less efficient in adsorbing at the interface [4,7,8].

Whey protein isolate (WPI) microgels have demonstrated to have strong potential for stabilizing Pickering emulsions, as they comply with the above-mentioned prerequisites and have shown improved functionality as a stabilizer when compared to native WPI [7,8]. Additional strategies have been investigated in order to produce protein microgels of well-defined size and shape and with suitable wetting properties to favour adsorption at interfaces, including jet homogenization, sonication, and enzymatic crosslinking [9,10].

Due to their high nucleophilic amino acid content, proteins are able to engage in various crosslinking reactions. Chemical crosslinking of proteins is mostly performed by reaction with aldehydes, mainly glutaraldehyde and formaldehyde. However, these substances have toxic potential and are not allowed in food [11]; food-grade alternatives are the organic acids tannic acid and citric acid. Tannic acid is a phenolic

compound found in many plant sources, which reacts readily with amino acids through its phenolic group, which is an excellent proton donor capable of forming strong hydrogen bonds with the carboxyl groups present in the protein structure [12,13]. Citric acid is a weak organic acid widely used in the food industry as an acidulant and preservative. It is found naturally in citrus fruits, especially in lemon and lime. The carboxylic groups of citric acid react with the free amino groups of the protein to form crosslinks and make citric acid part of the protein network, thus contributing to its hydrophobicity balance [14,15]. Both acids are declared Generally Recognized as Safe (GRAS) by the Food and Drugs Administration (FDA). There are no limitations for adding citric acid into foodstuff, while for tannic acid, the established limit is up to 0.04% [16,17]. Tannic acid is recognized for its antioxidant properties and is widely used as an additive in food products, especially in baking mixes, beverages, and desserts [18,19], in spite of some antinutritional properties (i.e., reduction of protein's bioavailability during digestion). Tannic acid and citric acid have been demonstrated to improve the technological properties of protein structures, such as macroscopic gels, films, and delivery vehicles [20–25]. However, their effect on protein microgel properties and the resulting effects on Pickering emulsion stabilization are yet unknown.

In the present work, the focus is on the production and characterization of food-grade organic acid-crosslinked WPI microgels for applications in oil-in-water Pickering emulsions. The properties of WPI microgels are tweaked by crosslinking with organic acids, and the expectation is that physical properties relevant to their role in Pickering emulsion stabilization will be modified, especially in terms of size distribution, surface charge, and wetting properties. Tannic acid or citric acid is used as the crosslinker and roasted coffee oil as the dispersed phase. This oil is already applied in the food industry as flavouring agent [26], and its use in the present work is proposed as an opportunity to diverse a food material's application. The produced Pickering emulsions were evaluated for physicochemical characteristics and stability over 7 days of storage. WPI microgels, with and without a crosslinker, were characterized by particle size distribution, zeta potential, and contact angle. Furthermore, Fourier-transform infrared spectroscopy (FTIR), X-ray diffraction (XRD), and scanning electron microscopy (SEM) were performed in order to elucidate the chemical and structural aspects of the particles.

2 Materials and Methods

2.1 Materials

Whey Protein Isolate (WPI) 88% purity (CL 3987, Alibra Ingredients, Campinas, Brazil) was used to prepare WPI microgels. Tannic acid (99%, Sigma-Aldrich, Darmstadt, Germany – 1701.20 g mol^{-1}) and citric acid (99%, Synth, Diadema, Brazil – 192.12 g mol^{-1}) were used as crosslinking agents. Sodium azide (99%, 0.1 g L^{-1}, Dinâmica, Indaiatuba, Brazil) was used to prevent microbial growth. Sodium hydroxide and hydrochloric acid solutions (HCl, 0.1 mol L^{-1}, Dinâmica, Indaiatuba, Brazil) were used for pH adjustment. Roasted coffee oil was kindly donated by Linax—Essential Oils (Votuporanga, Brazil).

2.2 Production of WPI Microgels

WPI microgels were produced according to the methodology described elsewhere [21] with some modifications. In brief, solutions of 40 g L^{-1} WPI in deionized water were prepared, and 0.1 g L^{-1} of sodium azide was added as an antimicrobial agent. WPI solutions were stirred for 2 h at 200 rpm (IKA, HS7, Staufen, Germany) and incubated under refrigeration for 12 h in order to ensure complete protein hydration. For the production of conventional microgels (WP40), firstly, WPI solutions had their pH adjusted to 5.8 since this pH value has been demonstrated to allow gel structure formation with good sphericity [27]. Then, solutions were heated in a thermal bath at 80 ◦C for 15 min, after which the samples were quickly cooled to room temperature and sonicated (Sonic Rupter 4000, Omni International, Kennesaw, GA, USA) for 3 min (20 kHz, 400 W), using an ice bath to prevent sample overheating (homogenization temperature was 30 ± 2 ◦C). The crosslinker (tannic acid or citric acid) was added to the prepared and cold-incubated WPI solutions (see the previous description). From preliminary studies, we selected to work at 3:1 (crosslinker:protein) molar ratio based on the protein content in solution (the purity of WPI was taken into account, and the molar mass of the major constituent (β-lactoglobulin) was used as that of the protein material). After crosslinker addition, the pH was adjusted to 5.8, and the same procedure – as described above for conventional WPI microgels – was followed.

2.3 Characterization of WPI Microgels

2.3.1 Particle Size Distribution and Zeta Potential

Particle size distribution and zeta potential were measured through dynamic light scattering (DLS) and electrophoretic light scattering, respectively. Samples were diluted 1000x in deionized water and evaluated (Zetasizer Nano ZS, Malvern Panalytical, Malvern, UK) immediately after their production. Each sample was analyzed in triplicate at 25 °C, using 1.45 as material refraction index for the protein particles, 1.33 as dispersant (water) refraction index, and 0.8872 mPa s as dispersant viscosity.

2.3.2 Fourier-Transform Infrared Spectroscopy (FTIR)

The chemical structures of conventional and crosslinked WPI microgels were investigated by attenuated total reflection Fourier-Transform Infrared spectra (ATR-FTIR). The spectra were recorded (Vertex 70 Spectrometer, Bruker Corporation, Berlin, Germany) in absorbance mode in a spectral region of 4000—480 cm^{-1}, over 64 consecutive scans. Prior to analysis, the microgel dispersions were frozen in ultra-freezer at −35 °C (Liotop, Liobras, São Carlos, Brazil) right after preparation and subsequently freeze-dried for 24 h (L101, Liobras, São Carlos, Brazil).

2.3.3 X-ray Diffraction (XRD)

X-ray patterns of freeze-dried samples, including native WPI, were obtained in an X-ray diffractometer (Miniflex 300, Rigaku, Japan). The samples were held on a glass support and subjected to scans from 3 to 40° (2θ) at a rate of 1° min^{-1}; using Cu Kα radiation generated at 30 kV and 10 mA. The crystallinity indices (CrI) were calculated according to the Segal method (Equation (1)) [28], where I_{max} is the maximum intensity (height of the tallest peak in the diffractogram), and I_{am} is the intensity corresponding to the amorphous fractions of the samples.

$$Crl\ (\%) = \frac{(I_{max} - I_{am})}{I_{max}} x\ 100 \quad (1)$$

2.3.4 Scanning Electron Microscopy (SEM)

Microgel morphology was characterized by means of scanning electron microscopy with a field emission gun (XL-30 FEG, Philips). Before analysis, the samples were frozen at −35 °C for 12 h followed by drying for 24 h using a freeze dryer (Liotop L101, Liobras, Brazil). The freeze-dried samples were then diluted in deionized water, fixed on carbon tape, and metallized with gold. Images were acquired at magnifications of 2000x , 5000x, and 20,000x, with electron beam acceleration of 5.0 kV.

2.3.5 Contact Angle

For static contact angle measurements, the microgel dispersions were carefully pipetted on microscopy slides. The slides were put in a desiccator to evaporate water so that only the deposited microgels remained on the glass surface, forming a thin layer. These slides were then placed in a contact angle measurement system (CAM 101, KSV Instruments, Finland) with a coupled camera, and one drop of deionized water (2 µL) was deposited on each microgel film [29]. The experiment was performed in triplicate, and images were acquired immediately after the water drop was deposited on the microgel film.

2.4 Production of Pickering Emulsions Containing Roasted Coffee Oil

Microgel dispersions prepared with 40 g L^{-1} of WPI as described in Section 4.2.2, with and without crosslinker, were used as the continuous phase for preparing Pickering emulsions containing roasted coffee oil as the dispersed phase (10% w/w). As a blank, an emulsion prepared with a solution of native WPI (40 g L^{-1}) was used. The roasted coffee oil and the continuous phase were pre-homogenized using Ultra Turrax (T-25, IKA, Staufen, Germany) for 2 min at 9000 rpm. Then, the coarse emulsions were sonicated (Sonic Rupter 4000, Omni International, Kennesaw, United States) for 3 min (20 kHz, 400 W) while immersed in an ice bath to prevent overheating (homogenization temperature was 30 ± 2 °C).

2.5 Characterization of Pickering Emulsions Containing Roasted Coffee Oil

2.5.1 Morphology and Droplet Size

Images of the emulsion droplets were obtained using a bright-field microscope (CX31, Olympus, Japan) with a 100x magnification lens, with a coupled camera (SC30, Olympus). Around 20 µL of the emulsion was pipetted on a glass slide and coated with a coverslip, followed by adding one droplet of immersion oil. These microscopy images were evaluated using ImageJ (NIH) software to determine the diameter of 300 droplets in each sample, and frequency distribution graphs were made using the software GraphPad Prism v. 8 (San Diego, CA, United States), which enabled identification of D_{10}, D_{50}, and D_{90} for each distribution. The distribution width (Span) was calculated according to Equation (2), in which D_i is the diameter, below which i% of the sample is contained (i= 10, 50, 90) [30,31].

$$Span = \frac{(D_{90} - D_{10})}{D_{50}} \quad (2)$$

2.5.2 Evaluation of Emulsion Stability

Physical stability of the produced emulsions was evaluated by the creaming (CI) and sedimentation (SI) indexes. For this purpose, emulsions were transferred to test tubes in triplicate and stored for 7 days at room temperature. The CI was calculated according to Equation (3), where H_U is the height of the upper phase (lowest density), and H_T is the total height of the emulsion in the tube [32].

$$CI\ (\%) = \frac{H_U}{H_T} x100 \quad (3)$$

Similarly, the sedimentation index was calculated using Equation (4), where H_S is the sediment height in the test tube.

$$SI\ (\%) = \frac{H_S}{H_T} x100 \quad (4)$$

2.6 Statistical Analysis

The results of analytical determinations for WPI microgels (particle size, polydispersity index, and zeta potential) and Pickering emulsions (creaming and sedimentation indexes) were subjected to one-way analysis of variance (ANOVA). Samples were evaluated in triplicate, and statistical analyses were carried out using the software Statistica v. 12.0 (StatSoft, Hamburg, Germany), considering a significance level (p) of 0.05 and Tukey's test as post hoc.

3 Results and Discussion

3.1 Characterization of WPI Microgels

Particles used for Pickering stabilization must meet specific criteria related to size, charge, morphology, and partial wettability to accomplish a high performance as an emulsion stabilizer. In this section, these characteristics of the produced WPI microgels were assessed. The influence of organic acids during the crosslinking step was investigated, and hypotheses about the potential of the various microgels for Pickering stabilization were formulated, which will be experimentally studied in the next section.

3.1.1 Size and Zeta Potential

Particle size distributions of the produced microgels are summarized in Table 4.1, which shows that smaller and less polydisperse particles could be attained when a crosslinker was used. The DLS measurement of WP40 points to large particles (Table 4.1) and highly polydisperse size distribution, probably indicating that conventional microgels are forming aggregates. In fact, sedimentation can be observed within a few minutes, which can be related to gravitational separation due to the microgels' size and density difference with the continuous phase (water). The crosslinked microgels were 8–10 times smaller than the conventional microgels and did not present sedimentation.

Table 4.1 - Particle size, polydispersity index (PDI), and zeta potential of conventional microgels (WP40), tannic acid- (WPTA), and citric acid-crosslinked (WPCA) WPI microgels.

Sample	Particle Size (nm)	PDI	Zeta Potential (mV)
WP40	1852.6 ± 638.0^{a*}	0.981 ± 0.03^{a}	−32.1 ± 0.3^{ab}
WPTA	185.2 ± 2.2^{b}	0.123 ± 0.01^{c}	−33.4 ± 1.1^{a}
WPCA	257.6 ± 4.2^{b}	0.212 ± 0.01^{b}	−30.3 ± 0.5^{b}

Different letters in the same column indicate significant difference according to Tukey's mean test.

Data expressed as mean (n = 3) ± standard deviation.

* Analysis without quality criteria due to high polydispersity.

Farjami et al. [21] stated that the crosslinker increases the structural stability of proteins during heat treatment, preventing agglomeration and thus resulting in relatively smaller particles when compared to microgels produced in the absence of crosslinker.

These authors produced WPI microgels crosslinked by citric acid with sizes ranging from 80 to 130 nm, which are smaller than those obtained in the present work, although in a similar order of magnitude. The size difference may be the result of a different WPI source and ratio crosslinker: protein but was most probably caused by the method applied for size distribution analysis: atomic force microscopy, which is determined by a scanning probe instead of light scattering. Crosslinking with tannic acid yielded the smallest microgels and lowest polydispersity index (PDI) among all treatments. In fact, WPTA was the only treatment that resulted in PDI lower than 0.2, which is the limit generally used for monodisperse polymer-based nanoparticles [33].

The zeta potential values of the microgels in suspension were negative for all the samples (Table 4.1). The absolute values as measured for WPI microgel complexes are de-pendent on the protein concentration and can vary from positive to negative according to the acidity of the medium [34,35]. Values close to −30 mV are commonly found in the literature for WPI based microgels [36] and even lower values [37], with reasonable stability of the particles in suspension. The isoelectric point of WPI is stated as pH 5.0, and the dissociation of COOH groups above pH 5 led the particles to carry negative charges [29]. It is worth mentioning that in the present study, the microgels were processed at pH 5.8, with general results in good agreement with cited literature.

3.1.2 Fourier-Transform Infrared Spectroscopy (FTIR)

Figure 4.1 presents the ATR-FTIR spectra of native WPI, WP40, WPTA, and WPCA. All samples have similar fingerprints related to the specific functional groups of WPI.

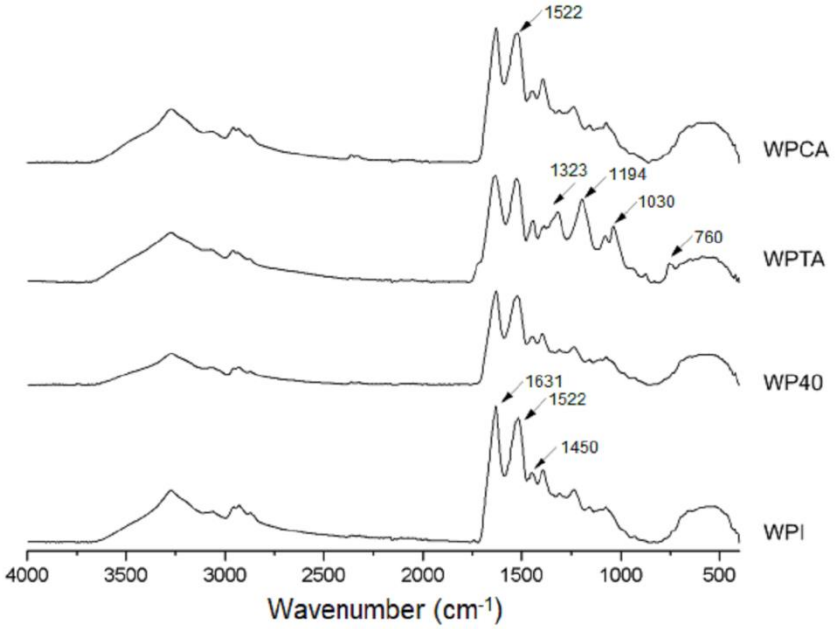

Figure 4.1 - Infrared spectra of native WPI, conventional microgels (WP40), tannic acid- (WPTA), and citric acid-crosslinked (WPCA) WPI microgels.

The two main peaks at 1631 cm^{-1} and 1522 cm^{-1} relate to peptide bonds of amide I (C=O stretching) and amide II groups (N–H folding and C–N stretching), respectively, which are very characteristic of protein structures. A peak centered at 1450 cm^{-1}, with lower intensity, corresponds to C–N stretching and N–H folding of the amide III group [38]. The amide I band (1631 cm^{-1}) gives information about the protein secondary structure; more specifically, the bands at around 1650–1660 cm^{-1} represent α-helix structures, whereas bands between 1610–1640 cm^{-1} refer to β-sheet structures [9]. The heating of WPI solutions leads to partial modification of the secondary structure [39], as can be observed by comparing the WPI and WP40 spectra (Figure 4.1). The band related to the secondary structure (1631 cm^{-1}) underwent intensity reduction after heat treatment (sample WP40), indicating partial unfolding or loss of some of the protein original helix configuration.

The effect of crosslinking can be also observed, mainly for tannic acid. Two features are important to be highlighted: a new band appears at 1030 cm^{-1} in the WPTA spectrum, which is related to C–O stretching vibration in the amide III region [11], whereas the peaks assigned at around 1323 cm^{-1} and 1194 cm^{-1} in the WPTA spectra correspond to the most strong absorptions identified in the tannic acid spectra (not shown), and are related to the Csp2–O bond of the acid aromatic rings [40]. These bands are not observed in the protein isolate structure. Thus, the presence in the WPTA spectra indicates the incorporation of the tannic acid in the microgel formation. Most of the interactions between TA and proteins are described as occurring in the amide regions involving the participation of TA phenolic hydroxyls and the amides in the proteins (CN and NH group). These interactions probably predominate hydrogen bonding rather than ionic crosslinking between species [40–42]. Additionally, the simultaneous occurrence of hydrophobic interactions is considered a possible cooperative mechanism in the formation of protein-tannin complexes [43–45].

The spectrum of WPCA microgels is mostly unchanged compared to WPI, indicating that the general structure of proteins is preserved. However, there is an increase in peak intensity in the amide II region (1522 cm^{-1}), which is likely due to the occurrence of inter-actions between C–N groups. This is consistent with the observation by Farjami et al. [21], who reported chemical linking between the carbonyl groups of citric acid and the amino groups of proteins.

Figure 4.2 shows the second derivative of the original spectra, which permits a much more detailed qualitative analysis. This evaluation focused mainly on the region between 1650 and 600 cm^{-1}, which comprises the amide I, amide II, and amide III structures of the whey protein. The smoothed derivative peaks follow a Lorentzian function shape, as well known from literature [46].

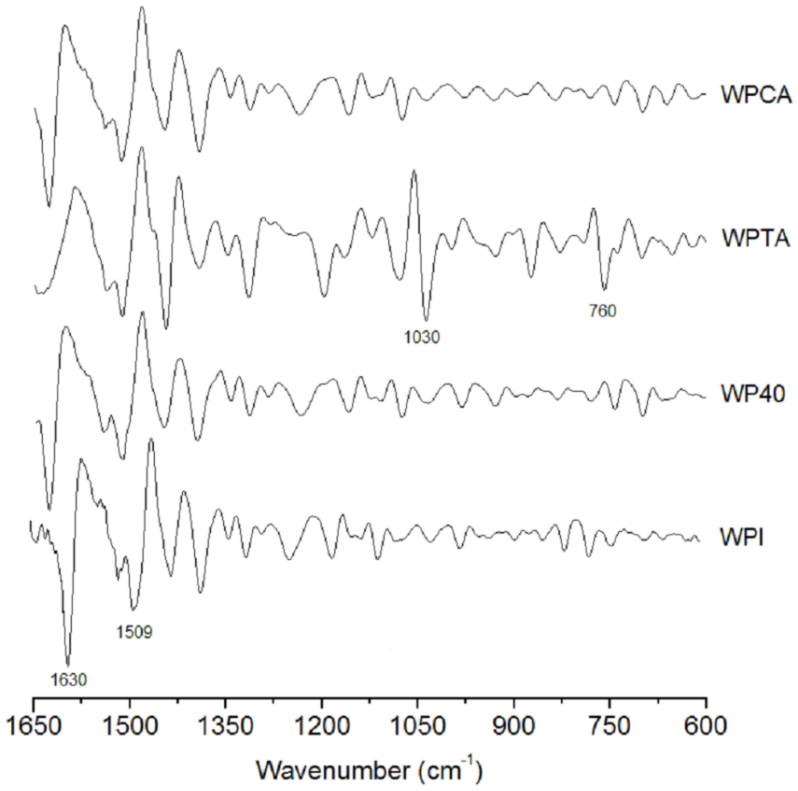

Figure 4.2 - The second derivative of the original FTIR spectra of native WPI, conventional microgels (WP40), tannic acid- (WPTA), and citric acid-crosslinked (WPCA) WPI microgels.

In the control WPI, two main peaks are worth signalling: the stronger band at 1630 cm^{-1}, related to β-segments, and a weaker one centred at 1509 cm^{-1} that is associated with the α-helix conformation. The peak corresponding to β-structure almost vanished in the tannic acid crosslinked sample, reflecting the strong interaction between TA and WPI that promotes a denaturation of secondary β-conformation protein structure, while the α-helix conformation is preserved.

It is evident that WPTA resulted in a structure that most differs from the original WPI control. Two more intense peaks appear at 1030 and 760 cm^{-1}. The first is ascribed to in-tense absorbance from C–O stretching and N–H deformation in the amide III groups [11]. The second less intense band could be related to the side-chain vibrations from the whey protein isolate [47], which probably reflects the tertiary structure associated with hydrogen bonding reaction between the amide and hydroxyl groups of the tannic acid.

3.1.3 X-ray Diffraction (XRD)

The diffractograms presented in Figure 4.3 confirm the semi-crystalline nature of WPI and the microgels. All samples show similar patterns with main diffraction peaks related to α-helix (9.2°) and β-sheet (19.6°) structures [48,49]. A crystallinity index of 58.6% was calculated for WPI, with a small decrease upon processing, except for the WPCA sample that retained the same crystallinity index as WPI (Table 4.2), as was also expected based on the FTIR result presented earlier. Similar results were reported by Mohammadian et al. [50] and Sun et al. [49] for conventional WPI microgels prepared at different pH values.

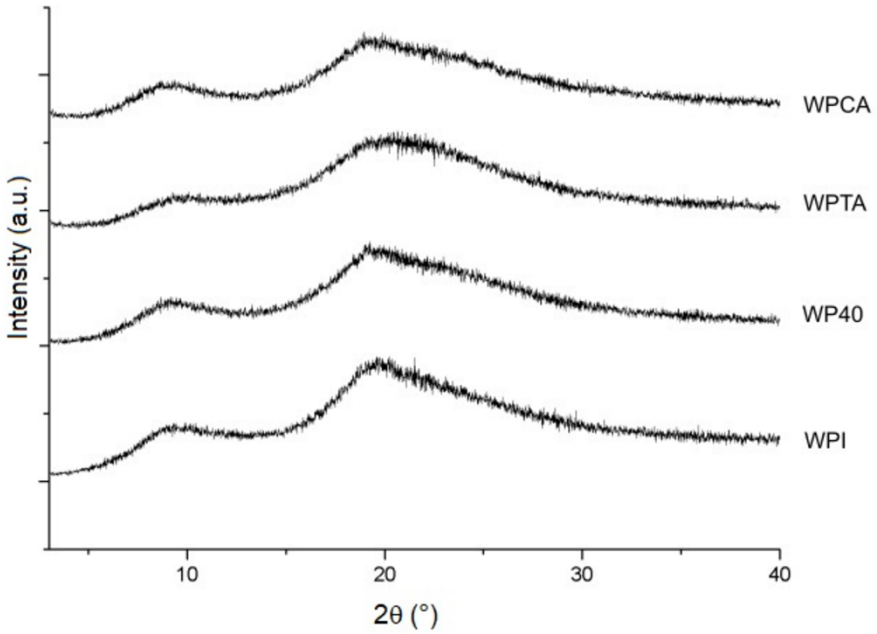

Figure 4.3 - X-ray diffraction patterns of native WPI, conventional microgels (WP40), tannic acid- (WPTA), and citric acid-crosslinked (WPCA) WPI microgels.

Table 4.2 - Crystallinity indices (Crl) of native WPI conventional microgels (WP40), tannic acid- (WPTA), and citric acid-crosslinked (WPCA) WPI microgels.

Sample	Crl (%)
WPI	58.6
WP40	53.9
WPTA	52.1
WPCA	60.0

In spite of the crystallinity indexes measured being a result of the drying procedure necessary to the analysis, the differences between samples may be related to the

organization degree of protein structure when dispersed in the aqueous medium. The degree of WPI crystallization, as obtained in dry conditions, reflects the limited mobility and rotations of the groups in the protein structure. In wet conditions, the access of water molecules to the hydrophilic groups is easier in a less crystalline structure, thus facilitating nucleation and more uniform size distribution of the microgels. The crosslinking with tannic acid resulted in a structure with lower crystallinity (Table 4.2). This justifies, to some degree, the average particle size and polydispersity values as displayed in Table 4.1.

3.1.4 Scanning Electron Microscopy with Field Emission Gun (SEM-FEG)

SEM images of the microgels are presented in Figure 4.4. After freeze-drying and redispersion in water, conventional microgels remained aggregated (Figure 4.4A), forming a spongy structure, as reported for WPI microgels by other researchers [51]. Conversely, the nanoparticles crosslinked with tannic acid, sample WPTA (Figure 4.4B), were small and with a nearly spherical shape, with a more homogenous distribution, revealing a lower tendency to form aggregates. The citric acid crosslinked nanoparticles (Figure 4.4C) have some similarities with WPTA microgels concerning size, although assumed a configuration of irregular aggregates when dried under microscopic observation.

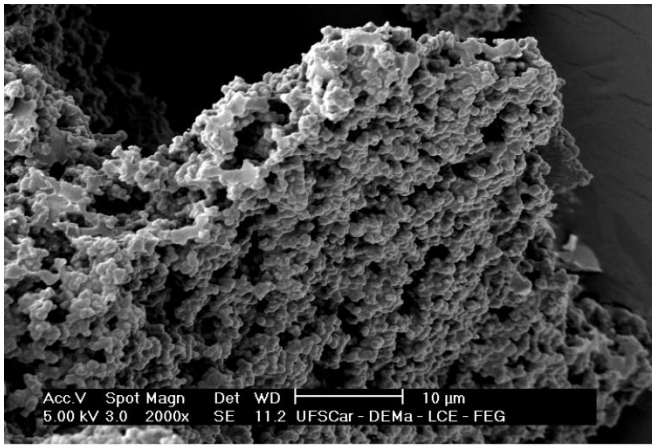

(A)

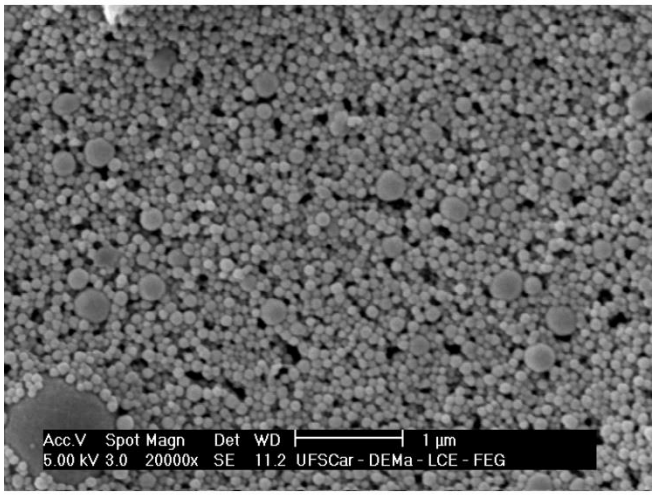

(B)

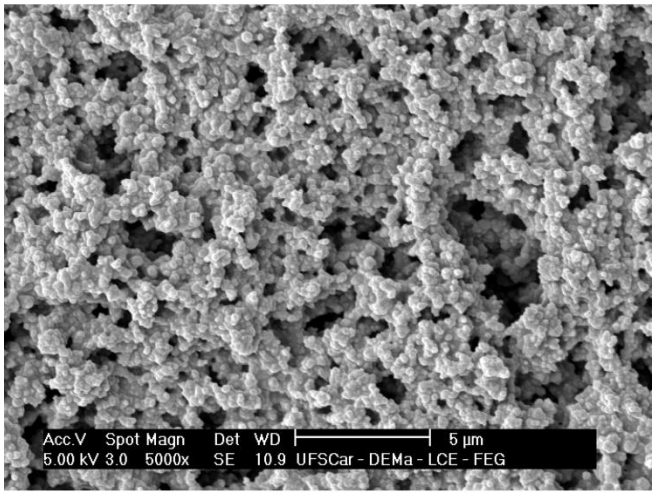

(C)

Figure 4.4 - SEM images of: (A) conventional microgels (WP40) (2000x); (B) tannic acid- (WPTA) (20,000x); (C) citric acid-crosslinked (WPCA) (5000x) WPI microgels.

In Pickering emulsions, particle shape is an important parameter for emulsion stability as it will determine how particles are going to pack themselves at the interface [52]. As

outlined by Berton-Carabin and Schroën [4], food-grade particles are very complex and may have irregular shapes; however, often their structure is soft, which allows for the particles to flatten at the O/W interface, resulting in efficient interfacial anchorage and possibly also network-formation, which contributes to emulsion stability. If this applies to the conventional and crosslinked microgels produced in this work, this may render them suitable for Pickering stabilization, as reported later.

3.1.5 Contact Angle

The contact angle measurements are an indication of the usefulness of particles for Pickering stabilization. Particles that are totally hydrophilic (contact angle $\theta = 0°$) will re-main in the water phase, and particles that are highly hydrophobic ($\theta = 180°$) would re-main in the oil phase [53]. For intermediate angles, the particle can be positioned at the O/W interface, although the effect on emulsion stability can vary greatly [54].
In the present study, the water contact angle measurements of the solid particles were performed in the air ($\theta_{sw(a)}$) by gently depositing a water droplet (2 µL) onto the layer of dried particles under ambient atmosphere. It is important to clarify that the exact value of the (water) contact angle of a single microgel particle at the O/W interface will differ from that measured on a dried film surface ($\theta_{sw(a)}$) for two main reasons: first, because of the different ambient phase, and second, due to the differences between the microscopic contact on a single (swollen) particle, and the macroscopic contact angle measured on a grafted microgel film [55]. However, the macroscopic contact angle in the air (see Figure 4.5) does show a strong correlation with the microscopic contact angle, which allows for the identification of trends in particle wettability, as was already discussed by Wu et al. [29]

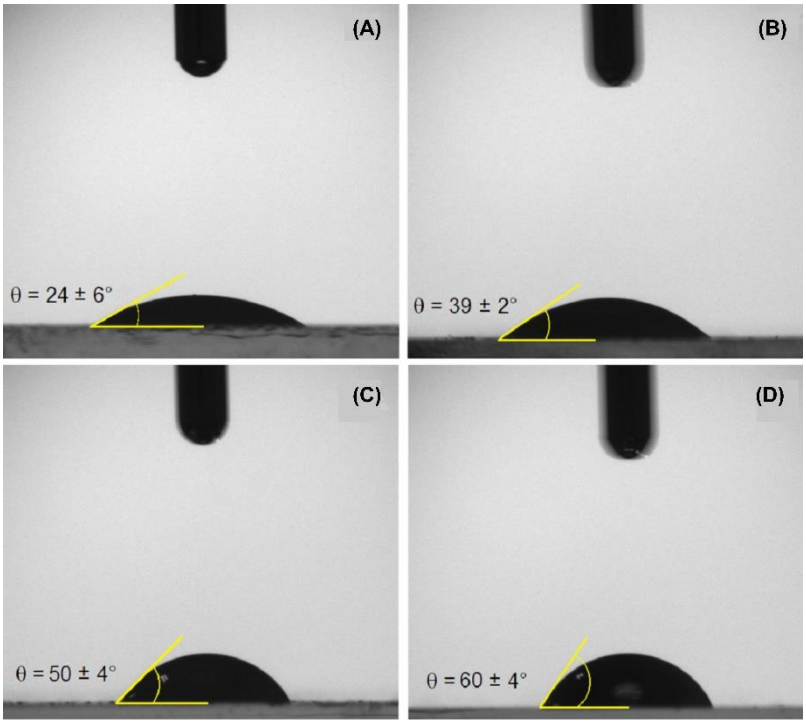

Figure 4.5 - The water contact angle (in air) on: (A) native WPI; (B) conventional microgels (WP40); (C) tannic acid-crosslinked (WPTA); (D) citric acid-crosslinked (WPCA) WPI microgels.

WPI consists of a group of globular proteins that, in their native state, present their hydrophilic fractions oriented outward, while hydrophobic groups are folded inside the molecule [56]. For this reason, depositing a water droplet onto the WPI film (Figure 5A) results in the smallest contact angle among the treatments, 24 ± 6°, confirming the surface predominance of hydrophilic groups. Particular attention was given to minimize the effect of protein dissolution by taking the measurement around 1 second after droplet deposition. For WPI microgels (Figure 4.5B), higher contact angles were found as for WPI, which can be indicative of exposure of hydrophobic groups as a result of previously discussed structural changes.

Both crosslinked particles (Figures 4.5C,D) show considerably higher contact angles than their non-crosslinked counterparts (Fig 4.5B), which is indicative of higher hydrophobicity. The polarity change may have occurred via chemical bonding between crosslinkers and carboxyl groups or amines in the protein structure, consequently reducing the number of polar side groups available to interact with water molecules [57]. The contact angle increased from 39 ± 2° for WP40 to a maximum of 60 ± 4° for

WPCA, which will allow these particles to attach more strongly to the emulsion interface compared to conventional microgel particles.

3.2 Characterization of Pickering Emulsions Containing Roasted Coffee Oil

Pickering emulsions were prepared using the produced WPI microgels as stabilizers and ultrasound as the dispersion method. In this section, the emulsions containing roasted coffee oil are evaluated regarding droplet size, morphology, and stability. This oil is an important byproduct of the coffee industry, and it has been applied as a flavoring agent, especially for baking products. Since Brazil is the largest coffee producer in the world, it is desirable to develop new technologies for expanding the use of coffee byproducts [58]. We would like to stress that WPI microgels can stabilize emulsions with other, more conventional, disperse phases, and demonstrated this for hexadecane. In this way, here, we focus on roasted coffee oil as a way to indicate the versatility of such emulsions in terms of application in the food industry.

3.2.1 Morphology and Droplet Size

Images of the produced emulsions were obtained by bright-field microscopy and are shown in Figure 6. The emulsions stabilized by crosslinked microgels (Figures 4.6C,D) have slightly smaller droplets, as shown in Table 3, which seem not to be flocculated, unlike the emulsion stabilized by regular WPI and WPI microgels (Figure 4.6A,B).

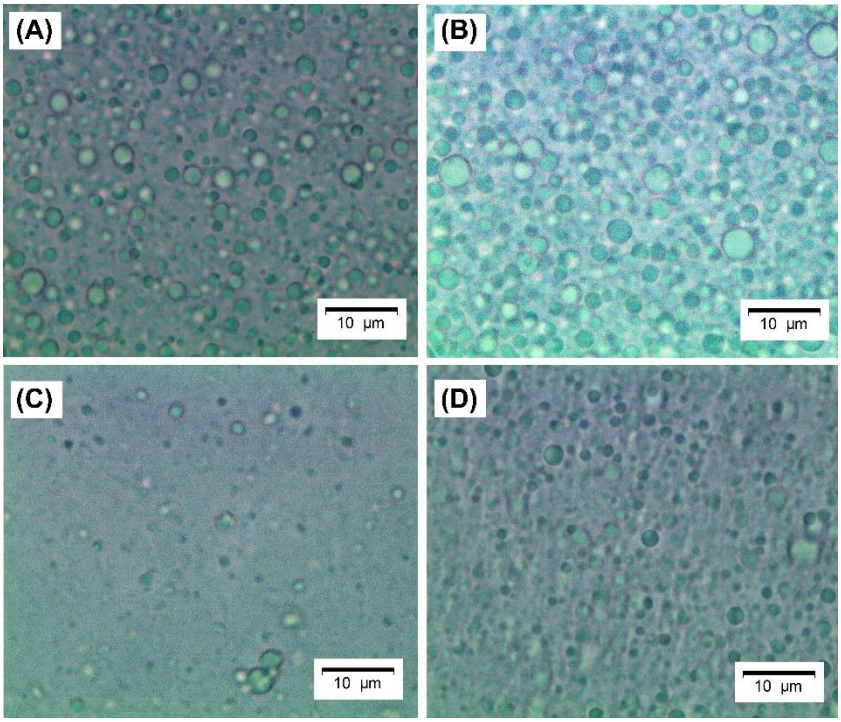

Figure 4.6 - Light microscopy images of emulsions stabilized by: (A) native WPI solution 40 mg mL^{-1}; (B) conventional microgels (WP40); (C) tannic acid-crosslinked (WPTA); (D) citric acid-crosslinked (WPCA) WPI microgels. Scale bars refer to 10 µm.

Table 4.3 - The mean droplet size (D_A) and polydispersity (span) of emulsions containing roasted coffee oil stabilized by native WPI, conventional microgels (WP40), tannic acid- (WPTA), and citric acid-crosslinked (WPCA) WPI microgels.

Continuous Phase	D_A (µm) *	Span	D_{10} (µm)	D_{50} (µm)	D_{90} (µm)
WPI	1.80	0.96	0.93	1.79	2.64
WP40	1.96	0.95	1.12	1.86	2.88
WPTA	1.26	0.98	0.75	1.15	1.88
WPCA	1.54	1.22	0.81	1.35	2.46

* Corresponds to the arithmetic mean of the diameter of 300 droplets in each sample.

In emulsions formulated with WPI and WP40, destabilization took place after 12 hours, probably due to droplet flocculation and further coalescence, generating creaming effects (see also Table 4.4). It is important to point out that it is unlikely that the large aggregates of WP40 microgels (see Table 4.1) can stabilize an emulsion with the average droplet size of 1.96 µm since it is necessary that particles are at least 10-fold smaller than the droplet size [4]. However, it is likely the large aggregates of conventional microgels were disintegrated during high-pressure homogenization. The

size of the (clustered) droplets is, of course, the most important reason for droplet creaming as, in accordance with Stokes' law [59,60], the particle radius has a squared effect on the upward (or downward) velocity of the dispersed phase. On the other hand, the crosslinked microgels might have resulted in a higher packing density at the interface that, in turn, may have reduced the density difference between the dispersed and continuous phase; another possible effect is that the more rigid crosslinked particles were less prone to form bridged interfaces that favors flocculation [61]; both effects reduce gravitational separation.

Table 4.4 - Creaming and sedimentation indexes of Pickering emulsions containing roasted coffee oil stabilized by native WPI, conventional microgels (WP40), tannic acid- (WPTA), and citric acid-crosslinked (WPCA) WPI microgels.

Continuous Phase	Creaming Index (%)	Sedimentation Index (%)
WPI	4.0 ± 0.5^{a}	0.0 ± 0.0^{c}
WP40	4.4 ± 0.1^{a}	10.4 ± 0.4^{a}
WPTA	0.0 ± 0.0^{b}	0.0 ± 0.0^{c}
WPCA	3.8 ± 0.5^{a}	2.4 ± 0.1^{b}

Different letters in the same column indicate significant difference according to Tukey's mean test. Data expressed as mean (n = 3) ± standard deviation.

3.2.2 Physical Stability of Pickering Emulsions

The emulsion stabilized with the microgels crosslinked with tannic acid is the only one that is stable to phase separation (Table 4.4) and shows creaming and sedimentation indexes of 0 after 7 days of storage. All other emulsions showed considerable creaming and, in two cases, also sedimentation.

The emulsion stabilized by native WPI did not show any sedimentation, which is logical since WPI is a soluble small molecule that, when dispersed properly, does not sediment. The emulsion stabilized by WPCA showed some sedimentation, indicating that these microgels are slightly prone to gravitational separation, albeit not as much as the standard microgels that are 10-fold larger in size (Table 4.1). The hypothesis is that the sedimented fraction is constituted by protein particles that were not adsorbed at the oil/water interface. This phenomenon was previously observed by de Folter et al. [62] and Anjali and Basavaraj [63] for hematite regular-shaped particles but also for food-grade particles based on WPI and soluble soybean polysaccharides, as reported by Cabezas and et al. [64]. These authors observed that the denatured protein particles

with larger sizes (around 240 nm) would be less prone to efficiently accommodate at the oil/water interface. In the present work, the samples in which there was sedimentation were those formulated with WPCA (around 258 nm) and WP40 (around 1853 nm). The appearance of sedimented particles also helps to explain the higher creaming indexes observed in these emulsions, as the less effective particle adsorption at the interface resulted in larger droplets, more susceptible to coalescence and further creaming. Ding et al. [65] produced Pickering emulsions stabilized by glutaraldehyde-crosslinked gelatin nanoparticles that were not that effective compared to the crosslinked WPI microgels used in the present study.

4. Conclusions

Crosslinking of WPI microgels with organic acids improves their physical and chemical characteristics by yielding particles that are smaller, less polydisperse, and more hydrophobic than conventional WPI microgels, which contribute to more effective adsorption at the O/W interface during the formation of Pickering emulsions. In particular, tannic acid demonstrated to be a very suitable WPI crosslinker for providing emulsions with higher stability. This is in stark contrast to emulsions stabilized by native WPI or conventional WPI microgels, in which droplet flocculation and coalescence were observed within a few minutes after emulsification. Even though the adsorption dynamics of WPI micro-gels is still unknown, the results presented in this work support the hypothesis that crosslinking of WPI microgels by organic acids, such as tannic acid and citric acid that are recognized as GRAS, is a promising strategy for producing crosslinked WPI microgels with tailored functionality for Pickering stabilization. However, the amount of emulsions stabilized by tannic acid-crosslinked microgels into foodstuff should be selected according to recommendations of regulatory agencies. On the other hand, the emulsification process with WPI microgels (with or without crosslinking) needs to be better understood. Residual soluble proteins may compete with microgels in stabilizing the O/W interface and thus influence the emulsion formation and/or stability. Our future research will be focused on a deeper understanding of the formation of crosslinked WPI microgels, including the fraction of proteins that remain in solution. It is also important to address the residual amount of crosslinking agent that carries astringency and thus may reduce consumer acceptance due to sensory inappropriateness. If this is the case, an additional step would need to

be added to the production line of the microgels, and although that is technically very feasible, it will add to the overall costs. To be complete, the stability of the emulsions under processing conditions will be to be checked.

Acknowledgments

The authors would like to thank the Brazilian Agricultural Research Corpo-ration—Embrapa Instrumentation for providing the general facilities, Marcia Perez dos Santos Cabrera for helping with particle size analysis, Alibra and Linax for the WPI and roasted coffee oil donation, respectively.

Funding source

This work was supported in part by the São Paulo Research Foundation – FAPESP (grant number 2016/22727-8) and in part by Coordenação de Aperfeiçoamento de Pessoal de Nível Superior – CAPES (finance code 001) through Program CAPES-PrInt-Unesp.

References

1. Gould, J.; Garcia-Garcia, G.; Wolf, B. Pickering particles prepared from food waste. *Materials (Basel).* **2016**, *9*, 1–14, doi:10.3390/ma9090791.
2. Marefati, A.; Bertrand, M.; Sjöö, M.; Dejmek, P.; Rayner, M. Storage and digestion stability of encapsulated curcumin in emulsions based on starch granule Pickering stabilization. *Food Hydrocoll.* **2017**, *63*, 309–320, doi:10.1016/j.foodhyd.2016.08.043.
3. Shah, B.R.; Zhang, C.; Li, Y.; Li, B. Bioaccessibility and antioxidant activity of curcumin after encapsulated by nano and Pickering emulsion based on chitosan-tripolyphosphate nanoparticles. *Food Res. Int.* **2016**, *89*, 399–407, doi:10.1016/j.foodres.2016.08.022.
4. Berton-Carabin, C.C.; Schroën, K. Pickering Emulsions for Food Applications: Background, Trends, and Challenges. *Annu. Rev. Food Sci. Technol.* **2015**, *6*, 263–297, doi:10.1146/annurev-food-081114-110822.
5. Dickinson, E. Food emulsions and foams: Stabilization by particles. *Curr. Opin. Colloid Interface Sci.* **2010**, *15*, 40–49, doi:10.1016/j.cocis.2009.11.001.
6. Tavernier, I.; Wijaya, W.; Meeren, P. Van Der; Dewettinck, K.; Patel, A.R. Food-grade particles for emulsion stabilization. *Trends Food Sci. Technol.* **2016**, *50*, 159–174, doi:10.1016/j.tifs.2016.01.023.
7. Destribats, M.; Rouvet, M.; Gehin-Delval, C.; Schmitt, C.; Binks, B.P. Emulsions stabilised by whey protein microgel particles: Towards food-grade Pickering emulsions. *Soft Matter* **2014**, *10*, 6941–6954, doi:10.1039/c4sm00179f.
8. Zamani, S.; Malchione, N.; Selig, M.J.; Abbaspourrad, A. Formation of shelf stable Pickering high internal phase emulsions (HIPE) through the inclusion of whey protein microgels. *Food Funct.* **2018**, *9*, 982–990,

doi:10.1039/c7fo01800b.
9. Jiang, Z.; Wang, C.; Li, T.; Sun, D.; Gao, H.; Gao, Z.; Mu, Z. Effect of ultrasound on the structure and functional properties of transglutaminase-crosslinked whey protein isolate exposed to prior heat treatment. *Int. Dairy J.* **2019**, *88*, 79–88, doi:10.1016/j.idairyj.2018.08.007.
10. Murray, B.S.; Phisarnchananan, N. Whey protein microgel particles as stabilizers of waxy corn starch + locust bean gum water-in-water emulsions. *Food Hydrocoll.* **2016**, *56*, 161–169, doi:10.1016/j.foodhyd.2015.11.032.
11. Azeredo, H.M.C.; Waldron, K.W. Crosslinking in polysaccharide and protein films and coatings for food contact - A review. *Trends Food Sci. Technol.* **2016**, *52*, 109–122, doi:10.1016/j.tifs.2016.04.008.
12. Mulaudzi, R.B.; Ndhlala, A.R.; Kulkarni, M.G.; Van Staden, J. Pharmacological properties and protein binding capacity of phenolic extracts of some Venda medicinal plants used against cough and fever. *J. Ethnopharmacol.* **2012**, *143*, 185–193.
13. Wu, J.; Liao, W.; Zhang, J.; Chen, W. Thermal behavior of collagen crosslinked with tannic acid under microwave heating. *J. Therm. Anal. Calorim.* **2019**, *135*, 2329–2335, doi:10.1007/s10973-018-7341-5.
14. Duquette, D.; Dumont, M.J. Comparative studies of chemical crosslinking reactions and applications of bio-based hydrogels. *Polym. Bull.* **2019**, *76*, 2683–2710, doi:10.1007/s00289-018-2516-6.
15. Galvão, A.C.; Robazza, W.S.; Arce, P.F.; Capello, C.; Hagemann, D.H. Experimental study and modeling of citric acid solubility in alcohol mixtures. *J. Food Eng.* **2018**, *237*, 96–102, doi:10.1016/j.jfoodeng.2018.05.032.
16. Food and Drug Administration (FDA) CRF - Code of Federal Regulations Title 21 Available online: https://www.accessdata.fda.gov/scripts/cdrh/cfdocs/cfCFR/CFRSearch.cfm?fr=184.1033 (accessed on May 27, 2021).
17. Food and Drug Administration (FDA) CFR -- Code of Federal Regulations Title 21 Available online: https://www.accessdata.fda.gov/scripts/cdrh/cfdocs/cfCFR/CFRSearch.cfm?fr=184.1097 (accessed on May 27, 2021).
18. Aewsiri, T.; Benjakul, S.; Visessanguan, W.; Wierenga, P.A.; Gruppen, H. Antioxidative activity and emulsifying properties of cuttlefish skin gelatin-tannic acid complex as influenced by types of interaction. *Innov. Food Sci. Emerg. Technol.* **2010**, *11*, 712–720, doi:10.1016/j.ifset.2010.04.001.
19. Shi, R.; Bi, J.; Zhang, Z.; Zhu, A.; Chen, D.; Zhou, X.; Zhang, L.; Tian, W. The effect of citric acid on the structural properties and cytotoxicity of the polyvinyl alcohol/starch films when molding at high temperature. *Carbohydr. Polym.* **2008**, *74*, 763–770, doi:10.1016/j.carbpol.2008.04.045.
20. Abaee, A.; Madadlou, A.; Saboury, A.A. The formation of non-heat-treated whey protein cold-set hydrogels via non-toxic chemical cross-linking. *Food Hydrocoll.* **2017**, *63*, 43–49, doi:10.1016/j.foodhyd.2016.08.024.
21. Farjami, T.; Madadlou, A.; Labba, M. Characteristics of the bulk hydrogels made of the citric acid cross-linked whey protein microgels. *Food Hydrocoll.* **2015**, *50*, 159–165.
22. Halim, A.L.A.; Kamari, A.; Phillip, E. Chitosan, gelatin and methylcellulose films incorporated with tannic acid for food packaging. *Int. J. Biol. Macromol.* **2018**, *120*, 1119–1126, doi:10.1016/j.ijbiomac.2018.08.169.
23. Hashemi, B.; Madadlou, A.; Salami, M. Functional and in vitro gastric digestibility

of the whey protein hydrogel loaded with nanostructured lipid carriers and gelled via citric acid-mediated crosslinking. *Food Chem.* **2017**, *237*, 23–29, doi:10.1016/j.foodchem.2017.05.077.

24. Picchio, M.L.; Linck, Y.G.; Monti, G.A.; Gugliotta, L.M.; Minari, R.J.; Alvarez Igarzabal, C.I. Casein films crosslinked by tannic acid for food packaging applications. *Food Hydrocoll.* **2018**, *84*, 424–434, doi:10.1016/j.foodhyd.2018.06.028.
25. Wang, T.; Fernandez, M.L.; Luo, Y.; Hu, S.; Wang, T.; Fernandez, M.L.; Luo, Y. Development of tannic acid cross-linked hollow zein nanoparticles as potential oral delivery vehicles for curcumin potential oral delivery vehicles for curcumin. *Food Hydrocoll.* **2016**, *61*, 821–831, doi:10.1016/j.foodhyd.2016.07.006.
26. Calligaris, S.; Munari, M.; Arrighetti, G.; Barba, L. Insights into the physicochemical properties of coffee oil. *Eur. J. Lipid Sci. Technol.* **2009**, *111*, 1270–1277, doi:10.1002/ejlt.200900042.
27. Nicolai, T. Formation and functionality of self-assembled whey protein microgels. *Colloids Surfaces B Biointerfaces* **2016**, *137*, 32–38, doi:10.1016/j.colsurfb.2015.05.055.
28. Hosseinnia, M.; Khaledabad, M.A.; Almasi, H. Optimization of Ziziphora clinopodiodes essential oil microencapsulation by whey protein isolate and pectin: A comparative study. *Int. J. Biol. Macromol.* **2017**, *101*, 958–966, doi:10.1016/j.ijbiomac.2017.03.190.
29. Wu, J.; Shi, M.; Li, W.; Zhao, L.; Wang, Z.; Yan, X.; Norde, W.; Li, Y. Pickering emulsions stabilized by whey protein nanoparticles prepared by thermal cross-linking. *Colloids Surfaces B Biointerfaces* **2015**, *127*, 96–104, doi:10.1016/j.colsurfb.2015.01.029.
30. Benetti, J.V.M.; Silva, J.T. do P.; Nicoletti, V.R. SPI microgels applied to Pickering stabilization of O/W emulsions by ultrasound and high-pressure homogenization: rheology and spray drying. *Food Res. Int.* **2019**, *122*, 383–391, doi:10.1016/j.foodres.2019.04.020.
31. Freitas, M.L.F.; Albano, K.M.; Telis, V.R.N. Characterization of biopolymers and soy protein isolate-high-methoxyl pectin complex. *Polimeros* **2017**, *27*, 62–67, doi:10.1590/0104-1428.2404.
32. Mwangi, W.W.; Ho, K.W.; Ooi, C.W.; Tey, B.T.; Chan, E.S. Facile method for forming ionically cross-linked chitosan microcapsules from Pickering emulsion templates. *Food Hydrocoll.* **2016**, *55*, 26–33, doi:10.1016/j.foodhyd.2015.10.022.
33. Danaei, M.; Dehghankhold, M.; Ataei, S.; Hasanzadeh Davarani, F.; Javanmard, R.; Dokhani, A.; Khorasani, S.; Mozafari, M.R. Impact of particle size and polydispersity index on the clinical applications of lipidic nanocarrier systems. *Pharmaceutics* **2018**, *10*, 1–17, doi:10.3390/pharmaceutics10020057.
34. Bédié, G.K.; Turgeon, S.L.; Makhlouf, J. Formation of native whey protein isolate-low methoxyl pectin complexes as a matrix for hydro-soluble food ingredient entrapment in acidic foods. *Food Hydrocoll.* **2008**, *22*, 836–844, doi:10.1016/j.foodhyd.2007.03.010.
35. Gbassi, G.; Yolou, F.; Sarr, S.; Atheba, P.; Amin, C.; Ake, M. Whey proteins analysis in aqueous medium and in artificial gastric and intestinal fluids. *Int. J. Biol. Chem. Sci.* **2012**, *6*, 1828–1837, doi:10.4314/ijbcs.v6i4.38.
36. Tercinier, L.; Ye, A.; Anema, S.; Singh, A.; Singh, H. Adsorption of milk proteins on to calcium phosphate particles. *J. Colloid Interface Sci.* **2013**, *394*, 458–466, doi:10.1016/j.jcis.2012.11.058.

37. Wang, S.; Chen, X.; Shi, M.; Zhao, L.; Li, W.; Chen, Y.; Lu, M.; Wu, J.; Yuan, Q.; Li, Y. Absorption of whey protein isolated (WPI)-stabilized β-Carotene emulsions by oppositely charged oxidized starch microgels. *Food Res. Int.* **2015**, *67*, 315–322, doi:10.1016/j.foodres.2014.11.041.
38. Karbasi, M.; Askari, G.; Madadlou, A. Surface decoration of whey protein microgels through the Maillard conjugation with maltodextrin. *Food Hydrocoll.* **2019**, *91*, 190–197, doi:10.1016/j.foodhyd.2019.01.003.
39. Nicolai, T.; Britten, M.; Schmitt, C. β-Lactoglobulin and WPI aggregates: Formation, structure and applications. *Food Hydrocoll.* **2011**, *25*, 1945–1962, doi:10.1016/j.foodhyd.2011.02.006.
40. Koupantsis, T.; Pavlidou, E.; Paraskevopoulou, A. Glycerol and tannic acid as applied in the preparation of milk proteins – CMC complex coavervates for flavour encapsulation. *Food Hydrocoll.* **2016**, *57*, 62–71, doi:10.1016/j.foodhyd.2016.01.007.
41. Guo, Y.; Bao, Y. hong; Sun, K. feng; Chang, C.; Liu, W. feng Effects of covalent interactions and gel characteristics on soy protein-tannic acid conjugates prepared under alkaline conditions. *Food Hydrocoll.* **2021**, *112*, 106293, doi:10.1016/j.foodhyd.2020.106293.
42. Muhoza, B.; Xia, S.; Zhang, X. Gelatin and high methyl pectin coacervates crosslinked with tannic acid: The characterization, rheological properties, and application for peppermint oil microencapsulation. *Food Hydrocoll.* **2019**, *97*, 105174, doi:10.1016/j.foodhyd.2019.105174.
43. Feng, Z.; Li, L.; Zhang, Y.; Li, X.; Liu, C.; Jiang, B.; Xu, J.; Sun, Z. Formation of whey protein isolate nanofibrils by endoproteinase GluC and their emulsifying properties. *Food Hydrocoll.* **2019**, *94*, 71–79, doi:10.1016/j.foodhyd.2019.03.004.
44. Frazier, R.A.; Papadopoulou, A.; Mueller-Harvey, I.; Kissoon, D.; Green, R.J. Probing protein-tannin interactions by isothermal titration microcalorimetry. *J. Agric. Food Chem.* **2003**, *51*, 5189–5195, doi:10.1021/jf021179v.
45. Thongkaew, C.; Gibis, M.; Hinrichs, J.; Weiss, J. Polyphenol interactions with whey protein isolate and whey protein isolate-pectin coacervates. *Food Hydrocoll.* **2014**, *41*, 103–112, doi:10.1016/j.foodhyd.2014.02.006.
46. Susi, H.; Michael Byler, D. Protein structure by Fourier transform infrared spectroscopy: Second derivative spectra. *Biochem. Biophys. Res. Commun.* **1983**, *115*, 391–397, doi:10.1016/0006-291X(83)91016-1.
47. Wen-Qiong, W.; Yi-Hong, B.; Ying, C. Characteristics and antioxidant activity of water-soluble Maillard reaction products from interactions in a whey protein isolate and sugars system. *Food Chem.* **2013**, *139*, 355–361, doi:10.1016/j.foodchem.2013.01.072.
48. Farrokhi, F.; Ehsani, M.R.; Badii, F.; Hashemi, M. Structural and thermal properties of nanofibrillated whey protein isolate in the glassy state. *LWT - Food Sci. Technol.* **2018**, *95*, 274–281, doi:10.1016/j.lwt.2018.05.001.
49. Sun, C.; Liang, B.; Sheng, H.; Wang, R.; Zhao, J.; Zhang, Z.; Zhang, M. Influence of initial protein structures and xanthan gum on the oxidative stability of O/W emulsions stabilized by whey protein. *Int. J. Biol. Macromol.* **2018**, *120*, 34–44, doi:10.1016/j.ijbiomac.2018.08.070.
50. Mohammadian, M.; Salami, M.; Momen, S.; Alavi, F.; Emam-Djomeh, Z. Fabrication of curcumin-loaded whey protein microgels: Structural properties, antioxidant activity, and in vitro release behavior. *LWT - Food Sci. Technol.* **2019**, *103*, 94–100, doi:10.1016/j.lwt.2018.12.076.

51. Zhang, W.; Zhong, Q. Microemulsions as nanoreactors to produce whey protein nanoparticles with enhanced heat stability by thermal pretreatment. *Food Chem.* **2010**, *119*, 1318–1325, doi:10.1016/j.foodchem.2009.08.043.
52. Low, L.E.; Siva, S.P.; Ho, Y.K.; Chan, E.S.; Tey, B.T. Recent advances of characterization techniques for the formation, physical properties and stability of Pickering emulsion. *Adv. Colloid Interface Sci.* **2020**, *277*, 102117, doi:10.1016/j.cis.2020.102117.
53. Chevalier, Y.; Bolzinger, M. Emulsions stabilized with solid nanoparticles : Pickering emulsions. *Colloids Surfaces A Physicochem. Eng. Asp.* **2013**, *439*, 23–34, doi:10.1016/j.colsurfa.2013.02.054.
54. Binks, B.. P.; Lumsdon, S.O. Influence of Particle Wettability on the Type and Stability of Surfactant-Free Emulsions. *Langmuir* **2000**, *16*, 8622–8631.
55. Paunov, V.N.; Cayre, O.J.; Noble, P.F.; Stoyanov, S.D.; Velikov, K.P.; Golding, M. Emulsions stabilised by food colloid particles: Role of particle adsorption and wettability at the liquid interface. *J. Colloid Interface Sci.* **2007**, *312*, 381–389, doi:10.1016/j.jcis.2007.03.031.
56. Walstra, P.; Wouters, J.T.M.; Geurts, T.J. *Dairy Science and Technology*; 2nd ed.; Taylor & Francis: Boca Raton, 2006; ISBN 9780824727635.
57. Peña, C.; de la Caba, K.; Eceiza, A.; Ruseckaite, R.; Mondragon, I. Enhancing water repellence and mechanical properties of gelatin films by tannin addition. *Bioresour. Technol.* **2010**, *101*, 6836–6842, doi:10.1016/j.biortech.2010.03.112.
58. Frascareli, E.C.; Silva, V.M.; Tonon, R. V.; Hubinger, M.D. Effect of process conditions on the microencapsulation of coffee oil by spray drying. *Food Bioprod. Process.* **2012**, *90*, 413–424, doi:10.1016/j.fbp.2011.12.002.
59. McClements, D.J.; Decker, E.A.; Weiss, J. Emulsion-based delivery systems for lipophilic bioactive components. *J. Food Sci.* **2007**, *72*, doi:10.1111/j.1750-3841.2007.00507.x.
60. McClements, D.J. *Food Emulsions: Principles, Practices, and Techniques*; 2nd ed.; CRC Press: Boca Raton, 2005; ISBN 978-0849320231.
61. Destribats, M.; Wolfs, M.; Pinaud, F.; Lapeyre, V.; Sellier, E.; Schmitt, V.; Ravaine, V. Pickering Emulsions Stabilized by Soft Microgels: Influence of the Emulsification Process on Particle Interfacial Organization and Emulsion Properties. *Langmuir* **2013**, *29*, 12367–12374, doi:10.1021/la402921b.
62. De Folter, J.W.J.; Hutter, E.M.; Castillo, S.I.R.; Klop, K.E.; Philipse, A.P.; Kegel, W.K. Particle shape anisotropy in pickering emulsions: Cubes and peanuts. *Langmuir* **2014**, *30*, 955–964, doi:10.1021/la402427q.
63. Anjali, T.G.; Basavaraj, M.G. Influence of pH and Salt Concentration on Pickering Emulsions Stabilized by Colloidal Peanuts. *Langmuir* **2018**, *34*, 13312–13321, doi:10.1021/acs.langmuir.8b02913.
64. Cabezas, D.M.; Pascual, G.N.; Wagner, J.R.; Palazolo, G.G. Nanoparticles assembled from mixtures of whey protein isolate and soluble soybean polysaccharides. Structure, interfacial behavior and application on emulsions subjected to freeze-thawing. *Food Hydrocoll.* **2019**, *95*, 445–453, doi:10.1016/j.foodhyd.2019.04.040.
65. Ding, M.; Zhang, T.; Zhang, H.; Tao, N.; Wang, X.; Zhong, J. Effect of preparation factors and storage temperature on fish oil-loaded crosslinked gelatin nanoparticle pickering emulsions in liquid forms. *Food Hydrocoll.* **2019**, *95*, 326–335.

5 ENHANCED COALESCENCE STABILITY OF DROPLETS THROUGH MULTI-FACETED MICROGEL ADSORPTION BEHAVIOUR

Jéssica Thaís do Prado Silva[1,2*], Vânia Regina Nicoletti[1], Karin Schroën[2] and Jolet de Ruiter[2]

[1]Unesp - São Paulo State University, Institute of Biosciences, Humanities and Exact Sciences, Cristóvão Colombo 2265, São José do Rio Preto 15054-000, São Paulo, Brazil

[2]Food Process Engineering Group, Wageningen University & Research, Wageningen 6700 AA, The Netherlands

Manuscript submitted to the Journal of Food Engineering

ISSN: 0260-8774

Abstract

Tannic acid-crosslinking of whey protein (WPI) microgels produces soft particles that can physically stabilize food emulsions. Here, we use these particles to investigate their compression at the air-water interface, and early-time stabilization of a model emulsion. Langmuir trough experiments showed that our microgels have a compression behaviour similar to synthetic microgels with a core-shell structure. The dangling chains provide protein-protein interactions at low surface coverage, while the partially-flattened cores provide thicker surface patches. Microfluidic experiments showed that at low continuous phase concentration, WPI microgels suppress coalescence due to bridging, which leads to improved stability compared to emulsions stabilized by native WPI. In contrast to classic Pickering emulsions, longer adsorption times lead to higher adsorbed amounts, which is expected due to the chains on the microgel surface, and possibly flattening of these microgels at the interface. Both features together are expected to be instrumental in obtaining highly stable microgel-stabilized food emulsions.

Keywords: WPI microgels, tannic acid, compression isotherm, microfluidics, emulsion stability, bridging flocculation.

1 Introduction

Pickering emulsions (Pickering, 1907) have received considerable attention recently, also in the food field, due to their outstanding physical stability. In such systems, particles are anchored at the O/W interface with desorption energy much larger than the thermal energy (k_bT), in a way that adsorption can be considered irreversible (Linke and Drusch, 2018). Different types of materials have been applied as Pickering stabilizer, such as polystyrene (Stancanelli et al., 2012), silica (Binks and Lumsdon, 2000; Whitby et al., 2017), hematite (Anjali and Basavaraj, 2018; De Folter et al., 2014), and clay (Wang et al., 2021). However, when aiming at food application, the material selection remains a challenge. This is because various parameters affect the ability of particles to act as stabilizer – such as partial wettability, size, and shape (Niroula et al., 2021) – and these are difficult to tune in food grade particles, due to the multiple composition and complexity of food materials (Berton-Carabin and Schroën, 2015). Furthermore, the presence of surface-active molecular species may influence particle anchoring at the interface indirectly through a reduction of the interfacial tension, and an effect on the particle wettability adsorbing at the droplet. Still, some advances have been accomplished using food components as starting material, such as gelatin (Jin et al., 2017), starch (Sjöö et al., 2015), chitosan (Ribeiro et al., 2020), zein (Zou et al., 2018), soy protein isolate (Benetti et al., 2019), and cellulose (Hu et al., 2015).

Microgel particles derived from proteins are a promising option for Pickering stabilization with added features because they combine the high desorption energy of solid particles with the surface activity of protein molecules that allow interaction beyond that of classical solid particles. Additionally, due to their ability to deform (and possibly de-swell) upon adsorption, a single microgel may cover a different interfacial area than its size in bulk. This may enhance anchoring to the interface and possibly lowers the amount of material needed to cover the same interfacial area (Bushuev et al., 2020; Murray, 2019), which presents an advantage for application in food.

Microgels have been successfully produced using whey protein isolate (WPI) as starting material (Destribats et al., 2014; Leon et al., 2018; Murray and Phisarnchananan, 2016; Wu et al., 2015). In a previous work, we studied the crosslinking of WPI microgels by tannic acid, which enabled to tune their physical properties such as size and wettability (do Prado Silva et al., 2021). These crosslinked

particles are very suitable for soft particle-stabilization as evidenced by smaller droplet size and enhanced emulsion stability. To better understand this stabilization process, it is necessary to consider time scales that are relevant during emulsion production, *i.e.* the sub-second events of droplet formation and collisions that are known to co-determine, amongst others, the droplet size.

Emulsions are usually produced through mechanical agitation, in which newly-generated droplets are only partially stabilized and coalesce repeatedly upon collision with adjacent droplets, to establish a final size distribution. The dynamic analysis of droplet formation, stabilization – in this case through particle adsorption –, and posterior coalescence is inherently difficult, in a way that evaluation of droplet size is restricted to average values measured in bulk emulsions (Yao et al., 2018). With microfluidic tools it is possible to uncouple droplet formation and coalescence, and thus enable separate studies of these two phenomena that occur at millisecond time scales. A typical device consists of micrometre size channels with a junction where two fluids meet, which allows excellent control over the size of droplets formed at this junction. This system is particularly relevant for emulsions stabilized by fragile particles, since there is no extensive mechanical shear that could disrupt these particles (Albert et al., 2019).

Microfluidics has been proven to be a useful tool in measuring how fast certain emulsifiers stabilise emulsions (Krebs et al., 2012b, 2012a), and how emulsification can be optimized in terms of processing conditions and ingredient formulation (Hinderink et al., 2020; Muijlwijk et al., 2017; Schröder et al., 2018). Important findings were acquired using microfluidics to investigate the formation of ‘classic’ Pickering emulsions. A sufficiently high continuous flow rate is necessary to stabilize these emulsions, which has been explained by the kinetic energy needed to adsorb hard particles to the interface (Schröder et al., 2018) or the fast removal of droplets from the microchannel to avoid collisions (Xu et al., 2005). Furthermore, Tatry et al (2019) demonstrated that reduction of surface tension is concentration dependent. Even though stable droplets are obtained at much lower amounts of microgels under high-shear conditions, the trends observed in microfluidic devices give valuable insights for emulsion design.

The spread and two-dimensional organization of microgel particles at interfaces can be assessed by means of Langmuir trough experiments. Surface pressure isotherms give insights into the subsequent interaction regimes that occur during compression of

interfacial layers due to the softness and responsiveness of microgels (Fernandez-Rodriguez et al., 2021). Several aspects of interfacial layers have been explored: for example to establish a 2D state equation for the dynamic adsorption of soft microgel particles (Deshmukh et al., 2014); and to explore similarities between interfacial films formed by protein assemblies of different sizes and at different ionic strength (Mahmoudi et al., 2010). Furthermore, it is possible to visualise the interfacial microstructure of protein aggregates and gel beads, when the compressed interfacial layer is transferred to a mica substrate and studied with atomic force microscopy (Yang et al., 2020).

In this study, we aim to gain understanding of the early-time stabilization of O/W emulsions by tannic acid-crosslinked WPI microgels. For this we use a microfluidic device to produce monodisperse droplets and subsequently monitor the extent of droplet coalescence and flocculation – in presence of either microgels or the constituting protein. We combine these experiments with surface pressure isotherms obtained in a Langmuir trough, which gives insights about interfacial behaviour of adsorbed microgel layers, and the surface coverage of microgels versus proteins. This approach enabled us to measure the influence of emulsion formulation on the stability of particle-stabilized emulsions; and is used here to characterize the emulsification potential of tannic acid-crosslinked WPI microgels. The developed methodology could be applied to other soft particles to expand the existing knowledge on particle stabilization, which represents an important advancement for the application of these systems in foodstuff production.

2 Materials and methods

2.1 Materials

Whey Protein Isolate (WPI), 97.0% - 98.4% purity (BiPro®, Davisco, Switzerland) and tannic acid (Sigma Aldrich, United States) were used as received. N-hexadecane (99%) (Alfa Aesar, Thermo Scientific, Germany) was used as model oil phase. Sodium phosphate dibasic, sodium phosphate monobasic, Nile blue A, and Nile Red were purchased from Sigma Aldrich (United States). Ultrapure water (18 MΩ) was obtained from a Milli-Q system (Millipore Corporation, Billerica, MA, United States) and was used to prepare all solutions and dilutions.

2.2 Production of WPI microgels

Tannic acid crosslinked WPI microgels were produced according to our previous work (do Prado Silva et al., 2021) with some modifications to further decrease particle size. Firstly, 40 g/L WPI aqueous solution was prepared under magnetic stirring for 2 h, followed by refrigerated incubation for at least 12 h to ensure complete protein hydration. Afterwards, tannic acid was added slowly to the continuously-stirred WPI solution at a molecular ratio of 1:2 (crosslinker:protein). Following crosslinker addition, the mixture had its pH adjusted to 5.8 using HCL solution (0.1 M) and was placed into a thermal bath at 80 °C for 15 min, to initiate microgel formation. The resulting microgel dispersion was rapidly cooled to room temperature using running tap water.
In order to remove residual WPI molecules that did not crosslink to form microgels, 100 grams of the microgel dispersion was washed repeatedly via ultrafiltration. We washed 7 times using an Amicon Stirred Cell (Merck Millipore, United States) with polyethersulfone membrane filter (0.03 µm, Sterlitech, United States), under an operating pressure of 3 bars and continuous stirring at 380 rpm. In each step, 50 grams of filtrate was removed, after which 50 grams of water was added to retain a constant mass of sample.

2.3 Particles size and zeta potential

Particle size distribution and zeta potential were measured through multi angle dynamic light scattering (MADLS) and electrophoretic light scattering, respectively, using the Zetasizer Ultra (Malvern Instruments, United Kingdom). Samples were diluted 100× in water and evaluated in triplicate at 25 °C, using 1.45 and 1.33 as refraction index for proteins and water, respectively.

2.4 Transmission Electron Microscopy (TEM)

For Transmission Electron Microscopy (TEM), the microgel dispersion was diluted 10× and deposited onto a freshly glow-discharged carbonized copper grid (200 mesh). Excess solvent was removed with standard filter paper and the microgels were stained with phosphotungstic acid solution. Images were taken with a JEM1011 transmission

electron microscopy (JEOL, Peabody, USA) operating at 80 kV in combination with a 2K x 2K SIS Veleta camera.

2.5 Surface tension of filtrates

The surface tension of filtrates (obtained after each washing step of the microgel dispersion, see section 2.4) was measured using an automated drop tensiometer (Tracker, Teclis, France). A pendant drop with a surface area of 20 mm² was formed at the tip of a needle, inside an empty glass cuvette. The pendant drop was monitored during 5,000 s (under volume conservation) and the surface tension over time was calculated by fitting the Young-Laplace equation to the extracted droplet shape. In an attempt to estimate the WPI content of the filtrates, reference curves of native WPI solutions with known concentrations were also recorded.

2.6 Behaviour of microgels and proteins under compression

Surface pressure versus area (π – A) isotherms were recorded using a Langmuir trough KN 2002 (KSV Nima, Biolin Scientific, Finland) with surface area of 364 x 76 mm. The trough was filled with water at room temperature, and $V_0 = 34$ µL of the filtered microgel dispersion was carefully spread on the surface using a Hamilton syringe, to deposit a known amount of microgels at the interface. The system was allowed to equilibrate for 30 minutes, and, afterwards, the barriers started compressing the interface at a constant rate of 5 mm/min to gradually increase the surface coverage (Γ, in mg/m^2). The surface pressure (π, in mN/m) was recorded by a force sensor attached to a platinum Wilhelmy-plate at a rate of one measurement per second. To account for the limited size of the trough and displacement of barriers, different concentrations of microgel dispersion ($c_0 = 1.67$, 2.5, 5, and 10 g/L) were evaluated in order to obtain a complete compression curve of surface pressure versus normalized area $A/(V_0 c_0)$ (m^2/mg protein), assuming that all spread proteins adsorbed to the interface. This set of curves shows good overlap for sections where the normalized area is the same, which confirms the reproducibility of the compression curves.

A second set of experiments was done to compare the surface pressure of microgels, native WPI, and a blend of them. Based on preliminary studies, we estimated the mass ratio needed to obtain roughly equal coverage of surface area by microgels and native

WPI to be 6:1 (microgels:WPI) in the blend. The measurement of surface pressure was performed in the same way as described above and the data were plotted in terms of surface pressure (π) as function of the total surface coverage (Γ). In addition, the dilatational modulus (ϵ) was calculated from the slope of π – A isotherms ($\in = -A\,\partial\pi/\partial A$) (Mahmoudi et al., 2010), and plotted as function of total surface coverage (Γ). To reduce small fluctuations, the slope was averaged over small intervals of 10 data points on the π – A isotherm.

2.7 Microscale evaluation of emulsions stabilized by WPI microgels

2.7.1 Microfluidics setup

Borosilicate glass microfluidic chips (Micronit Microtechnologies B.V., The Netherlands) composed of a T-junction, a meandering adsorption channel, and a collision channel were used to produce emulsions and evaluate their stability at the microscale (Figure 5.1). Droplets are formed in the T-junction (100 µm channel width), and then pass through the meandering channel (100 µm width) until they arrive at the collision channel (500 µm width, $L_{coal} = 30.0$ mm length) where droplets meet and may coalesce. All channels have a uniform depth of 45 µm. Two different lengths of meandering channel (9.6 mm and 25.6 mm) were used to study the effect of the adsorption time on emulsion stability (35 ms and 94 ms, respectively). Three inlets are available in the chips, however, for this study only two were used: one for the continuous phase and another one for the disperse phase. The third inlet is closed (indicated by the cross). One outlet is available at the end of the collision channel. Before use, the chips were cleaned by sonication (Branson ultrasonic bath, Hatch, United States) in four steps of 15 minutes each, using different cleaning solutions: ethanol, water, piranha solution (2 h), and water again; followed by a bake-out step in an oven at 550 °C for 2 h.

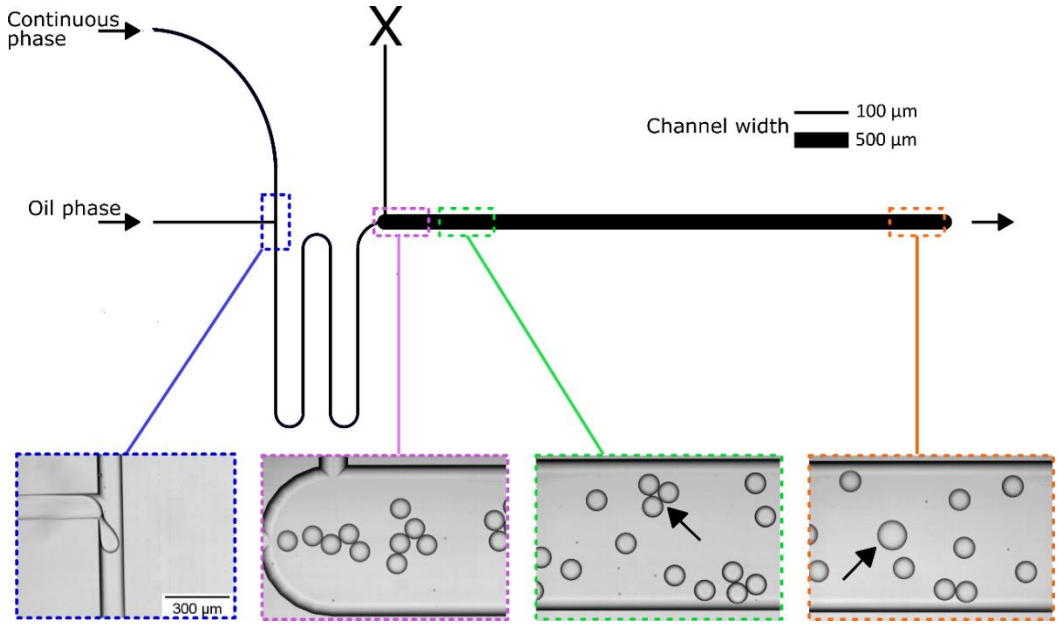

Figure 5.1 - Schematical representation of the microchip used, and snapshots that show droplet behaviour in the T-junction (blue box), and at three locations in the coalescence channel: the inlet frame is just after the meandering channel (purple box); the downstream frame is right after the inlet frame, at a position 1 mm from the inlet of the channel (green box); and the outlet frame is at the outlet of coalescence channel (orange box). Arrows point to examples of flocculated droplets (green box) and coalesced droplets (orange box). The scale bar refers to 300 µm (see blue box, applying to all frames). Channel dimensions in the sketch are not to scale.

The microfluidic chip was placed into a chip holder (Micronit Microtechnologies B.V., The Netherlands) and its inlet and outlet holes were connected to glass capillaries (ID 150, Polymicro Technologies). In this study, hexadecane was used as disperse phase, while the continuous phase was composed either of a microgel dispersion or native WPI solution, both prepared in various concentrations by dilution in phosphate buffer (pH 6.8). Flow rates of continuous (q_c = 70 µL/min) and disperse phase (q_d = 3 µL/min) were controlled using a pressure controller (OB1, Elveflow, France) and flow sensors (mini CORI-Flow, Bronkhorst B.V., The Netherlands). The chip was placed under an inverted light microscope (Axiovert 200 MAT, Carl Zeiss, The Netherlands) connected to a high-speed camera (MotionPro HS-4, IDT Inc., United States) recording images at 30 – 5000 Hz, and with a resolution of 1.57 µm/pixel. The passing of droplets through the coalescence channel, and their collective behaviour, was recorded at three

locations: at the inlet frame, the downstream frame (approximately 1 mm from the inlet of the collision channel) and the outlet frame of the channel (see figure 1).

2.7.2 Control of droplet collision conditions

To study the collective behaviour of droplets – either coalescence or flocculation – in a systematic way, their collision probability should be tightly controlled across all experiments (*i.e.* when varying the composition of the continuous phase or the length of meandering channel). We verify that the droplets are formed at the T-junction, and thus released into the collision channel, at a constant frequency $f_D = 349 \pm 25$ s^{-1}; and have a constant top-view diameter, $D =$ 70 ± 3 µm (standard deviation across conditions). Note that these droplets are only slightly squeezed between the walls of the 45 µm deep channels (with the diameter of the equivalent sphere being 63 µm). The droplets formed at the T-junction have high monodispersity with a typical coefficient of variation $CV\ (\%) = \left(\frac{\sigma}{D}\right) \times 100$ below 5% (σ: standard deviation of the droplet distribution). The mean droplet velocity (v_D) inside the collision channel was measured to be 0.022 ± 0.003 m s^{-1} across experiments, for a total flow rate of 73 µL/min. As a result, the droplets have a constant residence time $t_{res} = L_{coal}/v_{drop} = 1.19 \pm 0.14$ seconds in the collision channel. In conclusion, with constant flow rates, droplet size, release frequency and residence time, we take great care to keep the conditions for collision as similar as possible.

2.7.3 Coalescence analysis

The images obtained at the inlet (purple box in Figure 1) and outlet (orange box) of the collision channel were processed in Image J (NIH) software using a custom-written script (Muijlwijk et al., 2017). It measures the average two-dimensional (top-view) areas of the droplets at the inlet (A_i) and outlet (A_f). The arrow in the orange box (Figure 1) points at a coalesced droplet. The mean number of coalescence events was calculated as $N_{coal} = A_f/A_i - 1$. The mean coalescence frequency was calculated as $f_{coal} = N_{coal}/t_{res}$, with t_{res} the (constant) residence time in the coalescence channel, as discussed above.

2.7.4 Flocculation analysis

Images recorded at a position 1 mm downstream of the channel inlet (green box in Figure 1) were manually inspected for the presence of flocs (indicated by an arrow). A *floc* is defined as a cluster of droplets that stay together (see Movies S1 and S2) – in contrast to a *transient event* after which droplets (partially) split up (see Movies S3 and S4). It is important to note that the classification may depend on the time scale of observation: what is a floc at short time scales, can be a transient event at longer time scales. To study this we determine the size of flocs at two different time scales, namely after 3 and 35 ms. The typical number of droplets included in the analysis is 370 and 250 for these two recordings, respectively. The number of flocs of each size ($i = 1$, 2, 3, 4, 5 droplets etc.) is counted. Subsequently we calculate the probability distribution of a droplet being included in a floc of certain size i, and the average of this probability distribution, N_{floc}. (We find a small off-set < 0.3 due to random droplet collisions that are mis-identified as floc, especially for shorter analysis time scale).

3 Results and discussion

3.1 Properties of TA-WPI microgels

The microgel particles had a narrow size distribution (polydispersity index of 0.115 ± 0.004), mean hydrodynamic size of 90.4 ± 1.9 nm, and $D_{3,2}$ of 78.0 ± 2.3 nm. Their small size is attributed to the crosslinking effect of tannic acid. Phenolic hydroxyls of tannic acid interact with amides of WPI through hydrogen bonding, which increases the structural stability of WPI during heat treatment, preventing agglomeration and thus inducing the formation of small particles (do Prado Silva et al., 2021). The zeta potential of WPI microgels was -38.5 ± 1.3 mV indicating that a suspension with very high physical stability was obtained (Low et al., 2020). At pH above 5 (the isoelectric point of WPI), dissociation of $COOH^-$ groups is favoured, providing a negative net charge to the microgels (Wu et al., 2015).

The stability of the dispersion allows to wash out WPI from the microgels using 7 steps of ultrafiltration, without significantly changing the size distribution of the microgels (Figure 5.2A). TEM evaluation of these washed microgels showed that particles were

overall spherical, with some roughness on the surface, as can be seen in Figure 5.2B. In addition, their size distribution seems to be shifted to smaller microgel size than predicted by DLS analysis, as confirmed by Figure 5.A1 in the Appendix. Both observations can be attributed to the responsiveness of microgels to environmental conditions: in aqueous media (as is the case for DLS analysis), microgels are expected to be swollen, and thus likely retain their spherical shape. On the other hand, in the (partially) dried state (as is the case for samples prepared for TEM), water molecules have been expelled from the microgel network, giving rise to de-swollen particles.

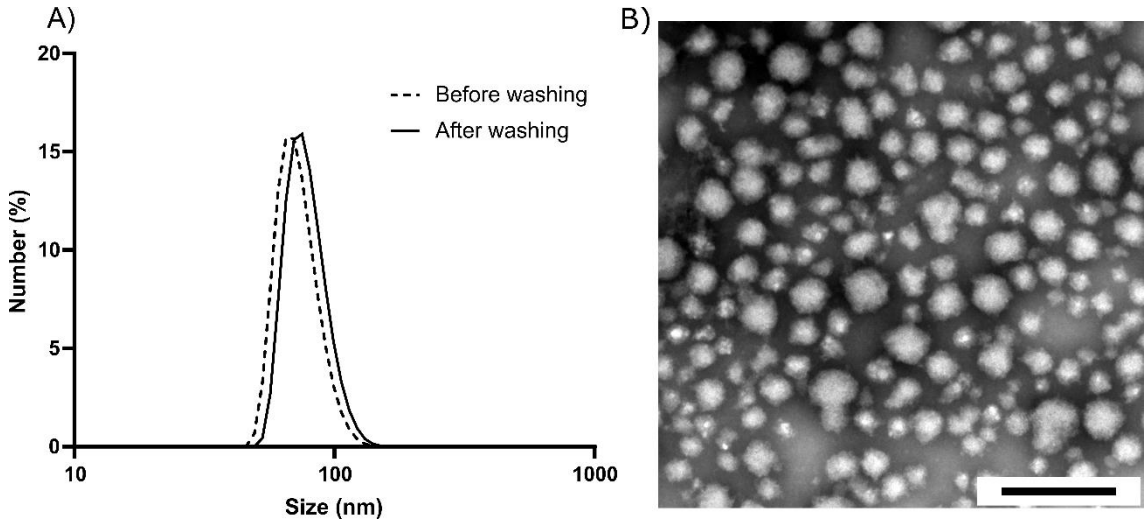

Figure 5.2 - Size distribution of microgels. (A) Comparison of size distribution (DLS) before and after the washing procedure. Curves are averages of triplicate measurements. (B) TEM image of washed microgels. Scale bar refers to 200 nm.

3.2 Composition of the (washed) microgel dispersion

The microgel dispersion was washed repeatedly to remove residual free whey proteins. The surface pressure of all seven filtrates was evaluated in a pendant drop tensiometer to evaluate the presence of surface-active molecules. Figure 5.3 shows that for increasing filtration step number, surface pressure increases more-and-more slowly, and reaches a lower quasi-equilibrium value. (Conformational changes of adsorbed proteins may induce a further small increase of surface pressure at longer time scales (Yang et al., 2020)). This indicates that the content of free surface-active molecules decreased at each filtration step; and demonstrated the efficacy of membrane ultrafiltration to purify the dispersion. Figure 5.3 also shows two reference

curves for ‘native’ WPI solutions with known concentrations. Assuming that the composition of residual protein in the dispersion (either before or after filtration) is similar to that of native WPI, it is possible to estimate that the content of free protein in the filtrates ranged from 15 g/L in the first step down to 0.1 g/L in the seventh step.

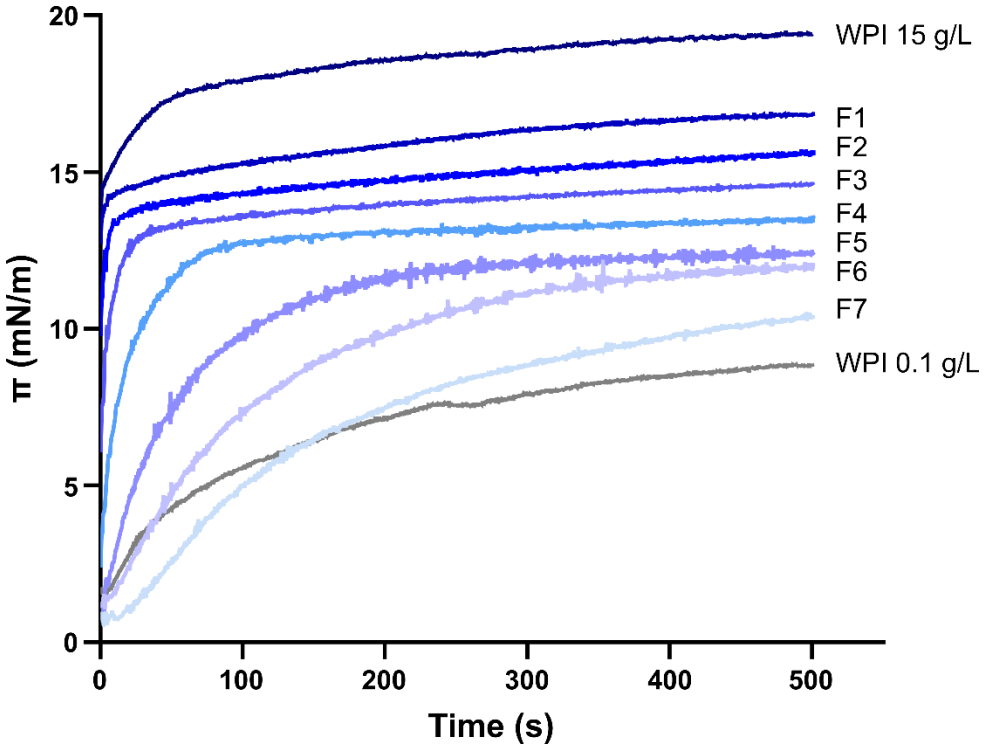

Figure 5.3 - Surface pressure curves of the seven filtrates (F1 – F7) obtained in the washing procedure of the microgel dispersion. Native WPI curves (15 g/L and 0.1 g/L) indicate the concentration range of free whey protein in the filtrates.

An extensive scan of surface pressure at intermediate WPI concentrations (0.1 – 15 g/L) was performed (data not shown). This enabled estimation of the amount of free protein in each filtrate by matching with respective WPI solution. Summation of the protein content of all filtrates yields the total amount removed from the microgel dispersion during the washing procedure, with an accuracy based on the matching with the WPI calibration series. The conversion factor of WPI into WPI microgels was estimated as (54 ± 9)% and (71 ± 6)% for samples used for analysis in the Langmuir trough and microfluidic investigation, respectively. This means that, in terms of microgel composition, each sample had 21 ± 4 g/L and 28 ± 2 g/L microgels, respectively. We also estimated the remaining amount of native WPI in each microgel dispersion after the washing procedure (based on the concentration in filtrate 7), which

was 0.5 ± 0.2 g/L and 0.1 ± 0.2 g/L, respectively. Despite the small differences between the results corresponding to the two prepared microgel dispersion batches, they are sufficiently similar to show the reproducibility of the microgel production and washing procedures.

3.3 Microgels behaviour under compression

A Langmuir trough was used to create a well-defined and well-controlled flat interface for microgels' compression. Since the general shape of compression curves obtained for microgel particles are very similar at the oil-water (O/W) and air-water interface (Picard et al., 2017; Pinaud et al., 2014), we chose to work at the air-water (A/W) interface in order to avoid the influence of possible impurities coming from the oil. The result is shown in Figure 5.4.

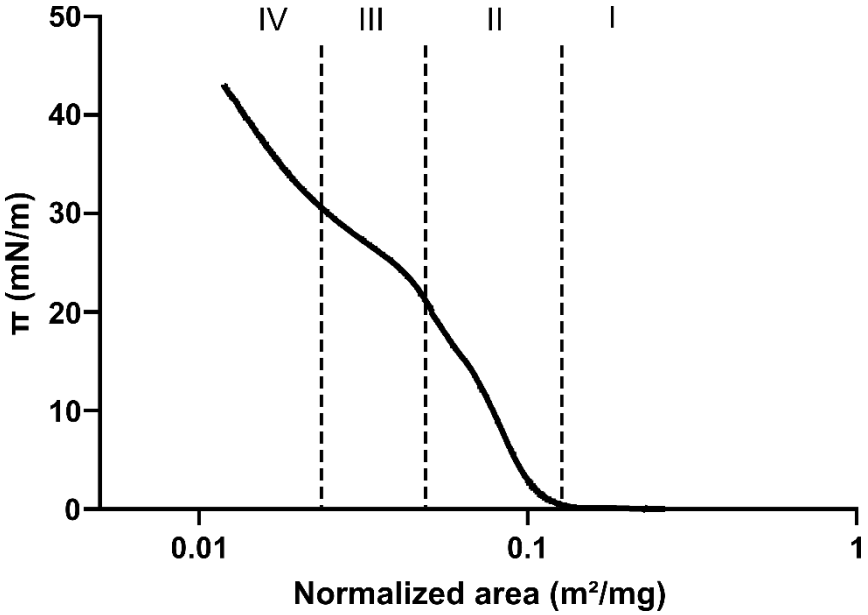

Figure 5.4 - Surface pressure isotherm of WPI microgels at the A/W interface. Dashed lines indicate transitions between regimes, based on the features in the curve as described by Pinaud et al. (2014).

The result in Figure 5.4 is similar as found for other soft microgels that have a core-shell structure. When at the interface, a balance between surface activity (driving chain spreading) and microgel internal elasticity drives a conformational change such that microgels lose their sphericity. The microgels assume a "fried egg-like" structure, in

which the less deformable core remains like a bump, yet the shells flatten out (Destribats et al., 2011). These microgel monolayers are highly compressible to an extend that depends, again, on the internal elasticity and adsorption strength of the particles (Bushuev et al., 2020), as was reported for soft model poly(N-isopropylacrylamide) microgels (Picard et al., 2017; Pinaud et al., 2014). Figure 4 can accordingly be divided into 4 different regimes. (I) Microgels are in their flattened state at the interface and sufficiently far away from each other to not experience inter-particle interactions. Here, the surface pressure is null. (II) Microgels start to interact when the inter-particle distance is of the order of the flattened microgel size, and it is then energetically more favourable for them to stretch less (Deshmukh et al., 2015), until they reach their non-deformed size. Here, the surface pressure increases at a high rate due to shell interpenetration. (III) Most of microgels are highly compressed and now the deformation occurs perpendicularly to the interface, leading to slower increase in surface pressure. (IV) Microgels are in fully-contracted state and, rather than compressing and dehydrating, it is more energetically favourable that microgels either desorb into the subphase or form multilayers, leading to steeper increase in surface pressure, similar to solid particles.

If indeed the dangling chains of core-shell microgels determine the (initial) increase of surface pressure, we may expect similarities in the isotherms of microgels and native proteins – albeit at higher total surface coverage for microgels. To study this, we compare (π – Γ) surface pressure isotherms of microgels, native WPI and a blend of microgels and native protein, as shown in Figure 5.5.

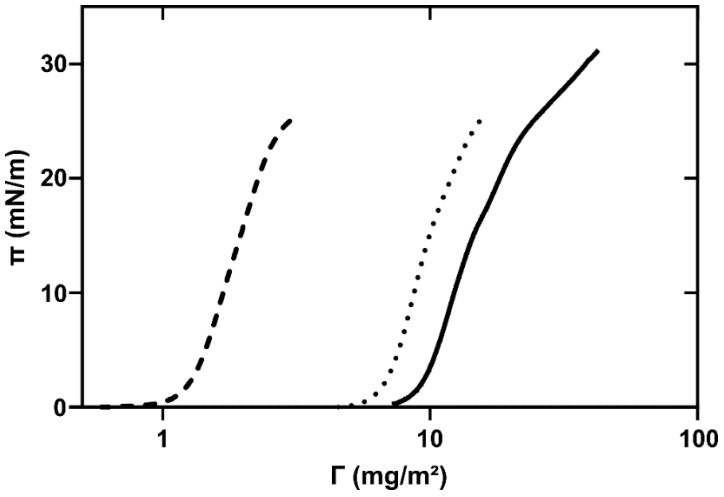

Figure 5.5 - Surface pressure isotherms of native WPI (– –), WPI microgels (——), and a blend of 6:1 (microgels:WPI) mass ratio (· - -).

Indeed, a similar increase in surface pressure is obtained albeit at roughly 10-fold higher surface coverage for microgels compared to native WPI. This effect cannot be attributed to residual WPI in the microgel dispersion after washing as its concentration (calculated to be 0.07 g/L) is too low to promote such effect.

To closer compare the compression behaviour, the dilatational modulus (ϵ) was calculated from the isotherm and plotted as function of surface pressure (π), or the corresponding surface coverage (Γ), as done in Figure 5.6A and B respectively. Each (local) maximum in dilatational modulus marks the onset of a conformational change in the monolayer. Particularly, the first peak is associated with the collapse of hydrophilic parts of the molecules, forming loops and tails into the subphase (Cicuta and Hopkins, 2001; Graham and Phillips, 1979).

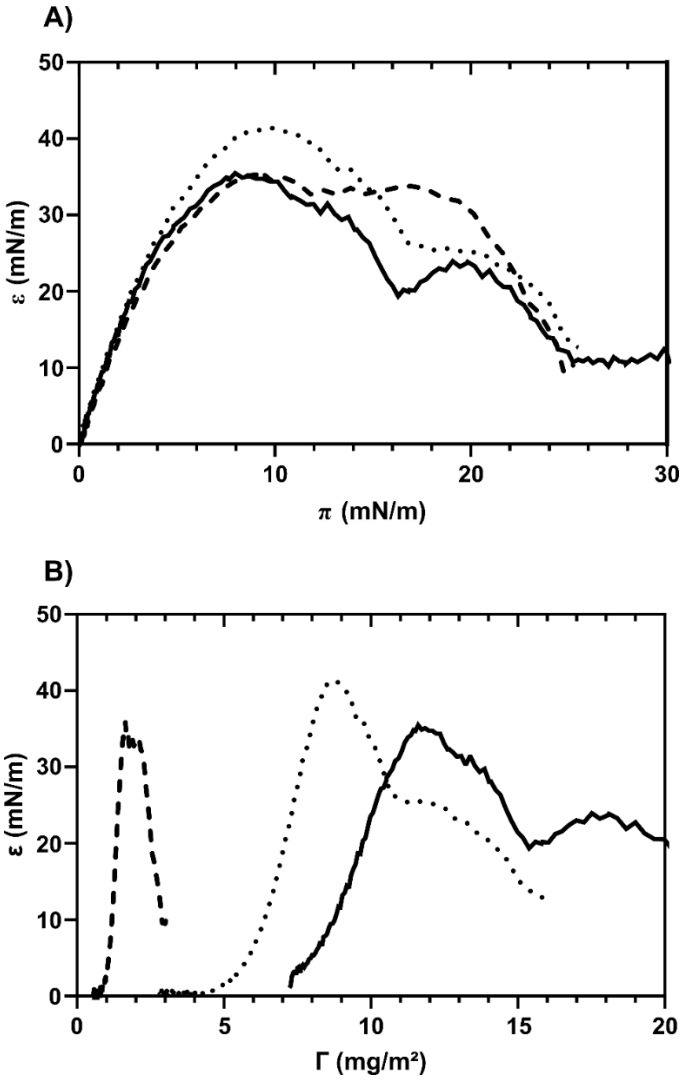

Figure 5.6 - Dilatational modulus as function of (A) surface pressure and (B) total surface coverage of native WPI (– –), WPI microgels (——), and a blend formed at 6:1 (microgels:WPI) mass ratio (· - ·).

For all samples tested, the dilatational modulus has an absolute maximum at relatively low π; followed by a second local maximum or shoulder at higher π. The maximum dilatational modulus is ϵ* ~ 36 mN/m for either native WPI or WPI microgels; and ϵ* ~ 42 mN/m for the blend. The latter seems to be systematically larger, based on blends with other mass ratios that we investigated. The maximum dilatational modulus is obtained at similar surface pressures for all samples, π* ~ 9 – 10 mN/m, and the overlap of curves shows that interfacial elasticity initially increases very similarly for all samples (Figure 5.6A). When comparing based on corresponding surface coverage at which the maximum elasticity is obtained (Figure 5.6B), Γ* at the first maximum increases from 1.6 mg/m² for native WPI, to Γ* = 8.8 mg/m² for the blend, and Γ* = 11.6 mg/m² for the microgels. This implies 7.3 times the surface coverage of the native WPI for the microgels (and 5.5 times for the blend), to obtain a similar increase in elasticity (and pressure) up to the first maximum in ϵ (see Figure 5.A2). This may be determined by three main effects. (1) Microgels have a thick core that adds a substantial amount of material, as illustrated in Figure 5.7. Fully swollen microgels are 78 nm, and a corresponding interfacial layer would be in the order of 50 mg/m^2 when considering close packing at the interface, indicating that the cores are indeed flattened. They are expected to remain flattened for coverages below Γ*, so regimes I – II (Figure 5.4). (2) The dangling chains of WPI microgels have been denatured, giving rise to molecules that may spread more (Murray, 2019; Picard et al., 2017), but have fewer hydrophilic parts to collapse at the subphase comparing to the native WPI. And (3) the dangling chains have limited movement since they are attached to the core of the microgel. The blend provides an intermediate case in which surface behaviour involves both native proteins and the dangling chains from the microgels.

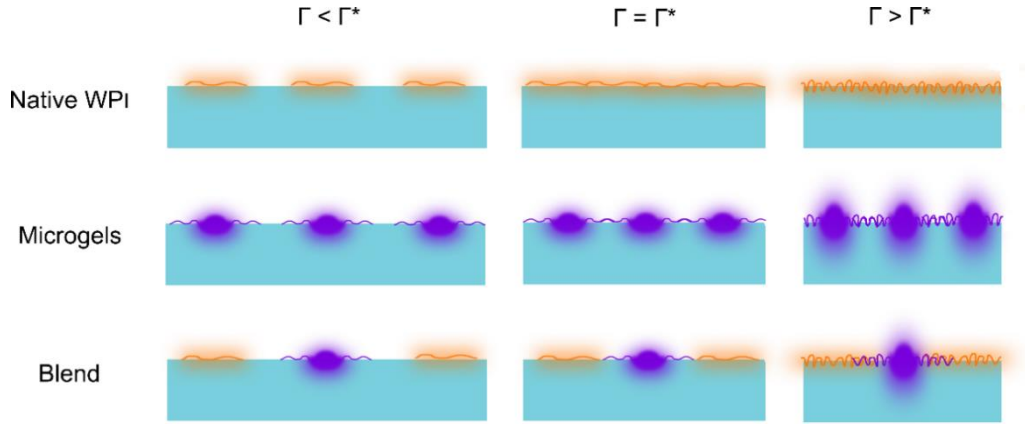

Figure 5.7 - Schematic representation of the structures at the A/W interface for different surface coverage: native WPI, microgels, and blend of microgels and WPI

(6:1 mass ratio). At Γ* loops start to form, whereas for Γ > Γ* the microgels start to compress.

A second local maximum or shoulder was observed for each sample on the dilatational modulus curves, corresponding to ϵ-values of ~ 34 mN/m; ~ 29 mN/m and ~ 24 mN/m for native WPI, blend and microgels, respectively. The presence of a second local maximum has been related to changes in the surface conformation of protein molecules due to interactions between opposite local charges. The magnitude of this second peak was shown to be function of pH and ionic strength both for β-casein monolayers (Cicuta et al., 2001; Cicuta and Hopkins, 2001) and for WPI self-assemblies (Mahmoudi et al., 2010). For the microgels, not only the value of the second maximum is decreased, but we also observe a stronger decrease of dilatational modulus after the first maximum – leading to more pronounced peaks. This may be related to enhanced entanglement and eventually, compression of the microgel core (Figure 5.7). The blend shows mixed behaviour with a second shoulder rather than a maximum.

Even though we use a flat A/W interface with pre-adsorbed layer, similar conformational changes will be expected upon adsorption to the O/W interfaces in emulsions (Zembyla et al., 2019). Thus in our microfluidic emulsification experiments in which dynamic adsorption plays a role, we use the compression isotherms as calibration for the surface coverage (similar to e.g. Deshmukh (2014): we assume that Γ* = 11.6 mg/m² of microgels is equivalent to Γ* = 1.6 mg/m² of native proteins (Figure 5.6), which is roughly the amount needed to obtain monolayer coverage (Tcholakova et al., 2002)).

3.4 Microfluidic investigation of emulsions stabilized by WPI microgels

3.4.1 Coalescence stability inside microfluidic chips

We investigated the effect of microgel concentration in the continuous phase on the stability of emulsion droplets against coalescence and compare this with emulsions stabilized by different concentrations of native WPI. With a 94 ms adsorption time in our microfluidic device, stable emulsions ($f_{coal} < 0.002$) were obtained above the following critical protein concentrations: 0.2 g/L when native WPI solution was used as

continuous phase and 0.9 g/L when the microgel dispersion was used. The microgel dispersion can thus be used to stabilize an emulsion. The higher mass of WPI microgels necessary to produce stable emulsions was expected, since they form thicker layers than the (much smaller) native WPI molecules and thus, a higher interfacial amount is needed to obtain similar surface pressure and elasticity, as demonstrated in the Langmuir trough compression experiments. Hence, to compare stabilization by either microgels or native WPI we introduced the nondimensional parameter $F^* = \left(C_{cp}/A_T\right)/\Gamma^*$. F^* is the ratio between maximum surface coverage after adsorption of all available emulsifier from the continuous phase (C_{cp}/A_T), and the surface coverage Γ^* (at peak elastic modulus). Here, C_{cp} is the continuous phase concentration and $A_T = 4.1$ m^2/L is the total interfacial area per volume of continuous phase that needs to be stabilized.

Figure 5.8 shows the mean coalescence frequency of droplets as function of F^* for each continuous phase, containing microgels or native proteins.

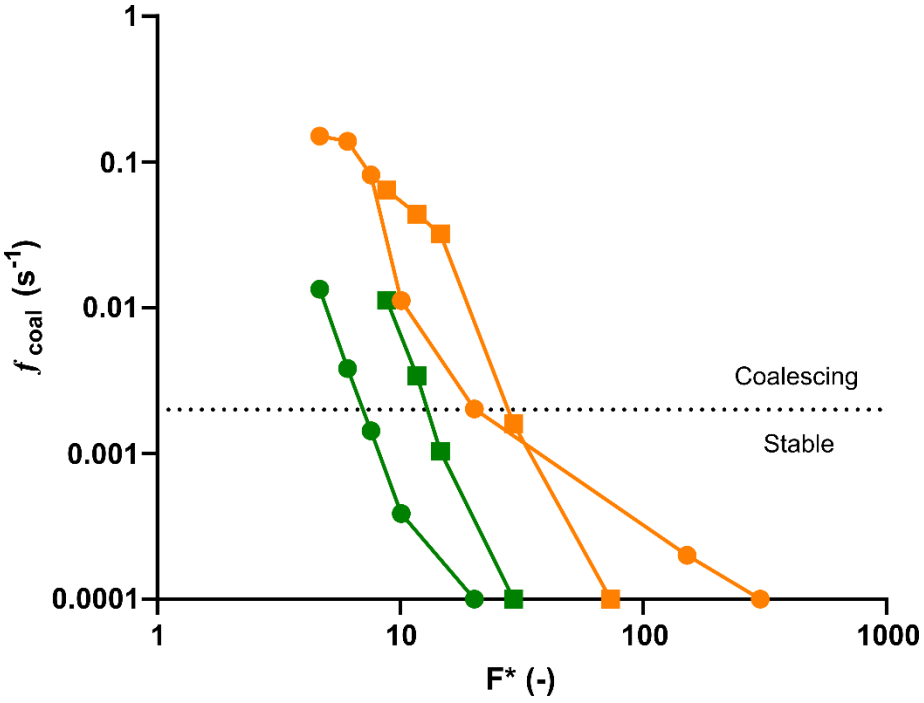

Figure 5.8 - Mean coalescence frequency as function of F^*. Data are shown for droplets stabilised by microgels (●) and native WPI (■) at adsorption times of 94 ms (green curves) and 35 ms (orange curves). Coalescence frequencies below 0.0001 s^{-1} are insignificant and have been collapsed at the baseline of the graph.

A surplus of proteins or microgels ($F^* > 10$) is needed to stabilize the emulsion droplets as not all available material will be adsorbed to the interface, or even reach it. As expected, coalescence frequency increases with decreasing amount of emulsifier (decreasing F^*) because droplets that are poorly covered, collide and merge until they achieve a fully stabilized interface.

The adsorption time (35 or 94 ms) that is imposed between droplet formation and droplet-droplet interactions (see Figure 5.1) also played an important role in droplet stability. Under otherwise identical conditions, the coalescence frequency is higher for shorter adsorption time (see Figure 5.8), which is in agreement with previous studies with native food proteins (Hinderink et al., 2019; Muijlwijk et al., 2017). For small proteins, the transport mechanism is typically convective in this type of microfluidic channels (Muijlwijk et al., 2016) and protein adsorption is likely kinetically-limited. A longer adsorption time then allows a higher amount of protein to be adsorbed to the interface (for sub-monolayer coverage). Surprisingly, adsorption time shows a very similar effect on the stability of microgel-stabilized emulsions. This again confirms that the microgels are not behaving as classical (rigid) Pickering particles, which have a high adsorption barrier (Berton-Carabin and Schroën, 2015; Tcholakova et al., 2008) and are thus expected to preferentially adsorb under the high-shear conditions at the formation junction; in that case, they would be expected to show a (much) weaker dependency on adsorption length and to present improved emulsion stability only upon increasing the continuous phase flow rate. The fact that, in reality, microgels show increased emulsion stability when they are allowed a longer adsorption time shows that further adsorption takes place in the channel. This can be explained by the surface activity of the polymeric shell, which facilitates spontaneous adsorption. For soft microgels, increasing adsorption time then allows for a higher adsorbed amount. In addition the relaxation of microgels at the interface takes a finite time (Destribats et al., 2013), in such way that longer adsorption times may also allow for further spreading of the polymeric shell. and possibly these microgels also spread further.

Finally, we compare the stabilization by microgels versus native proteins. Microgel-stabilized emulsions are stable down to slightly lower values of F^*. As the parameter F^* captures equivalent surface layer properties (in terms of pressure and dilatational modulus), this difference points to kinetic differences between the systems, either the approach of the stabilizer to the interface, or very soon after that. Several factors may play a role: adsorption speed, necessary adsorption events, and the role of the

adsorbed layer in dynamic collision events. In spite of the high surface activity of their dangling chains, the adsorption of microgels is likely slower due to their increased size that limits their diffusion, but once adsorbed, each microgel contributes a high amount of mass since they are almost 20 times larger than β-lactoglobulin, the major constituent of WPI (Nicolai et al., 2011). Finally, we postulate that the thick microgel cores provide steric hindrance, which suppresses coalescence in favour of the occurrence of bridging flocculation.

3.4.2 Flocculation analysis

In the downstream frame of the coalescence channel, we observed that droplets stabilized by microgels form clusters of various sizes (Figure 9B); a phenomenon known as flocculation. The average floc size of each emulsion as function of F^* and adsorption time is presented in Figure 9A.

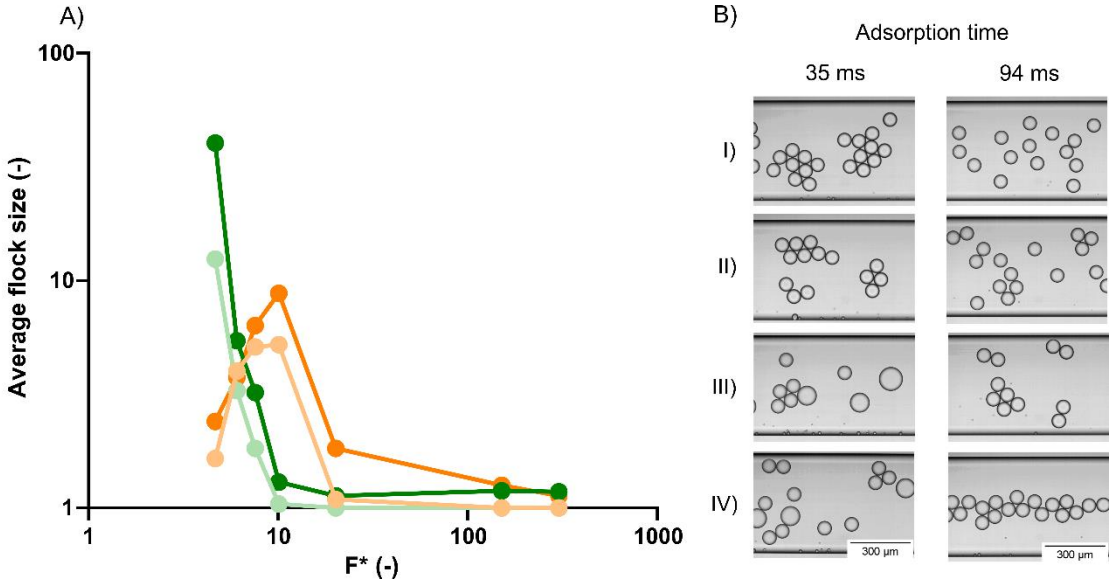

Figure 5.9 - Flocculation of microgel-stabilized emulsion droplets. (A) Average floc size as function of F^*. Analysis was carried out at two different timescales: 3 ms (dark colour) and 35 ms (light colour), at adsorption times of 35 ms (orange curve) and 94 ms (green curve). B) Representative microscopic images of the downstream frame (green box in Figure 1), for both adsorption times (35 and 94 ms) at decreasing F^*: 10.1 (I); 7.6 (II); 6.1 (III) and 4.7 (IV). Scale bars refer to 300 µm.

Figure 5.9A shows that, for both adsorption times (35 and 94 ms), the average floc size (initially) increases when decreasing F^*. As flocculation is induced in the microgel-poor regime (and is absent for native protein-stabilized droplets), the mechanism by which these clusters are formed is bridging flocculation: at low surface coverage, colliding droplets may share one or more adsorbed particle(s) that are partially wetted by each droplet, but still maintain an intervening film of bulk continuous phase. Several mechanisms act to maintain the colloidal stability, preventing the displacement of particles away from or within the bridging layer, namely the adhesion energy of the individual particles, the steric hindrance restricting lateral particle movement, and the capillary pressure within the thin intervening liquid film (Dickinson, 2017).

Adsorption time plays a role in the extent of flocculation. For emulsions with shorter (35 ms) adsorption time, the surface coverage is lower under otherwise identical conditions of bulk concentration (due to the lower amount of adsorption and possibly limited spreading of microgels at the interface). Thus, flocculation is initiated at higher microgel bulk concentrations. In this case we also observe that at low $F^* \sim$ 7.6 flocculation decreases again, which is caused by initiation of coalescence due to low surface coverage, as shown in Figure 5.9B (III & IV, $F^* < 6.1$) and, previously, in Figure 5.8. Indeed, for the longer adsorption time of 94 ms, coalescence is only initiated at the lowest tested concentration (see Figure 5.8), and thus a decrease in flocculation has not been observed.

It should be noted that all flocs are transient in our experiments, and in time they separate (or coalesce). At longer observation time (35 ms), the average floc size is smaller than at shorter observation time (3 ms) for all concentrations and adsorption times (see the light lines in Figure 5.9A); and at the end of the channel all flocs have been split up. This transient behaviour may be explained by flow-induced rupture of flocs; or the gradual flattening of microgels at the interface that enables more completely coverage, and the consequent rupture of flocs. Droplets in a floc that have low surface coverage may instead coalesce. Figure 5.9B shows examples of droplet pairs having coalesced, but also supressed coalescence of droplets that are present within a (larger) floc. Moreover, when observing the image sequences, we noticed that coalesced droplets occasionally were able to detach themselves from a floc (Movie S5). This is probably because upon coalescence the total interfacial area suddenly decreases, leading to higher surface coverage and energy release in the form of kinetic

energy. At that point, the large floc is separated into several smaller flocs, which reduces the average floc size.

4 Conclusion

Tannic acid-crosslinked whey protein microgels were successfully produced and purified, showing no disintegration after 7 washing steps. The implemented ultrafiltration procedure was able to remove at least 97% of non-reacted protein. These microgels flatten out when adsorbed in low concentrations to an A/W interface. Upon compression of the interface, the flattened microgels are squeezed laterally until they cannot deform further. When comparing the surface pressure and dilatational modulus of interfacial layers formed by microgels with native WPI, it is possible to conclude the native WPI and the microgels have similar effects on surface pressure at low surface concentrations. This is probably due to the dangling chains of the microgel that are available to stretch out and provide chain interactions. The onset of conformational changes in the monolayer (at peak elastic modulus) takes place at a higher surface coverage for the microgels ($\Gamma^* = 11.6$ mg/m²) than for native WPI ($\Gamma^* = 1.6$ mg/m²). The thick cores of the microgels add a significant amount of material to the surface coverage.

Through microfluidic investigation it was possible to achieve comprehensive insights in droplet-droplet interactions, including the transient bridging of droplets and their subsequent separation or coalescence. The adsorption time had an important role on the stability of the droplets, not only for native proteins but also for microgels. Longer adsorption times allow a higher adsorbed amount (due to the surface activity of the dangling chains and possibly spreading of the gel particle). Compared to emulsions stabilized by native WPI, within a certain window of operation, emulsions stabilized by soft microgels showed an improved stability against coalescence as droplets experience transient bridging flocculation instead of coalescence. As flocs do not reform after separation it is likely that microgels have flattened at the O/W interface to complete surface coverage, thus leading to no flocs present after 1.4 seconds of travel time. Thus, transient flocculation allows droplets to stabilize in time, and keeps them from coalescing immediately as would happen in absence of microgels that provide bridging. It would be interesting to perform microfluidic emulsification tests with blends

of varying ratio of microgels to native WPI, to study competitive adsorption effects and resulting emulsion stability.

Acknowledgements

The authors would like to thank Anja van Osch-Schröder for Transmission Electron Microscopy analysis.

Funding source

This work was supported by Coordenação de Aperfeiçoamento de Pessoal de Nível Superior – CAPES (finance code 001) through the Program CAPES-PrInt-Unesp, process number 88887.194785/2018-00, Mobility number 88887.374187/2019-00.

References

Albert, C., Beladjine, M., Tsapis, N., Fattal, E., Agnely, F., Huang, N., 2019. Pickering emulsions: Preparation processes, key parameters governing their properties and potential for pharmaceutical applications. J. Control. Release 309, 302–332. https://doi.org/10.1016/j.jconrel.2019.07.003

Anjali, T.G., Basavaraj, M.G., 2018. Influence of pH and Salt Concentration on Pickering Emulsions Stabilized by Colloidal Peanuts. Langmuir 34, 13312–13321. https://doi.org/10.1021/acs.langmuir.8b02913

Benetti, J.V.M., Silva, J.T. do P., Nicoletti, V.R., 2019. SPI microgels applied to Pickering stabilization of O/W emulsions by ultrasound and high-pressure homogenization: rheology and spray drying. Food Res. Int. 122, 383–391. https://doi.org/10.1016/j.foodres.2019.04.020

Berton-Carabin, C.C., Schroën, K., 2015. Pickering Emulsions for Food Applications: Background, Trends, and Challenges. Annu. Rev. Food Sci. Technol. 6, 263–297. https://doi.org/10.1146/annurev-food-081114-110822

Binks, B.. P., Lumsdon, S.O., 2000. Influence of Particle Wettability on the Type and Stability of Surfactant-Free Emulsions. Langmuir 16, 8622–8631.

Bushuev, N. V., Gumerov, R.A., Bochenek, S., Pich, A., Richtering, W., Potemkin, I.I., 2020. Compression and Ordering of Microgels in Monolayers Formed at Liquid-Liquid Interfaces: Computer Simulation Studies. ACS Appl. Mater. Interfaces 12, 19903–19915. https://doi.org/10.1021/acsami.0c01600

Cicuta, P., Hopkins, I., 2001. Studies of a weak polyampholyte at the air-buffer interface: The effect of varying pH and ionic strength. J. Chem. Phys. 114, 8659–8670. https://doi.org/10.1063/1.1365401

Cicuta, P., Hopkinson, I., Petrov, P.G., 2001. Photocontrol of protein conformation in a Langmuir monolayer. J. Chem. Phys. 115, 9991–9994. https://doi.org/10.1063/1.1423666

De Folter, J.W.J., Hutter, E.M., Castillo, S.I.R., Klop, K.E., Philipse, A.P., Kegel, W.K., 2014. Particle shape anisotropy in pickering emulsions: Cubes and peanuts. Langmuir 30, 955–964. https://doi.org/10.1021/la402427q

Deshmukh, O.S., Ende, D. van den, Stuart, M.C., Mugele, F., Duits, M.H.G., 2015.

Hard and soft colloids at fluid interfaces: Adsorption, interactions, assembly & rheology. Adv. Colloid Interface Sci. 222, 215–227.

Deshmukh, O.S., Maestro, A., Duits, M.H.G., Van Den Ende, D., Stuart, M.C., Mugele, F., 2014. Equation of state and adsorption dynamics of soft microgel particles at an air-water interface. Soft Matter 10, 7045–7050. https://doi.org/10.1039/c4sm00566j

Destribats, M., Lapeyre, V., Wolfs, M., Sellier, E., Leal-Calderon, F., Ravaine, V., Schmitt, V., 2011. Soft microgels as Pickering emulsion stabilisers: Role of particle deformability. Soft Matter 7, 7689–7698. https://doi.org/10.1039/c1sm05240c

Destribats, M., Rouvet, M., Gehin-Delval, C., Schmitt, C., Binks, B.P., 2014. Emulsions stabilised by whey protein microgel particles: Towards food-grade Pickering emulsions. Soft Matter 10, 6941–6954. https://doi.org/10.1039/c4sm00179f

Destribats, M., Wolfs, M., Pinaud, F., Lapeyre, V., Sellier, E., Schmitt, V., Ravaine, V., 2013. Pickering emulsions stabilized by soft microgels: Influence of the emulsification process on particle interfacial organization and emulsion properties. Langmuir 29, 12367–12374. https://doi.org/10.1021/la402921b

Dickinson, E., 2017. Biopolymer-based particles as stabilizing agents for emulsions and foams. Food Hydrocoll. 68, 219–231. https://doi.org/10.1016/j.foodhyd.2016.06.024

do Prado Silva, J.T., Benetti, J.V.M., Alexandrino, T.T. de B., Assis, O.B.G., de Ruiter, J., Schroën, K., Nicoletti, V.R., 2021. Whey Protein Isolate Microgel Properties Tuned by Crosslinking with Organic Acids to Achieve Stabilization of Pickering Emulsions. Foods 10, 1296. https://doi.org/10.3390/foods10061296

Fernandez-Rodriguez, M.A., Martín-Molina, A., Maldonado-Valderrama, J., 2021. Microgels at interfaces, from mickering emulsions to flat interfaces and back. Adv. Colloid Interface Sci. 288, 102350. https://doi.org/10.1016/j.cis.2020.102350

Graham, D.., Phillips, M.., 1979. Proteins at liquid interfaces. J. Colloid Interface Sci. 70, 427–439. https://doi.org/10.1016/0021-9797(79)90050-x

Hinderink, E.B.A., Kaade, W., Sagis, L., Schroën, K., Berton-Carabin, C.C., 2020. Microfluidic investigation of the coalescence susceptibility of pea protein-stabilised emulsions: Effect of protein oxidation level. Food Hydrocoll. 102, 105610. https://doi.org/10.1016/j.foodhyd.2019.105610

Hinderink, E.B.A., Münch, K., Sagis, L., Schroën, K., Berton-Carabin, C.C., 2019. Synergistic stabilisation of emulsions by blends of dairy and soluble pea proteins: Contribution of the interfacial composition. Food Hydrocoll. 97, 105206. https://doi.org/10.1016/j.foodhyd.2019.105206

Hu, Z., Ballinger, S., Pelton, R., Cranston, E.D., 2015. Surfactant-enhanced cellulose nanocrystal Pickering emulsions. J. Colloid Interface Sci. 439, 139–148. https://doi.org/10.1016/j.jcis.2014.10.034

Jin, W., Zhu, J., Jiang, Y., Shao, P., Li, B., Huang, Q., 2017. Gelatin-Based Nanocomplex-Stabilized Pickering Emulsions: Regulating Droplet Size and Wettability through Assembly with Glucomannan. J. Agric. Food Chem. 65, 1401–1409. https://doi.org/10.1021/acs.jafc.6b04146

Krebs, T., Schroen, K., Boom, R., 2012a. A microfluidic method to study demulsification kinetics. Lab Chip 12, 1060–1070. https://doi.org/10.1039/c2lc20930f

Krebs, T., Schroën, K., Boom, R., 2012b. Coalescence dynamics of surfactant-stabilized emulsions studied with microfluidics. Soft Matter 8, 10650–10657. https://doi.org/10.1039/c2sm26122g

Leon, A.M., Medina, W.T., Park, D.J., Aguilera, J.M., 2018. Properties of microparticles

from a whey protein isolate/alginate emulsion gel. Food Sci. Technol. Int. 24, 414–423. https://doi.org/10.1177/1082013218762210

Linke, C., Drusch, S., 2018. Pickering emulsions in foods - opportunities and limitations. Crit. Rev. Food Sci. Nutr. 58, 1971–1985. https://doi.org/10.1080/10408398.2017.1290578

Low, L.E., Siva, S.P., Ho, Y.K., Chan, E.S., Tey, B.T., 2020. Recent advances of characterization techniques for the formation, physical properties and stability of Pickering emulsion. Adv. Colloid Interface Sci. 277, 102117. https://doi.org/10.1016/j.cis.2020.102117

Mahmoudi, N., Gaillard, C., Boué, F., Axelos, M.A.V., Riaublanc, A., 2010. Self-similar assemblies of globular whey proteins at the air-water interface: Effect of the structure. J. Colloid Interface Sci. 345, 54–63. https://doi.org/10.1016/j.jcis.2010.01.036

Muijlwijk, K., Colijn, I., Harsono, H., Krebs, T., Berton-Carabin, C., Schroën, K., 2017. Coalescence of protein-stabilised emulsions studied with microfluidics. Food Hydrocoll. 70, 96–104. https://doi.org/10.1016/j.foodhyd.2017.03.031

Muijlwijk, K., Huang, W., Vuist, J.E., Berton-Carabin, C., Schroën, K., 2016. Convective mass transport dominates surfactant adsorption in a microfluidic Y-junction. Soft Matter 12, 9025–9029. https://doi.org/10.1039/c6sm01677d

Murray, B.S., 2019. Microgels at fluid-fluid interfaces for food and drinks. Adv. Colloid Interface Sci. 271, 1–7. https://doi.org/10.1016/j.cis.2019.101990

Murray, B.S., Phisarnchananan, N., 2016. Whey protein microgel particles as stabilizers of waxy corn starch + locust bean gum water-in-water emulsions. Food Hydrocoll. 56, 161–169. https://doi.org/10.1016/j.foodhyd.2015.11.032

Nicolai, T., Britten, M., Schmitt, C., 2011. β-Lactoglobulin and WPI aggregates: Formation, structure and applications. Food Hydrocoll. 25, 1945–1962. https://doi.org/10.1016/j.foodhyd.2011.02.006

Niroula, A., Gamot, T.D., Ooi, C.W., Dhital, S., 2021. Biomolecule-based pickering food emulsions: Intrinsic components of food matrix, recent trends and prospects. Food Hydrocoll. 112, 106303. https://doi.org/10.1016/j.foodhyd.2020.106303

Picard, C., Garrigue, P., Tatry, M.C., Lapeyre, V., Ravaine, S., Schmitt, V., Ravaine, V., 2017. Organization of Microgels at the Air-Water Interface under Compression: Role of Electrostatics and Cross-Linking Density. Langmuir 33, 7968–7981. https://doi.org/10.1021/acs.langmuir.7b01538

Pickering, S.U., 1907. Emulsions. J. Chem. Soc. 91, 2001–2021.

Pinaud, F., Geisel, K., Massé, P., Catargi, B., Isa, L., Richtering, W., Ravaine, V., Schmitt, V., 2014. Adsorption of microgels at an oil-water interface: Correlation between packing and 2D elasticity. Soft Matter 10, 6963–6974. https://doi.org/10.1039/c4sm00562g

Ribeiro, E.F., de Barros Alexandrino, T.T., Assis, O.B.G., Junior, A.C., Quiles, A., Hernando, I., Nicoletti, V.R., 2020. Chitosan and crosslinked chitosan nanoparticles: synthesis, characterization and their role as Pickering emulsifiers. Carbohydr. Polym. 250, 116878. https://doi.org/10.1016/j.carbpol.2020.116878

Schröder, A., Sprakel, J., Schroën, K., Spaen, J.N., Berton-Carabin, C.C., 2018. Coalescence stability of Pickering emulsions produced with lipid particles: A microfluidic study. J. Food Eng. 234, 63–72. https://doi.org/10.1016/j.jfoodeng.2018.04.007

Sjöö, M., Emek, S.C., Hall, T., Rayner, M., Wahlgren, M., 2015. Barrier properties of heat treated starch Pickering emulsions. J. Colloid Interface Sci. 450, 182–188. https://doi.org/10.1016/j.jcis.2015.03.004

Stancanelli, R., Løjkner, L.D., Larsen, K.L., Guardo, M., Cannavà, C., Tommasini, S., Ventura, C.A., Calabrò, M.L., Micali, N., Villari, V., Mazzaglia, A., 2012. Structural and spectroscopic features of lutein/butanoyl-β-cyclodextrin nanoassemblies. J. Pharm. Biomed. Anal. 71, 214–218. https://doi.org/10.1016/j.jpba.2012.07.034

Tatry, M.C., Laurichesse, E., Perro, A., Ravaine, V., Schmitt, V., 2019. Kinetics of spontaneous microgels adsorption and stabilization of emulsions produced using microfluidics. J. Colloid Interface Sci. 548, 1–11.

Tcholakova, S., Denkov, N.D., Ivanov, I.B., Campbell, B., 2002. Coalescence in β-lactoglobulin-stabilized emulsions: Effects of protein adsorption and drop size. Langmuir 18, 8960–8971. https://doi.org/10.1021/la0258188

Tcholakova, S., Denkov, N.D., Lips, A., 2008. Comparison of solid particles, globular proteins and surfactants as emulsifiers. Phys. Chem. Chem. Phys. 10, 1608. https://doi.org/10.1039/b715933c

Wang, F., Yin, Y., Chen, B., Cuan, S., Wang, Z., Wang, A., Li, G., Shi, H., 2021. Pickering medium internal phase emulsions based on natural clay particles: Route to a macroporous adsorbent. J. Mol. Liq. 322, 114995. https://doi.org/10.1016/j.molliq.2020.114995

Whitby, C.P., Scarborough, H., Ngothai, Y., 2017. Drying oil-in-water Pickering emulsions to make redispersible powders. Adv. Powder Technol. 28, 2940–2946. https://doi.org/10.1016/j.apt.2017.09.001

Wu, J., Shi, M., Li, W., Zhao, L., Wang, Z., Yan, X., Norde, W., Li, Y., 2015. Pickering emulsions stabilized by whey protein nanoparticles prepared by thermal cross-linking. Colloids Surfaces B Biointerfaces 127, 96–104. https://doi.org/10.1016/j.colsurfb.2015.01.029

Xu, Q.Y., Nakajima, M., Binks, B.P., 2005. Preparation of particle-stabilized oil-in-water emulsions with the microchannel emulsification method. Colloids Surfaces A Physicochem. Eng. Asp. 262, 94–100. https://doi.org/10.1016/j.colsurfa.2005.04.019

Yang, J., Thielen, I., Berton-Carabin, C.C., van der Linden, E., Sagis, L.M.C., 2020. Nonlinear interfacial rheology and atomic force microscopy of air-water interfaces stabilized by whey protein beads and their constituents. Food Hydrocoll. 101, 105466. https://doi.org/10.1016/j.foodhyd.2019.105466

Yao, X., Liu, Z., Ma, M., Chao, Y., Gao, Y., Kong, T., 2018. Control of Particle Adsorption for Stability of Pickering Emulsions in Microfluidics. Small 14, 1–7. https://doi.org/10.1002/smll.201802902

Zembyla, M., Lazidis, A., Murray, B.S., Sarkar, A., 2019. Water-in-oil pickering emulsions stabilized by synergistic particle-particle interactions. Langmuir 35, 13078–13089. https://doi.org/10.1021/acs.langmuir.9b02026

Zou, Y., van Baalen, C., Yang, X., Scholten, E., 2018. Tuning hydrophobicity of zein nanoparticles to control rheological behavior of Pickering emulsions. Food Hydrocoll. 80, 130–140. https://doi.org/10.1016/j.foodhyd.2018.02.014

Appendix

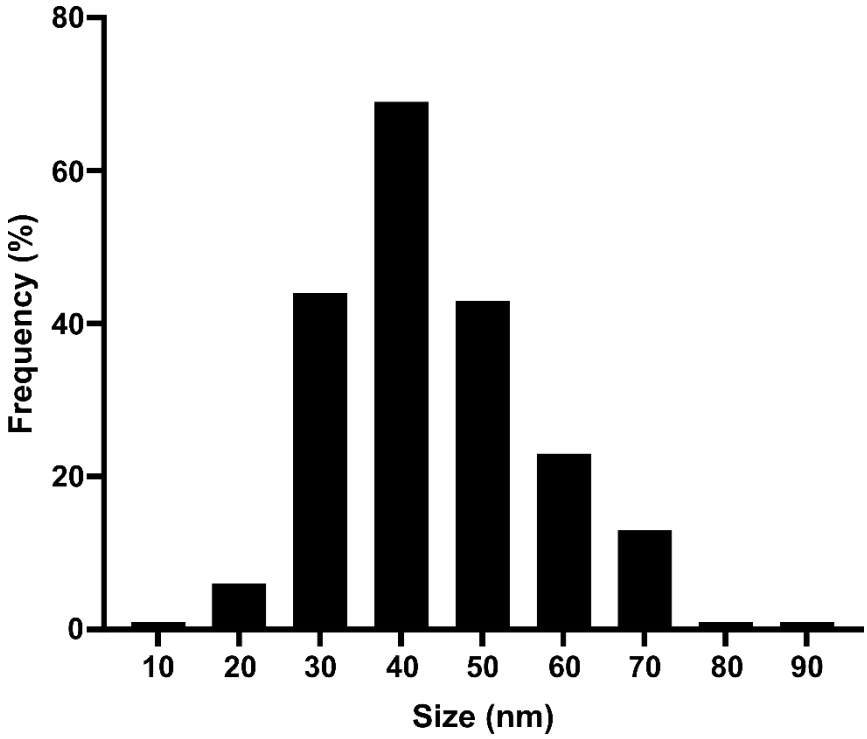

Figure 5.A1 - *Size distribution of microgel particles based on TEM micrography*.

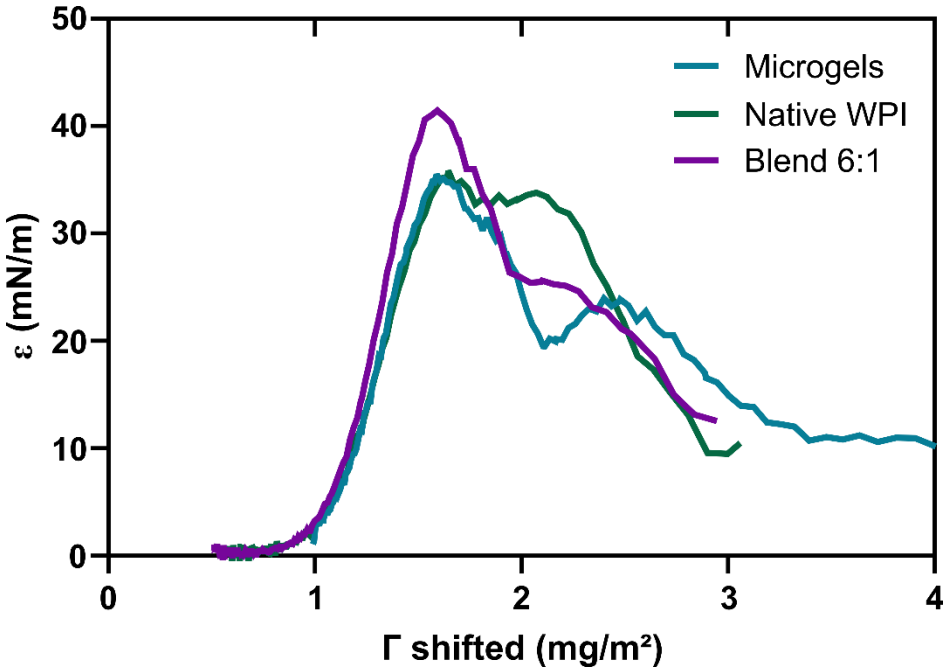

Figure 5.A2 - Dilatational modulus as function of the shifted surface coverage for native WPI, WPI microgels, and a blend formed at 6:1 (microgels:WPI) mass ratio. Shifts are performed with a constant multiplication factor with respect to the native WPI curve.

6 SYNERGISTIC EFFECT OF WHEY PROTEINS AND THEIR DERIVED MICROGELS IN THE STABILIZATION OF O/W EMULSIONS

Jéssica Thaís do Prado Silva[1,2*], Annabel Janssen[2], Vânia Regina Nicoletti[1], Karin Schroën[2] and Jolet de Ruiter[2]

[1]Unesp - São Paulo State University, Institute of Biosciences, Humanities and Exact Sciences, Cristóvão Colombo 2265, São José do Rio Preto 15054-000, São Paulo, Brazil

[2]Food Process Engineering Group, Wageningen University & Research, Wageningen 6700 AA, The Netherlands

Abstract

Tannic acid-crosslinked whey protein isolate (WPI) microgels are particles suitable for Pickering stabilization. Their production is often accompanied by remaining un-reacted WPI, which may play a role in physical stability of emulsions. Here, these microgels were produced and carefully characterized regarding the presence of surface-active molecules after an extensive ultrafiltration procedure. The results showed that the majority of native WPI was removed from the dispersion (90%), however, completely purification is not feasible. The physical characteristics of emulsions stabilized by blends of microgels and native WPI showed to be dependent on the homogenization protocol. Native WPI was able to disrupt bridging flocculation between droplets after 14 days of storage for emulsions prepared using rotor-stator equipment. However, high pressure homogenizer gave rise to very viscous emulsion, which may impair WPI diffusion to the interface for disrupting flocs. The microgels were not removed from droplets' interface during storage, pointing out that native WPI had a synergistic effect rather than competition for adsorption during emulsification.

Keywords: WPI microgels, tannic acid, surface-active molecules, Pickering emulsions, synergistic stabilization.

1 Introduction

Particle-stabilized emulsions – Pickering emulsions (Pickering, 1907) show extraordinary stability against coalescence compared to those stabilized by conventional emulsifiers, primarily as a result of the high desorption energy required to remove particles from the interface and the thicker interfacial layers they provide, forming a physical barrier that prevents droplet coalescence (Berton-Carabin & Schroën, 2015). Such systems offer emulsions a surfactant-free character (Leal-Calderon & Schmitt, 2008) and therefore may comply with consumer demands for clean labels (Green et al., 2013; McClements & Gumus, 2016). These reasons justify the many efforts that have been made to design Pickering emulsions suitable for food applications (Du et al., 2019; Ribeiro et al., 2020; Schröder et al., 2019; Wang et al., 2020).

Proteins stand out among the food-grade components that offer opportunities as starting material for the production of Pickering particles. This is because they are highly surface-active molecules, allowing protein particles to combine the high desorption energy of Pickering particles with the ability of protein molecules to adsorb at any interface (Murray, 2019). Usually, protein molecules are treated by a simple heating protocol to form microgel particles. Heat treatments alter the secondary structure of proteins by molecular unfolding. This causes hydrophobic groups initially present in the core of globular proteins to be exposed, improving the protein's wettability by the oil phase (Dickinson, 2011; Nicolai et al., 2011; Wu et al., 2015).

Microgels are soft, deformable particles formed by a water-swollen polymeric network that is internally crosslinked through a combination of hydrophobic bonds, hydrogen bonding, electrostatic interactions or disulphide bonds, depending on the method of preparation (Yan et al., 2020). Such particles have a core-shell morphology, in which the shell is less crosslinked than the microgel core, therefore the shells are capable of distorting, giving to microgels the appearance of "fried-egg" when adsorbed at interfaces. Flattening the spherical shape increases the interfacial area occupied by the microgel, in such a way that the desorption energy of microgels should be higher than the one for classical Pickering particles. The expectation is, therefore, that microgel particles are better stabilizers for emulsions than hard spheres (Murray, 2019).

Whey protein is a co-product in cheese production and therefore is regarded as a widely available and accepted protein source (Li et al., 2018). It contains a mixture of globular proteins such as β-lactoglobulin (β-LG), α-lactalbumin (α-LA), bovine serum albumin (BSA) and immunoglobulins (Haug et al., 2007). Microgels produced from whey protein have been reported to function as effective Pickering stabiliser (Destribats et al., 2014; Murray & Phisarnchananan, 2016; Wu et al., 2015; Zamani et al., 2018). In addition, we demonstrated that physical properties of microgels made of whey protein isolate (WPI) can be tuned by adding a crosslinking step using tannic acid. This enables the production of smaller particles compared to conventional WPI microgels, thus reflecting on a more structured physical barrier and enhancing the emulsion stability (do Prado Silva et al., 2021).

Due to the heterogeneity in composition of food ingredients, production of food-grade particles for Pickering stabilization often results in mixtures of these particles with unreacted surface-active constituents. These cannot be easily removed and consequently may play a role in emulsion formation and interfacial stabilization (Destribats et al., 2014). How these interactions establish themselves typically depends on the homogenization protocol and the nature of the surface-active molecules involved.

A tendency for synergistic interactions is generally observed when surface-active molecules are present in low concentrations. In this domain of concentrations, surface-active molecules may facilitate the breakage of droplets during homogenisation and thereby offer additional time for particle adsorption (Lan et al., 2007; Pichot et al., 2010), as well as they may strengthen the interfacial layers (Gülseren & Corredig, 2013; Murray et al., 2011), and can adjust the wettability of particles (Binks et al., 2007; Hu et al., 2015). On the other hand, when concentrations of surface-active molecules are increased, antagonistic effects may become more prominent, which are due to different phenomena such as increased competition for interfacial adsorption (Gülseren & Corredig, 2013), reduction desorption energy of particles as a result of the significant decrease in interfacial tension (Murphy et al., 2018), in addition to extensive changes in particle wettability that cause the particles to lose their role as an effective Pickering stabilizer (Binks et al., 2007; Binks et al., 2013).

The challenge to produce pure Pickering emulsions from materials of food origin, highlights the importance of understanding the interaction pathways between Pickering particles and residual surface-active constituents. In this context, the present work

aims to investigate the effects of the presence of native whey protein isolate on the physical stability and interfacial properties of emulsions stabilized by tannic acid-crosslinked WPI microgels.

2 Materials and methods

2.1 Materials

Whey Protein Isolate (WPI), purity 97.0% - 98.4% (BiPro, Davisco, Switzerland) and tannic acid, purity >99% (Sigma Aldrich, United States) were used as received. N-hexadecane (99%) (Alfa Aesar, Thermo Scientific, Germany) was used as model oil phase. Sodium dodecyl sulfate (SDS, >99%), dimethyl sulfoxide (DMSO, >99.7%), Nile blue A, Nile red, potassium sorbate (>99%), and aspartic acid (>98%) were purchased from Sigma Aldrich (United States). 2-Propanol (HPLC grade), n-hexane (PEC grade), and hydrochloric acid (HCL, 37-38%) were purchased from Actu-All Chemicals (Oss, Netherlands). Polyethersulfone (PES) membrane filters with a pore size of 0.03 µm were obtained from Sterlitech Corporation (United States). Acetonitrile ULC-MS (30%, Actu-All Chemicals, Netherlands) and trifluoroacetic acid (TFA) (Sigma Aldrich, United States) was used for HPSEC analysis. All solutions were made in ultrapure water (Millipore Corporation, Billerica, Massachusetts, United States).

2.2 Production and characterization of tannic acid-crosslinked WPI microgels

The production of WPI microgels followed the procedure described elsewhere (do Prado Silva et al., 2021). Initially, WPI solution (40 g/L) was prepared by mixing deionized water and WPI trough magnetic stirring (350 rpm) during 2 hours at 20 °C. The solution was incubated overnight for at least 12 hours at 4 °C to ensure complete protein hydration. Tannic acid was carefully added to the WPI solution at room temperature in a molar ratio of 0.5:1 (tannic acid:WPI) under magnetic stirring (200 rpm). The solution had its pH adjusted to 5.8 by drop-wise addition of 1 M HCl and was heated for 15 minutes in a water bath operating at 80 °C in absence of stirring. The resulting microgel dispersion was then rapidly cooled to room temperature using running tap water.

The microgels were characterized regarding to particle size distribution by Dynamic Light Scattering (DLS) and zeta potential using the Smoluchowski model (Zetasizer Nano ZS, Malvern Instruments, United Kingdom). Experiments were performed at 25 °C using a disposable folded capillary cell (DS1080). Microgel dispersions were diluted 100x in ultrapure water prior to analysis to avoid multiple scattering effects. Samples were evaluated in triplicate, using a refractive index of 1.45 for the dispersed phase and 1.33 for the dispersant.

2.3 Purification of the microgel dispersion

In order to remove possible non-reacted WPI molecules from the microgel dispersion, a purification procedure based on ultrafiltration process was implemented. Right after preparation, the microgel dispersion was washed 10 times in an Amicon Stirred Cell (Merck Millipore, United States), stirred at 380 rpm under an operating pressure of 3 bars, using a PES membrane filter (0.03 µm). In every step, 50 grams of filtrate were removed, after which 50 grams of ultrapure water were added to keep a constant total mass of approximately 100 g inside the filtration cell. After 5 filtrations, the membrane filter was replaced by a new one, in an attempt to improve the separation performance. The native WPI concentrations (mg/mL) in the microgel dispersion before and after purification were determined using a high-pressure size exclusion chromatography (HPSEC) instrument (Thermo UltiMate 3000, Thermo Scientific, Germany), equipped with a standard quaternary pump (Pump LPG-3400SD), auto sampler (WPS-3000), column-oven (TCC-3000), and photodiode array detector (PDA-3000). Samples (180 µL) were collected in glass vials and measured in duplicate. Two columns were used to perform the separation (TSKGel G3000SWXL and TSKGel G2000SWXL), (Sigma Aldrich, United States) at 30 °C. Acetonitrile (30%) with 0.1% TFA was used as eluent at 1.5 mL/min flowrate, over a runtime of 20 minutes. Samples were detected at 214 nm wavelength.

2.4 Production of emulsions stabilized by blends of WPI microgels and native WPI

2.4.1 Continuous phase design

In order to evaluate the effect of free surface-active molecules on stabilization of Pickering emulsions, different continuous phases were designed containing a fixed

amount of WPI microgels and increased amounts of native WPI. The composition of each continuous phase was calculated in terms of the critical content of the individual components (see Supplementary Information). Right after preparation, the washed microgel dispersion was diluted to 33% of the critical content of WPI microgels in ultrapure water. Then, pre-determined amounts of native WPI were added to the diluted microgel dispersion (25 to 200% of WPI critical concentration), under magnetic stirring. The stabilizer compositions of the continuous phases are summarized in Table 6.1.

Table 6. 1 – Stabilizer composition of emulsions and treatment codification.

Treatment	Stabilizer in the continuous phase		
	TA-WPI microgels (%)[+]	Native WPI prone to homogenization (%)[+]	Native WPI added after homogenization (%)[+]
25G	33	25*	0
200G		200	
25/175G		25*	175
25B	0	25	0
200B		200	
25/175B		25	175

[+]Percentages are relative to the critical content.

*This native WPI content was inherent in the dispersion of TA-WPI microgels. No additional WPI was added.

2.4.2 Production of emulsions

The continuous phases referred on Table 6.1 were used to produce 10 wt.% oil-water emulsions with hexadecane as the oil phase. Hexadecane was added carefully to each continuous phase and potassium sorbate (1 wt.%) was added as antimicrobial agent. Initially, a coarse emulsion was made using a high-speed blender (Ultra-Turrax IKA T18 Basic, Germany) operating at 11.000 rpm for 1 minute. Afterwards, in order to evaluate the influence of shear rate on emulsions' characteristics, the coarse emulsion was passed through two different homogenization techniques: either rotor-stator homogeniser or high-pressure homogenizer. The equipment selected for this purpose were a colloid mill (IKA MagicLab, Germany) connected to a water bath at 20 °C,

operating at 15.000 rpm for 2 minutes, and a microfluidizer (M-110Y, Microfluidics, United States) at 400 bars for 5 passes.

2.5 Droplet size distribution

The droplet size distribution in the emulsions was measured by Static Light Scattering (Mastersizer 3000, Malvern Instruments, United Kingdom). A refractive index of 1.43 was used for the dispersed phase (hexadecane) and 1.33 for the dispersant (water). An absorption index of 0.01 was applied. Emulsions that presented bimodal distribution were diluted in 1 w/w% SDS (1:1, v/v) prior to analysis to assess the presence of flocculation.

2.6 Microscopic evaluation

Emulsion droplets were visualized using a light microscope (Axioscope, Zeiss, Germany) at 40x magnification. For this purpose, 10 µL of diluted emulsions (1:1, v/v) were placed onto a microscopy slide and covered with a cover slide.

Confocal laser scanning microscopy (CLSM) was used to gain more qualitative insights about the interfacial organization. Nile red (1 w/w% in DMSO) and Nile blue A (1 wt.% in ultrapure water) solutions were used as stain for hexadecane and WPI (either microgels or native molecules), respectively. Immediately after preparation, 1 mL of each emulsion was added to 10 µl Nile red solution and 5 µl Nile blue A solution in a test tube protected from light. The tubes were rotated for 2 hours prior to analysis to incubate the stains. Aliquots of 50 µL of stained emulsion were pipetted onto a glass slide that was covered carefully by another slide and visualized in a confocal laser scanning microscope (Zeiss LSM 5 Exciter, Breda, NL). Nile red and Nile blue A were excited by 488 nm Argon and 633 nm Helium-Neon laser, respectively. Images obtained by both microscopic techniques were further edited with Fiji (NIH) software.

Transmission Electron Microscopy (TEM) was performed in order to gain additional insights about the morphology of microgels and their adsorption at the droplet interface. As TEM is only able to provide quality images for very small objects, only the microgel dispersions and emulsions prepared with microfluidizer were evaluated. Samples were deposited onto a freshly glow-discharged carbon coated copper grid (200 mesh). Excess solvent was removed with standard filter paper, followed by

staining with phosphotungstic acid solution (2 wt.%). Images were taken with a JEM1011 transmission electron microscope (JEOL, United States) operating at 80 kV in combination with a 2K x 2K SIS Veleta camera.

3 Results and discussion

3.1 Characterization of tannic acid-crosslinked WPI microgels

The tannic acid-crosslinked WPI (TA-WPI) microgels showed unimodal size distribution ranging between 30 – 200 nm, with a mean z-average diameter of 85.4 ± 0.6 nm and a polydispersity index (PDI) of 0.11. The microgels subjected to the ultrafiltration treatment had a similar size distribution (Figure 6.1A), confirming that this procedure did not substantially affect the microgel integrity. This agrees with the exceptional stability reported in earlier studies in which WPI microgels that were subjected to even harsher treatments (e.g. spray drying or sonication) remained unharmed (Destribats et al., 2014; Schmitt et al., 2010), which is attributed to the internal covalent crosslinks of microgels. TEM micrographs of the filtered microgels (Figure 6.1, B and C) show that the particles had a spherical morphology with some irregularities, in addition to allowing observation of a denser central region surrounded by a less dense border. The appearance of the TA-WPI microgels supports the expected core-shell morphology, in which the shell is less crosslinked than the microgel core, similarly as it was previously reported (Schmitt et al., 2011)

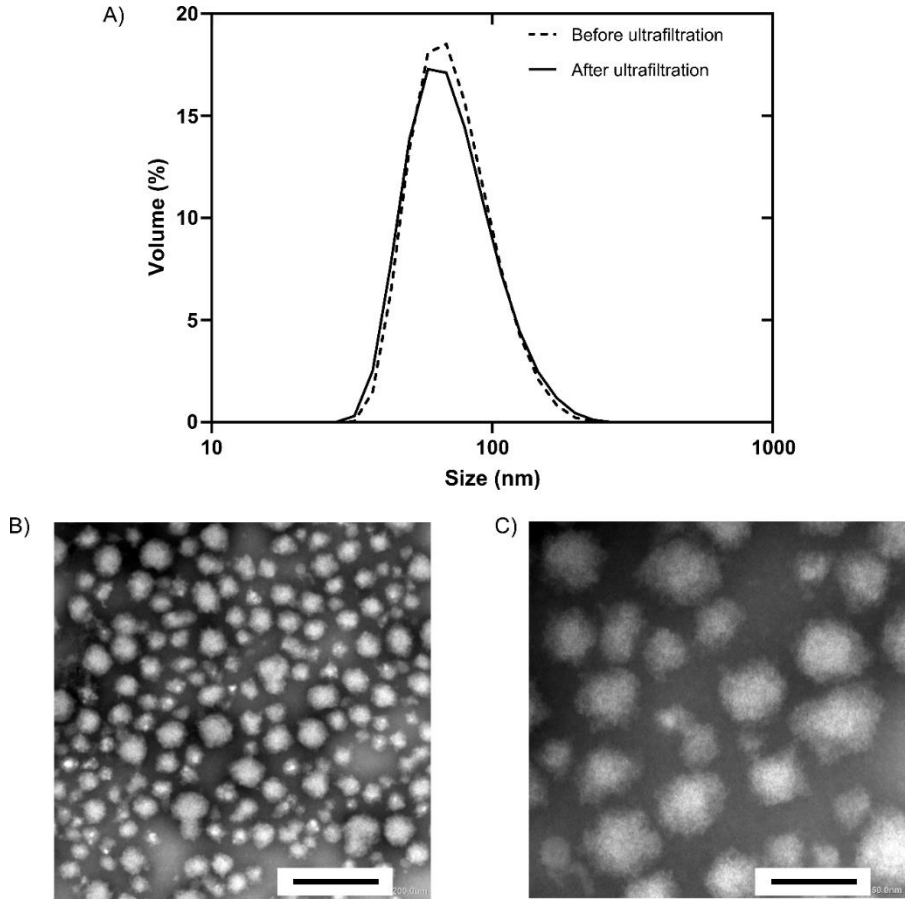

Figure 6.1 – Particle size distribution measured by DLS (A) and TEM micrographs of tannic acid-crosslinked WPI microgels; scale bars represent 200 nm (B) and 50 nm (C), respectively.

The zeta potential of the washed microgels was -47.8 ± 0.7 mV. This value is in accordance with those observed by other researchers and is a result of protons' dissociation in the -COOH groups of WPI at pH lower than the isoelectric point (≈ 4.7); the highly negative value of zeta potential establishes dispersion stability as a result of electrostatic repulsion between particles (Araiza-Calahorra & Sarkar, 2019; Destribats et al., 2014; Murray & Phisarnchananan, 2016; Wu et al., 2015; Zamani et al., 2018). Upon producing the TA-WPI microgels, we determined that 64 ± 3.5% of the native WPI was converted to particles. This value was based on the experimental α-LA and β-LG concentrations calculated from HPSEC chromatograms of native WPI solution and unwashed microgel dispersion. The formation of microgels was accompanied by a decrease in the ratio between the concentration of unbound native β-LG and α-LA, which was reduced from 3.0 in native WPI (Figure 6.A1) to 0.9 in the unwashed

microgel dispersion (Figure 6.2). This observation implies that β-LG is more involved in the formation of TA-WPI microgels than α-LA.

Multiple factors make β-LG a better candidate for microgel formation than α-LA, including the proline content, the size, the free thiol groups and the polarity. As stated by Schmitt (2011), microgels cannot be produced from pure α-LA, which mainly result in the formation of precipitates and soluble aggregates. Microgel formation requires the presence of substantial amounts of β-LG, either in its pure form or coexisting with small amounts of α-LA. The relatively higher proportion of proline embedded within the structure of β-LG (8 of the 162 amino acids) compared to α-LA (2 of the 123 amino acids) (Kilara & Vaghela, 2018), could facilitate the formation of protein-tannin complexes (Asquith & Butler, 1986; Frazier et al., 2003; Hagerman & Butler, 1981). Moreover, tannins are more likely to bind to higher molecular weight proteins (Hagerman & Butler, 1981), which would also slightly favour the complexation with β-LG dimers over α-LA monomers. The presence of a buried free thiol group, which becomes exposed during protein unfolding upon heating, makes β-LG especially more vulnerable to intermolecular disulphide aggregation reactions than α-LA, which is deficient in this reactive group (Broersen, 2020; Schmitt et al., 2011). Additionally, the deep hydrophobic core of β-LG that becomes exposed upon heat treatment is very effective at ligand binding and could be responsible for the described hydrophobic interactions of protein-tannin complexation (Broersen, 2020; Frazier et al., 2003). Large amounts of α-LA, on the other hand, may suppress the occurrence of these hydrophobic interactions, impairing the formation of microgels (Schmitt et al., 2011).

3.2 Evaluation of the ultrafiltration procedure as purifying method for microgel dispersion

The effectiveness of the ultrafiltration in removing unreacted WPI molecules was evaluated by means of HPSEC analysis of the TA-WPI microgel dispersion before and after purification. The results showed that the adopted procedure was able to remove considerable amount of native WPI from the mixture (Figure 6.2).

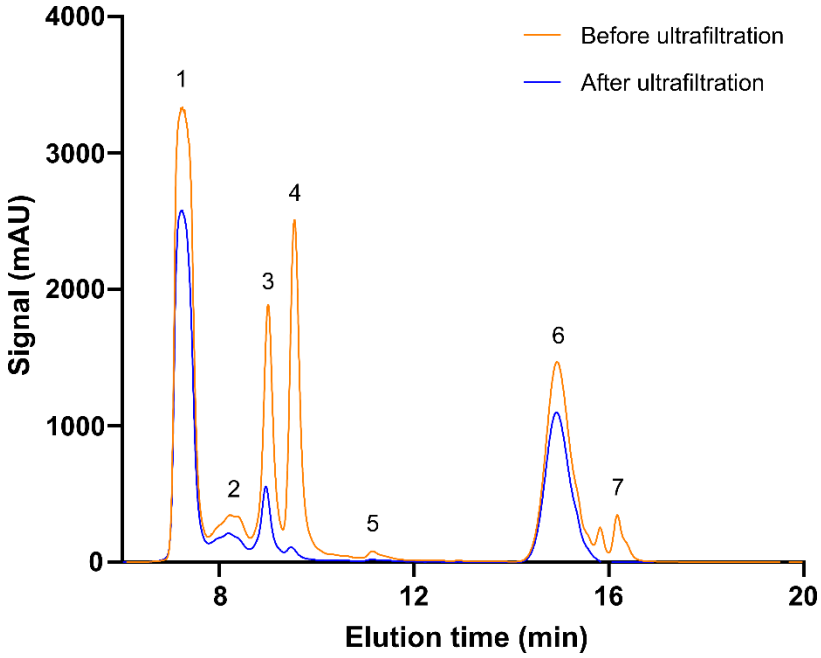

Figure 6.2 – Protein composition of TA-WPI microgel dispersion (40 g/L) measured by HPSEC before and after ultrafiltration. Peaks correspond to: (1) large protein aggregates and microgels; (2) BSA and smaller aggregates; (3) β-LG dimers; (4) α-LA monomers; (5) peptides; (6) tannic acid; (7) minerals and salts.

Interestingly, it can be observed that the ratio β-LG:α-LA, which was reduced from 3.0 in native WPI (Figure A1) to 0.9 in the unwashed microgel dispersion, as previously discussed in Section 3.1, increased again from 0.9 to 10.2 after ultrafiltration, suggesting that the filter was more efficient in removing α-LA than β-LG. The slightly higher selectivity of polyethersulfone (PES) membranes for α-LA compared to β-LG has been reported before and could be related to the larger size of β-LG dimers (Cowan et al., 2007). Another explanation for the lower permeability of β-LG could be related to the aforementioned higher tendency of β-LG to participate in aggregation reactions upon unfolding during heat treatment, irreversibly exposing its hydrophobic core. On the other hand, the fact that α-LA is less likely to be involved in these reactions allows it to renature upon cooling, returning to its initially more hydrophilic conformation by burying all hydrophobic groups inside (Wit & Klarenbeek, 1984). This mechanism, combined to the high hydrophilic nature of the PES membranes, may favour the permeance of the relatively more hydrophilic renatured α-LA over the irreversibly denatured β-LG.

The decrease in the sum of the areas of peaks 3 and 4 (Figure 6.2) is equivalent to a reduction of 11.3 to 1.3 mg/mL of native WPI in the dispersion upon filtration, which

means that 90% of the unreacted WPI was effectively removed. This result indicates that even after 10 wash steps, TA-WPI microgels still coexist with some native WPI, hindering complete purification through this procedure.

The microgel dispersion after the final ultrafiltration step was composed by approximately 25.6 mg/mL TA-WPI microgels and 1.3 mg/mL native WPI (mainly composed by β-LG). The residual native WPI concentration in the washed microgel dispersion was a fundamental parameter in the subsequent design of the final emulsions, in which the ratio between native WPI and TA-WPI microgels is of utmost importance.

3.3 Characterization of the emulsions

The results of ultrafiltration procedure proved that a complete purification of TA-WPI microgel dispersion was not feasible and some residual native WPI should be dealt with. Starting from this reasoning, the TA-WPI microgel dispersion was diluted in order to attain 33% of the microgel critical content, as discussed in Section 2.4.1, which resulted that the residual amount of unreacted protein in the mixture represented 25% of the native WPI critical concentration. This composition was considered to design continuous phases for producing the emulsions.

With the aim of understanding the effect of native WPI molecules on the physical properties of Pickering emulsions, we first compared emulsions stabilized by blends of TA-WPI microgels and native WPI with conventional emulsions (stabilized only by native WPI and named as blank emulsions), as described on Table 6.1.

Later, we investigated the effects of homogenization technique on the characteristics of emulsions stabilized by blends of TA-WPI microgels and native WPI, as the homogenization parameters might affect the relative adsorption rate of the different stabilizers. The composition of such emulsions in terms of microgels and native WPI, as well as the mixing protocol (addition of native WPI before or after homogenization), was comparable to that of treatments 25G, 200G and 25/175G.

3.3.1 Effect of surface-active molecules content on physical properties of microgel-stabilized emulsions

The stability of the emulsions against flocculation and coalescence was investigated by means of their droplet size distributions, which were determined in freshly prepared emulsions and after 14 days of storage at 20 °C (Figure 6.3).

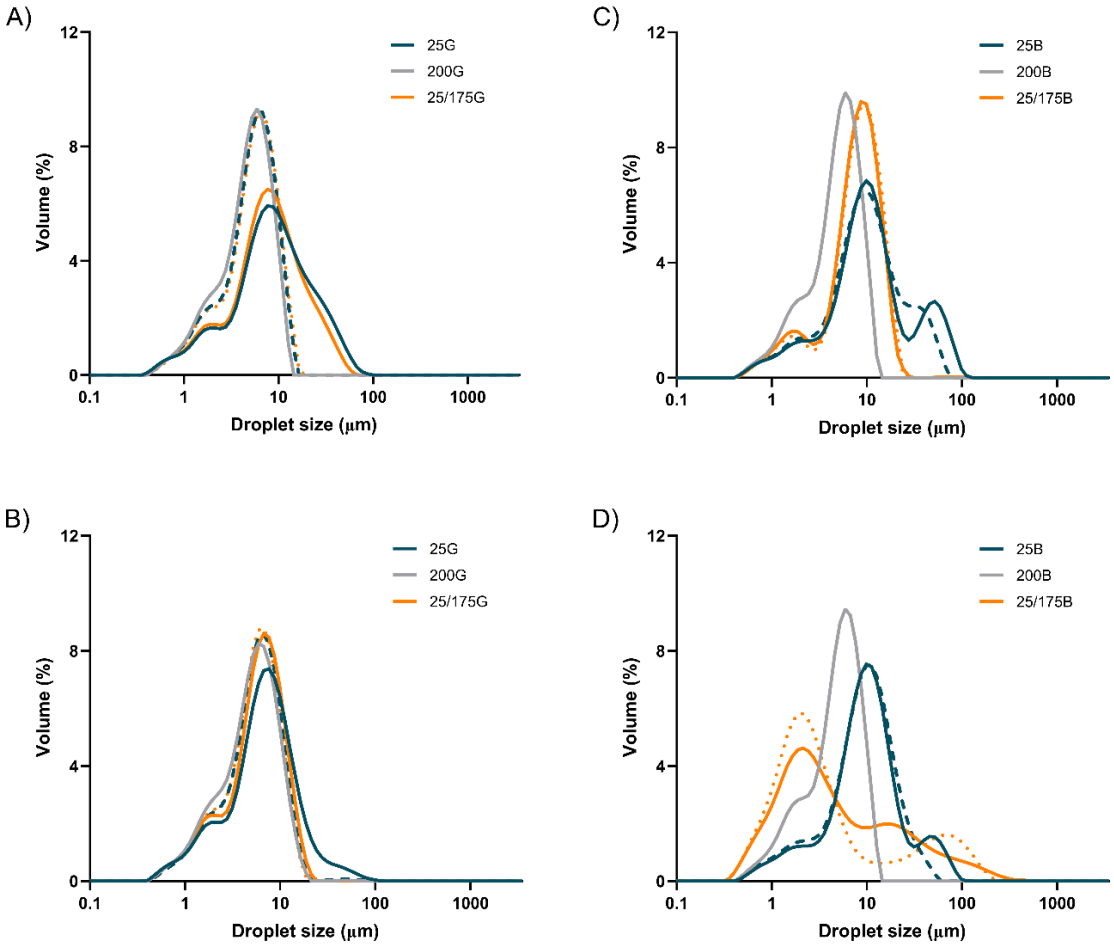

Figure 6.3 – Droplet size distributions in emulsions produced by rotor-stator homogenization on days 0 (A and C) and 14 (B and D). Samples that showed broader or bimodal distributions were diluted in 1 w/w% SDS (1:1, v/v), as represented by the non-continuous lines.

Emulsions produced in presence of the lowest native WPI concentration (25G and 25/175G) showed a remarkable shift towards larger sizes. However, by adding SDS solution, these emulsions reassumed a droplet size distribution similar to that of sample 200G (Figure 6.3A), suggesting the presence of flocs. The same behaviour was not observed for the blank emulsions (25B and 25/175B), in which the size distribution profile did not change after SDS addition (Figure 6.3C), indicating the

occurrence of coalescence rather than flocculation. This flocculation/coalescence behaviour of freshly prepared emulsions was confirmed by light microscopy images (Figure 6.4). These images show that the individual size of droplets in the emulsions containing microgel particles as stabilizer are similar (Figure 6.4A, B, and C); the images also make evident the presence of flocs in the treatments 25G and 25/175G, as it was already indicated by the analysis of size distribution. On the other hand, flocs were not observed in emulsions produced in absence of microgels (Figure 6.4D, E, and F). In contrast, they showed remarkable differences in individual droplets size.

It is important to point out that, in spite of all emulsions were designed to contain the same amount of native WPI, the treatments containing microgels summed up a higher overall stabilizer concentration in comparison to the blank emulsions. In addition, the ability of microgels to flatten at the interface contribute to provide an increased surface coverage compared to native WPI. At low overall stabilizer concentration, the interfacial area formed during homogenization is not completely covered and neighbouring droplets can merge until they achieve a full covered interface. During homogenization, the formation of droplets, adsorption of stabilizer, and re-coalescence phenomena happen simultaneously at milliseconds time scale (Muijlwijk et al., 2017). Thus, the WPI added after homogenization is not able to prevent the re-coalescence of droplets, which justify to some extent the similar droplet sizes of samples 25B and 25/175B.

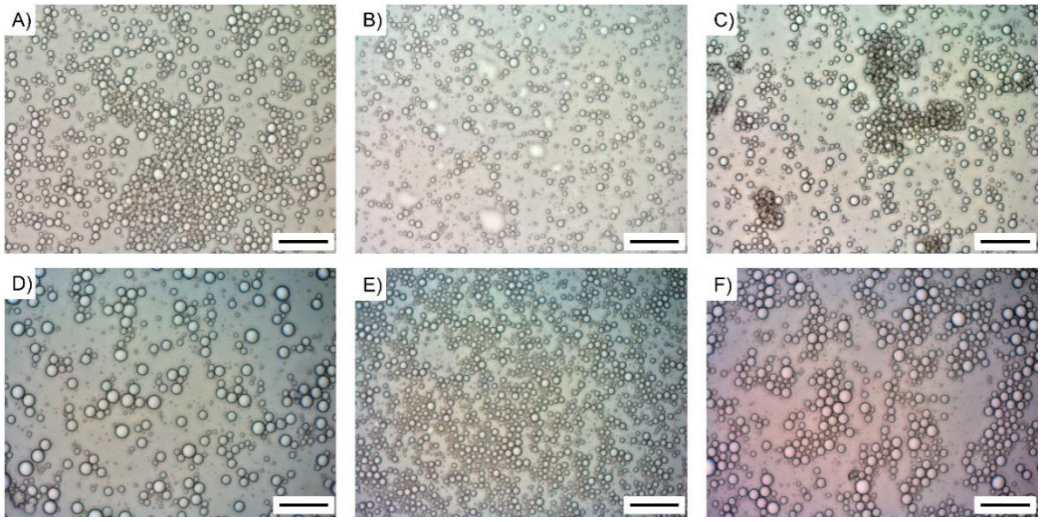

Figure 6.4 – Light microscope images of freshly prepared emulsions: (A) 25G; (B) 200G; (C) 25/175G; (D) 25B; (E) 200B; (F) 25/175B. Scale bars represent 50 µm.

After 14 days of storage, the shoulders present in the droplet size distribution profiles of treatments 25G and 25/175G (Figure 6.3A and B) vanished, suggesting that disruption of the flocks initially present took place in these emulsions. With regard to the blank emulsions, however, only the sample 200B was physically stable to coalescence over time. Emulsion 25/175B showed a clear shift towards larger sizes and the occurrence of macroscopic phase separation was visualized. The coalescence in this case could be attributed to depletion interactions during storage induced in the presence of the additional 175% WPI. In spite of its low emulsifier content, emulsion 25B did not show extensive macroscopic phase separation, as droplets were individually dispersed in the absence of induced depletion interactions. However, the droplet size distribution (Figure 6.3D) shows a shrinkage of the larger droplet population on day 14, which may indicate that part of the larger droplets detected on day 0 underwent phase separation, forming some tiny patches of oil that were observed on top of the emulsion.

Aiming to investigate further the flocculation behaviour of droplets over time, emulsions were characterized on days 0 and 14 by means of CLSM (Figure 6.5). The morphology revealed by CLSM images are in agreement with the observations based on the droplet size distribution of the emulsions, with flocculation being apparent for emulsion stabilized by TA-WPI microgels at low native WPI content during emulsification.

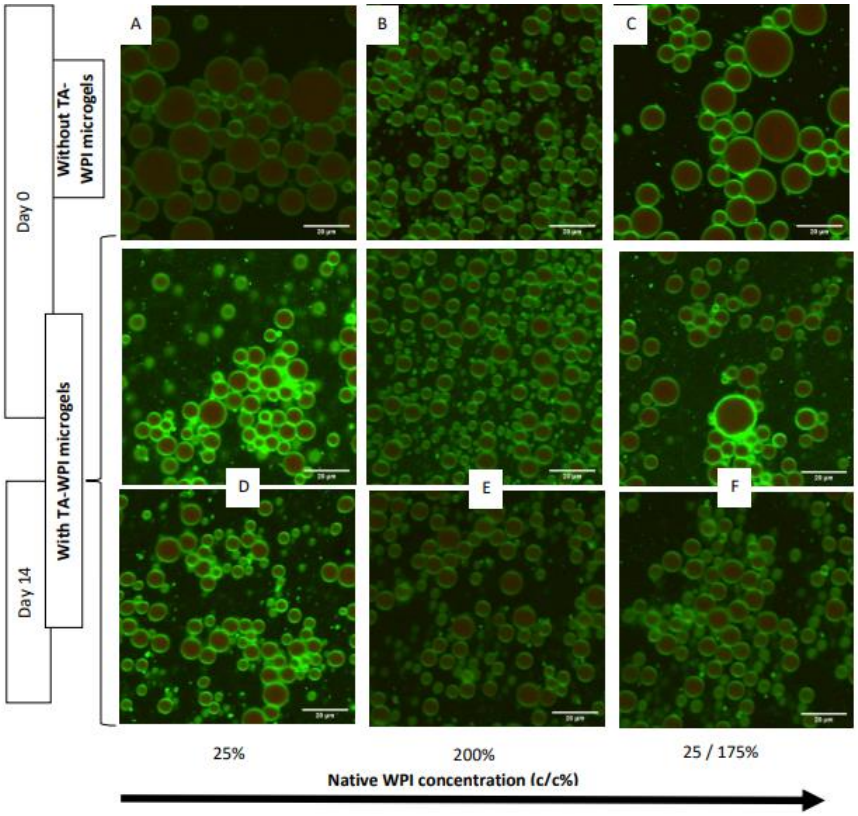

Figure 6.5 – CLSM images of: (A-C) blank emulsions on day 0, and (D-F) emulsions stabilized by blends of TA-WPI microgels and native WPI on day 0 and 14. Native WPI and microgels appear in green and hexadecane appears in red. (A) 25B, (B) 200B, (C) 25/175B, (D) 25G, (E) 200G, (F) 25/175G. Scale bars represent 20 µm.

The occurrence of flocculation only in emulsions produced in the presence of WPI microgels leads to the hypothesis that bridging flocculation took place on those samples, a common phenomenon for Pickering emulsions. Particle bridging occurs only when two partially covered droplets collide, being specific for emulsions with low particle content, as is the case in the present study, in which microgels were available to cover only 33% of the interface. In this configuration, a single layer of particles can simultaneously stabilize two colliding droplets. The strong capillary forces created by the formed menisci around the particles guarantee their positioning at the interfaces, forming a dense bridged monolayers between droplets, which prevents coalescence (French et al., 2015; Horozov & Binks, 2006).

The contact areas between the flocculated droplets reveal increased fluorescence (Figure 6.5D and F), which is in accordance with microscopic observations of poorly-covered droplets as reported by Destribats and Leal-Calderon (2007). These researchers suggested that increased fluorescence is an indicative of particle

reallocation at droplet contact zones (therefore predominant in flocculated emulsions) as a result of dipole-dipole interactions, which are especially favoured by the high electrostatic charge of the TA-WPI microgels.

The disruption of flocks is evidenced in CLSM images of treatments 25G and 25/175G on day 14 (Figure 6.5D and F), thus confirming the size distribution results previously discussed. This could be indicative of decreased bridging flocculation over time, which can be a result of post-emulsification interfacial reorganisation. Small amounts of residual non-adsorbed native WPI (25G) or the native WPI added after homogenization (25/175G) can replace part of the bridged TA-WPI microgels by reducing their desorption energy (Murphy et al., 2018; Vashisth et al., 2010). Additionally, proteins may undergo conformational changes during interfacial aging to optimise their interactions with both phases, which characteristically occurs over a time span of days to weeks for globular proteins present in WPI (McClements, 2004). As a result, the native WPI that was adsorbed could have acquired a more optimal and stretched conformation, squeezing out some of the bridged microgels, while ensuring the individual droplet integrity.

The absence of flocs in emulsion 200G was evidenced by its droplet size distribution as well as by the corresponding CLSM images. The logical reason for that is a synergistic interaction of WPI molecules and microgels upon adsorption. The presence of WPI prior to homogenization could guarantee enough stabilizer content to cover the interfacial area formed during homogenization. This reduced the extent of re-coalescence phenomena and generated smaller droplets. Once the interface was completely covered, bridging events were suppressed and stable individual droplets resisted over the storage period.

3.3.2 Effect of the homogenization technique on the emulsion physical properties

As the interfacial organization of microgel particles has been reported to be function of the preparation pathway (Destribats et al., 2013), we produced an additional batch of emulsions stabilized by blends of WPI microgels and native WPI using a high shear process. Interestingly, the emulsions produced by high-pressure homogenization appeared to have an increased viscosity than those produced by rotor-stator treatment. This was a first indication of increased flocculation into the samples.

The droplet size distribution profiles of emulsions produced by high-pressure homogenization (Figure 6.6) were shifted to larger values than the samples produced

by rotor-stator treatment, an additional indication of higher flocculation behaviour. The size distributions of treatments 25GT and 25/175GT were very similar (Figure 6.6A), indicating that the addition of native WPI post homogenization was not able to suppress bridging of droplets. On the other hand, the presence of additional native WPI before homogenization (treatment 200GT) gave rise to emulsions with smaller flocks. These observations reinforce that the presence of native WPI during emulsification has an impact on droplet formation and contributes to reduce the extent of bridging events, likewise its rotor-stator prepared counterpart (200G).

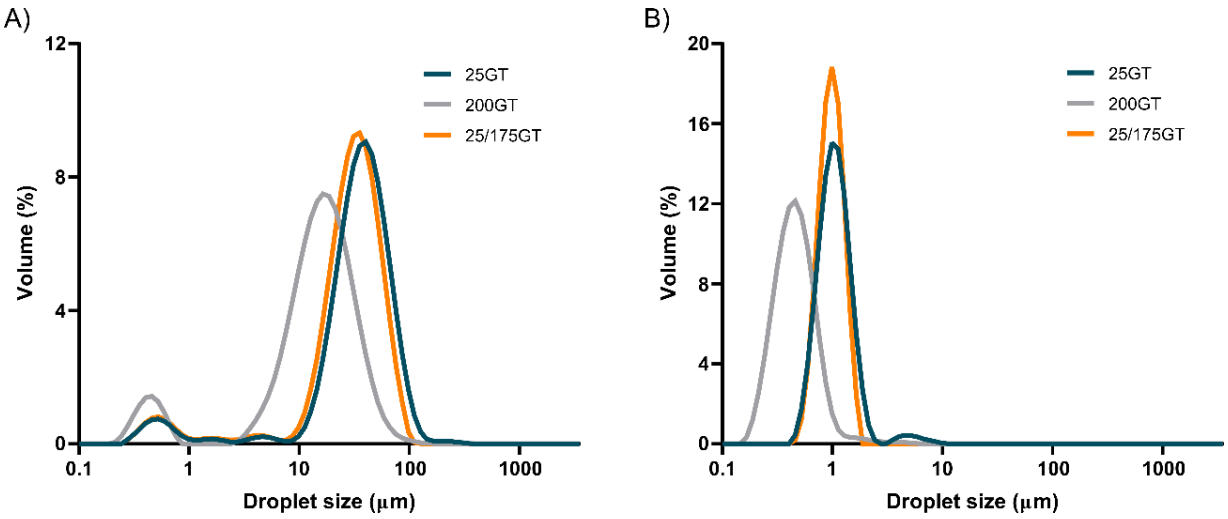

Figure 6.6 – Droplet size distributions of emulsions produced by high pressure homogenization on day 0: (A) freshly prepared emulsions and (B) emulsions diluted in 1 w/w% SDS (1:1, v/v).

After the disruption of flocks (Figure 6.6B), we can still observe that samples 25GT and 25/175GT had similar droplet size distribution. In the case of sample 25/175GT, if the interface was replaced by WPI molecules, droplets would be expected to be more prone to coalescence events than interfaces stabilised mostly by particles (sample 25GT), leading to an increase in droplet size (Hu et al., 2015; Pichot et al., 2010). In this way, since the addition of WPI post homogenization did not alter the individual droplet sizes and flocculation behaviour of emulsions produced by high shear homogenization, the interfacial composition of both samples probably remained similar over time.

On the other hand, sample 200GT presented a shift towards smaller sizes. This may be a result of the ability of native WPI molecules to reduce the interfacial tension. In this case, droplet breakage is facilitated in the presence of these molecules prior to emulsification (Berton-Carabin & Schroën, 2015; Bernard P. Binks et al., 2007; Pichot et al., 2009, 2010). As the mean droplet diameter in fresh emulsions is, among others, governed by the interfacial tension (Hinderink et al., 2019), the presence of native WPI allowed the formation of smaller droplets. However, the disruption of flocs was not clearly observed after 10 days of storage (see Figure 6.A2), indicating no interfacial replacement of particles for WPI molecules over time. Presumably, the high viscosity of emulsions and the fact that droplets were entrapped into networks of bridged droplets might have hindered the diffusion of native molecules to the interface.

The way that microgels adsorb and arrange at the interface is directly related to the mechanical strength of the interfacial layer and consequently to the stability of emulsions (DESHMUKH et al., 2015). Flexible microgels subjected to high shear emulsification adopt deformed configurations, resulting in strong deformation of microgels in the interfacial plane. Moreover, more interfacial area is created using high emulsification energy and, in such conditions, microgels have enough space to deform laterally. This lateral deformation of microgel particles lead to the instant coverage of larger interfacial area, but with lower density of microgels at the interface, which may promote the occurrence of bridging flocculation after relaxation time. In contrast, when using low shear emulsification, the deformation dynamics of microgel particles is too slow compared to droplets' recombination rate and the interfacial area created during homogenization is smaller. In this way, microgels neither have time nor space to extend. Thus, a highly dense interfacial layer is created, hindering bridging between droplets and consequently avoiding flocculation, as schematized in Figure 6.7 (Destribats et al., 2013).

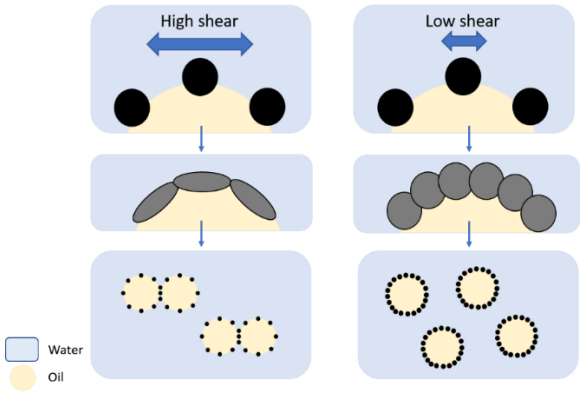

Figure 6.7 – Different microgel conformations under high or low shear homogenization. Adapted from Destribats et al. (2013).

WPI microgels were not removed from the interface, as confirmed by TEM images of the emulsions produced by high shear homogenizer on days 0 and 10 (Figure 6.8) - image of sample 25/175 GT on day 10 was not included because complications occurred with the TEM grid due to its high viscosity. WPI microgels remained adsorbed after 10 days of storage, meaning that native WPI molecules were not able to promote significant microgel desorption over time.

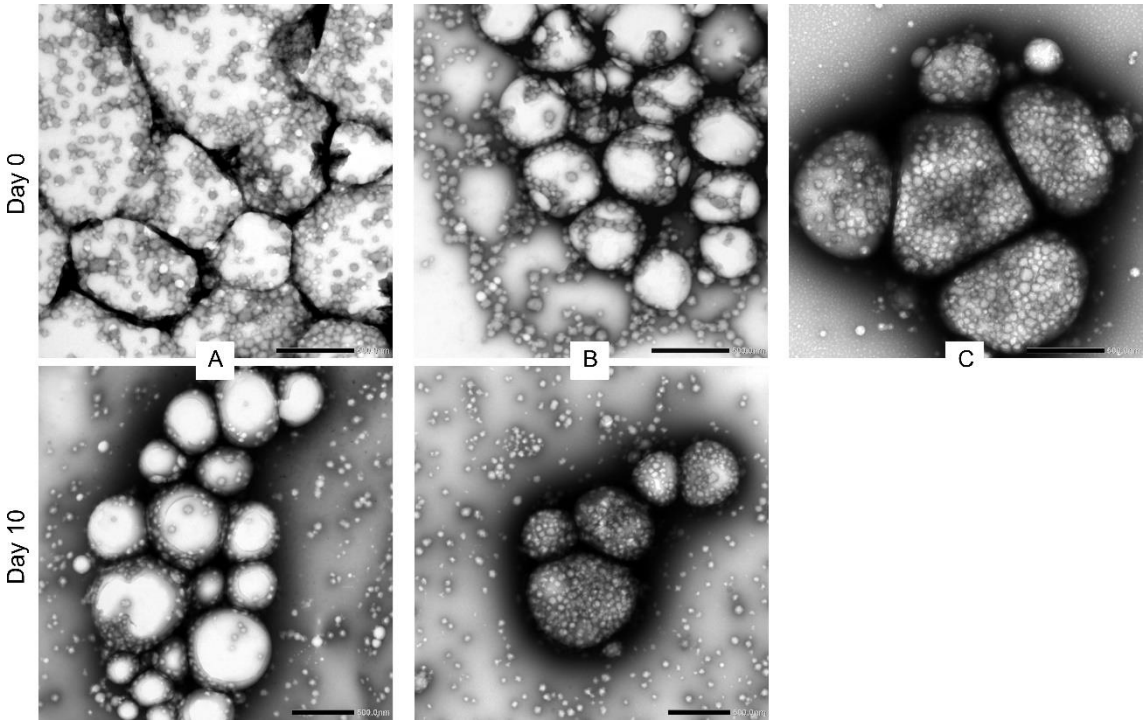

Figure 6.8 – TEM micrographs of emulsions produced by high pressure homogenization on days 0 and 10.: (A) 25GT, (B) 200GT and (C) 25/175GT. Scale bars represent 500 nm.

Based on the results presented in this work, a synergistic effect of WPI microgels and native WPI molecules is suggested: native WPI assisted droplets' breakage, without impairing the adsorption of microgels nor promoting their complete desorption over time.

4 Conclusion

WPI microgels were successfully produced by WPI crosslinking with tannic acid, followed by heating treatment. A multi-step filtration was able to remove 90% of non-reacted WPI from the microgel dispersion. This observation highlights the challenge to establish complete purification of food-grade Pickering particles and the necessity to take into account the presence of such surface-active molecules while designing emulsions.

Continuous phases composed by blends of microgels and native WPI were used to stabilize hexadecane emulsions. Droplet coalescence was supressed by bridging flocculation in emulsions produced in the presence of TA-WPI microgels, a phenomenon well-known for particle-stabilized emulsions. The physical characteristics of emulsions showed to be dependent on the homogenization technique. For emulsions produced by rotor-stator homogenizer in the presence of low native WPI content, native WPI was able to disrupt flocs over time by adsorbing at the interface and pushing bridged particles. At high native WPI content, droplets remained individually distributed, meaning that native WPI played considerable role on interfacial composition. For emulsions produced under high shear, the presence of native protein assisted the formation of droplets by reducing the interfacial tension, contributing to the formation of smaller droplets. The presence of native WPI in high amounts did not impair microgel adsorption, as also showed by TEM images. Due to the mobility limitation caused by the high viscosity of the obtained emulsion, the remaining WPI molecules in the continuous phase were unlikely to be adsorbed over time. Thus, the remaining WPI may acted as a thickening agent rather than establishing a competitive behaviour for adsorption.

Due to the incomplete purification, this study was not able to evaluate a pure WPI microgel-stabilised system, which would be a great future asset to function as a reference to evaluate physical stability. This consideration emphasizes the need for a more advanced and feasible purification procedure before WPI microgels can be

successfully and lucratively applied for its proposed benefits in both the academic and industrial sectors.

Acknowledgements

The authors would like to thank Anja van Osch-Schröder for Transmission Electron Microscopy analysis.

Funding source

This work was supported by Coordenação de Aperfeiçoamento de Pessoal de Nível Superior – CAPES (finance code 001) through the Program CAPES-PrInt-Unesp, process number 88887.194785/2018-00.

References

Araiza-Calahorra, A., & Sarkar, A. (2019). Pickering emulsion stabilized by protein nanogel particles for delivery of curcumin: Effects of pH and ionic strength on curcumin retention. *Food Structure*, *21*(March), 100113. https://doi.org/10.1016/j.foostr.2019.100113

Asquith, N. T., & Butler, G. L. (1986). Interactions of condensed tannins with selected proteins. *Pergamon Journals*, *25*(7), 3–5.

Aymard, P., Durand, D., & Nicolai, T. (1996). The effect of temperature and ionic strength on the dimerisation of β-lactoglobulin. *International Journal of Biological Macromolecules*, *19*(3), 213–221. https://doi.org/10.1016/0141-8130(96)01130-0

Berton-Carabin, C. C., & Schroën, K. (2015). Pickering emulsions for food applications: Background, trends, and challenges. *Annual Review of Food Science and Technology*, *6*(February), 263–297. https://doi.org/10.1146/annurev-food-081114-110822

Binks, Bernard P., Desforges, A., & Duff, D. G. (2007). Synergistic stabilization of emulsions by a mixture of surface-active nanoparticles and surfactant. *Langmuir*, *23*(3), 1098–1106. https://doi.org/10.1021/la062510y

Binks, Bernard Paul, Isa, L., & Tyowua, A. T. (2013). Direct measurement of contact angles of silica particles in relation to double inversion of pickering emulsions. *Langmuir*, *29*(16), 4923–4927. https://doi.org/10.1021/la4006899

Broersen, K. (2020). Milk Processing Affects Structure, Bioavailability and Immunogenicity of β -lactoglobulin. *MDPI, Foods*, *9*, 874.

Cowan, S., Ritchie, S., Cowan, S., & Ritchie, S. (2007). Modified Polyethersulfone (PES) Ultrafiltration Membranes for Enhanced Filtration of Whey Proteins Ultrafiltration Membranes for Enhanced. *Seperation Science and Technology*, *42*, 2405–2418. https://doi.org/10.1080/01496390701477212

Destribats, M., & Leal-Calderon, F. (2007). Pickering emulsions with stimulable particles: from highly- to weakly-covered interfaces. *Physical Chemistry Chemical Physics*, *9*(48), 6285–6488. https://doi.org/10.1039/b705094a

Destribats, M., Rouvet, M., Gehin-Delval, C., Schmitt, C., & Binks, B. P. (2014). Emulsions stabilised by whey protein microgel particles: Towards food-grade

Pickering emulsions. *Soft Matter*, *10*(36), 6941–6954. https://doi.org/10.1039/c4sm00179f

Destribats, M., Wolfs, M., Pinaud, F., Lapeyre, V., Sellier, E., Schmitt, V., & Ravaine, V. (2013). Pickering emulsions stabilized by soft microgels: Influence of the emulsification process on particle interfacial organization and emulsion properties. *Langmuir*, *29*(40), 12367–12374. https://doi.org/10.1021/la402921b

Dickinson, E. (2011). Mixed biopolymers at interfaces: Competitive adsorption and multilayer structures. *Food Hydrocolloids*, *25*(8), 1966–1983. https://doi.org/10.1016/j.foodhyd.2010.12.001

do Prado Silva, J. T., Benetti, J. V. M., Alexandrino, T. T. de B., Assis, O. B. G., de Ruiter, J., Schroën, K., & Nicoletti, V. R. (2021). Whey Protein Isolate Microgel Properties Tuned by Crosslinking with Organic Acids to Achieve Stabilization of Pickering Emulsions. *Foods*, *10*(6), 1296. https://doi.org/10.3390/foods10061296

Du, Z., Li, Q., Li, J., Su, E., Liu, X., Wan, Z., & Yang, X. (2019). Self-Assembled Egg Yolk Peptide Micellar Nanoparticles as a Versatile Emulsifier for Food-Grade Oil-in-Water Pickering Nanoemulsions. *Journal of Agricultural and Food Chemistry*, *67*(42), 11728–11740. https://doi.org/10.1021/acs.jafc.9b04595

Frazier, R. A., Papadopoulou, A., Mueller-Harvey, I., Kissoon, D., & Green, R. J. (2003). Probing protein-tannin interactions by isothermal titration microcalorimetry. *Journal of Agricultural and Food Chemistry*, *51*(18), 5189–5195. https://doi.org/10.1021/jf021179v

French, D. J., Taylor, P., Fowler, J., & Clegg, P. S. (2015). Making and breaking bridges in a Pickering emulsion. *Journal of Colloid and Interface Science*, *441*, 30–38. https://doi.org/10.1016/j.jcis.2014.11.032

Green, A. J., Littlejohn, K. A., Hooley, P., & Cox, P. W. (2013). Formation and stability of food foams and aerated emulsions: Hydrophobins as novel functional ingredients. *Current Opinion in Colloid and Interface Science*, *18*(4), 292–301. https://doi.org/10.1016/j.cocis.2013.04.008

Gülseren, I., & Corredig, M. (2013). Interactions of chitin nanocrystals with β-lactoglobulin at the oil-water interface, studied by drop shape tensiometry. *Colloids and Surfaces B: Biointerfaces*, *111*, 672–679. https://doi.org/10.1016/j.colsurfb.2013.06.058

Hagerman, A. E., & Butler, L. G. (1981). The Specificity of Proanthocyanidin-Protein Interactions *. *Journal of Biological Chemistry*, *256*(9), 4494–4497. https://doi.org/10.1016/S0021-9258(19)69462-7

Haug, A., Høstmark, A. T., & Harstad, O. M. (2007). Bovine milk in human nutrition - A review. *Lipids in Health and Disease*, *6*, 1–16. https://doi.org/10.1186/1476-511X-6-25

Hinderink, E. B. A., Münch, K., Sagis, L., Schroën, K., & Berton-Carabin, C. C. (2019). Synergistic stabilisation of emulsions by blends of dairy and soluble pea proteins: Contribution of the interfacial composition. *Food Hydrocolloids*, *97*(February), 105206. https://doi.org/10.1016/j.foodhyd.2019.105206

Horozov, T. S., & Binks, B. P. (2006). *Particle-Stabilized Emulsions: A Bilayer or a Bridging Monolayer?**. 773–776. https://doi.org/10.1002/anie.200503131

Hu, Z., Ballinger, S., Pelton, R., & Cranston, E. D. (2015). Surfactant-enhanced cellulose nanocrystal Pickering emulsions. *Journal of Colloid and Interface Science*, *439*, 139–148. https://doi.org/10.1016/j.jcis.2014.10.034

Kilara, A., & Vaghela, M. N. (2018). Whey proteins. In *Proteins in Food Processing* (Second Edi). Elsevier Ltd. https://doi.org/10.1016/B978-0-08-100722-8.00005-X

Lan, Q., Yang, F., Zhang, S., Liu, S., Xu, J., & Sun, D. (2007). Synergistic effect of

silica nanoparticle and cetyltrimethyl ammonium bromide on the stabilization of O/W emulsions. *Colloids and Surfaces A: Physicochemical and Engineering Aspects*, *302*(1–3), 126–135. https://doi.org/10.1016/j.colsurfa.2007.02.010

Leal-Calderon, F., & Schmitt, V. (2008). Solid-stabilized emulsions. *Current Opinion in Colloid and Interface Science*, *13*(4), 217–227. https://doi.org/10.1016/j.cocis.2007.09.005

Li, D., Chen, E., Chen, H., Zhou, H., Li, B., & Li, Y. (2018). Impact of whey protein isolates and concentrates on the formation of protein nanoparticles-stabilised Pickering emulsions. *International Journal of Food Science and Technology*, *53*(3), 644–653. https://doi.org/10.1111/ijfs.13578

McClements, D. J. (2004). Protein-stabilized emulsions. *Current Opinion in Colloid and Interface Science*, *9*(5), 305–313. https://doi.org/10.1016/j.cocis.2004.09.003

McClements, D. J., & Gumus, C. E. (2016). Natural emulsifiers — Biosurfactants, phospholipids, biopolymers, and colloidal particles: Molecular and physicochemical basis of functional performance. *Advances in Colloid and Interface Science*, *234*, 3–26. https://doi.org/10.1016/j.cis.2016.03.002

Muijlwijk, K., Colijn, I., Harsono, H., Krebs, T., Berton-Carabin, C., & Schroën, K. (2017). Coalescence of protein-stabilised emulsions studied with microfluidics. *Food Hydrocolloids*, *70*, 96–104. https://doi.org/10.1016/j.foodhyd.2017.03.031

Murphy, R., Zhu, L., Narsimhan, G., & Jones, O. (2018). Impacts of Size and Deformability of β-Lactoglobulin Microgels on the Colloidal Stability and Volatile Flavor Release of Microgel-Stabilized Emulsions. *Gels*, *4*(3), 79. https://doi.org/10.3390/gels4030079

Murray, B. S. (2019). Microgels at fluid-fluid interfaces for food and drinks. *Advances in Colloid and Interface Science*, *271*, 1–7. https://doi.org/10.1016/j.cis.2019.101990

Murray, B. S., Durga, K., Yusoff, A., & Stoyanov, S. D. (2011). Stabilization of foams and emulsions by mixtures of surface active food-grade particles and proteins. *Food Hydrocolloids*, *25*(4), 627–638. https://doi.org/10.1016/j.foodhyd.2010.07.025

Murray, B. S., & Phisarnchananan, N. (2016). Whey protein microgel particles as stabilizers of waxy corn starch + locust bean gum water-in-water emulsions. *Food Hydrocolloids*, *56*, 161–169. https://doi.org/10.1016/j.foodhyd.2015.11.032

Nicolai, T., Britten, M., & Schmitt, C. (2011). β-Lactoglobulin and WPI aggregates: Formation, structure and applications. *Food Hydrocolloids*, *25*(8), 1945–1962. https://doi.org/10.1016/j.foodhyd.2011.02.006

Pichot, R., Spyropoulos, F., & Norton, I. T. (2009). Mixed-emulsifier stabilised emulsions: Investigation of the effect of monoolein and hydrophilic silica particle mixtures on the stability against coalescence. *Journal of Colloid and Interface Science*, *329*(2), 284–291. https://doi.org/10.1016/j.jcis.2008.09.083

Pichot, R., Spyropoulos, F., & Norton, I. T. (2010). O/W emulsions stabilised by both low molecular weight surfactants and colloidal particles: The effect of surfactant type and concentration. *Journal of Colloid and Interface Science*, *352*(1), 128–135. https://doi.org/10.1016/j.jcis.2010.08.021

Pickering, S. U. (1907). Emulsions. *Journal of the Chemical Society*, *91*, 2001–2021.

Ribeiro, E. F., de Barros Alexandrino, T. T., Assis, O. B. G., Junior, A. C., Quiles, A., Hernando, I., & Nicoletti, V. R. (2020). Chitosan and crosslinked chitosan nanoparticles: synthesis, characterization and their role as Pickering emulsifiers. *Carbohydrate Polymers*, *250*, 116878. https://doi.org/10.1016/j.carbpol.2020.116878

Schmitt, C., Bovay, C., Vuilliomenet, A. M., Rouvet, M., & Bovetto, L. (2011). Influence of protein and mineral composition on the formation of whey protein heat-induced microgels. *Food Hydrocolloids*, *25*(4), 558–567. https://doi.org/10.1016/j.foodhyd.2010.05.010

Schmitt, C., Moitzi, C., Bovay, C., Rouvet, M., Bovetto, L., Donato, L., Leser, M. E., Schurtenberger, P., & Stradner, A. (2010). Internal structure and colloidal behaviour of covalent whey protein microgels obtained by heat treatment. *Soft Matter*, *6*(19), 4876–4884. https://doi.org/10.1039/c0sm00220h

Schröder, A., Sprakel, J., Boerkamp, W., Schroën, K., & Berton-Carabin, C. C. (2019). Can we prevent lipid oxidation in emulsions by using fat-based Pickering particles? *Food Research International*, *120*, 352–363. https://doi.org/10.1016/j.foodres.2019.03.004

Silva, J. T. do P., Benetti, J. V. M., Alexandrino, T. T. de B., Assis, O. B. G., Ruiter, J. de, Schroën, K., & Nicoletti, V. R. (2020). *WPI microgel properties tuned by crosslinking with organic acids to achieve stabilization of Pickering emulsions containing roasted coffee oil*.

Vashisth, C., Whitby, C. P., Fornasiero, D., & Ralston, J. (2010). Interfacial displacement of nanoparticles by surfactant molecules in emulsions. *Journal of Colloid and Interface Science*, *349*(2), 537–543. https://doi.org/10.1016/j.jcis.2010.05.089

Wang, Z., Zhang, N., Chen, C., He, R., & Ju, X. (2020). Rapeseed Protein Nanogels As Novel Pickering Stabilizers for Oil-in-Water Emulsions. *Journal of Agricultural and Food Chemistry*, *68*(11), 3607–3614. https://doi.org/10.1021/acs.jafc.0c00128

Wit, N. J., & Klarenbeek, G. (1984). Effects of Various Heat Treatments on Structure and Solubility of Whey Proteins. *Journal of Dairy Science*, *67*(11), 2701–2710. https://doi.org/10.3168/jds.S0022-0302(84)81628-8

Wu, J., Shi, M., Li, W., Zhao, L., Wang, Z., Yan, X., Norde, W., & Li, Y. (2015). Pickering emulsions stabilized by whey protein nanoparticles prepared by thermal cross-linking. *Colloids and Surfaces B: Biointerfaces*, *127*, 96–104. https://doi.org/10.1016/j.colsurfb.2015.01.029

Yan, X., Ma, C., Cui, F., McClements, D. J., Liu, X., & Liu, F. (2020). Protein-stabilized Pickering emulsions: Formation, stability, properties, and applications in foods. *Trends in Food Science and Technology*, *103*(July), 293–303. https://doi.org/10.1016/j.tifs.2020.07.005

Zamani, S., Malchione, N., Selig, M. J., & Abbaspourrad, A. (2018). Formation of shelf stable Pickering high internal phase emulsions (HIPE) through the inclusion of whey protein microgels. *Food and Function*, *9*(2), 982–990. https://doi.org/10.1039/c7fo01800b

Appendix

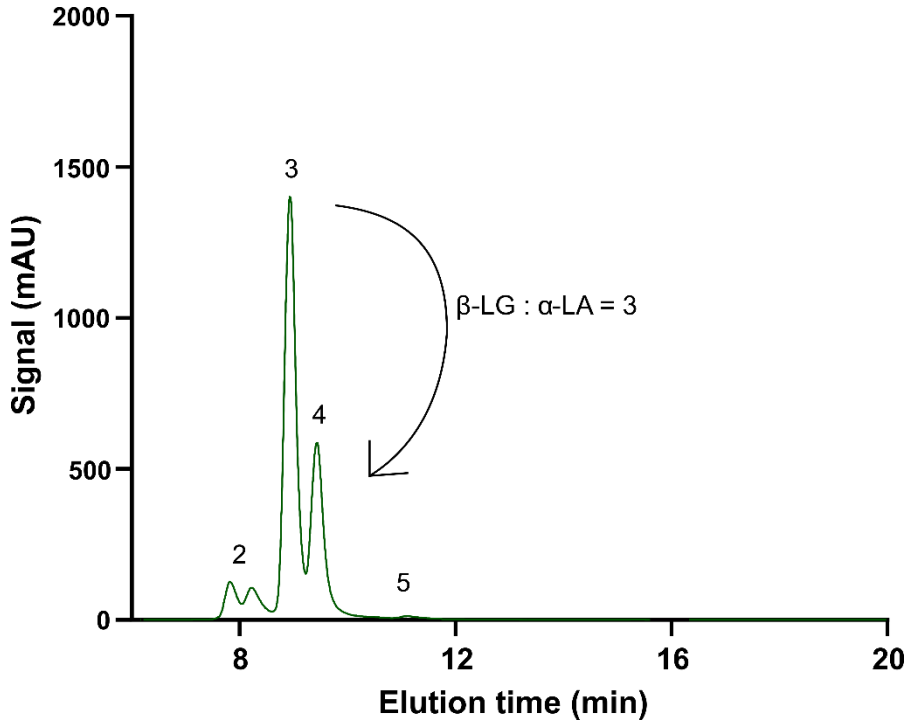

Figure 6.A1 – Characterization of protein composition of a native WPI solution (8 g/L) measured by HPSEC. Peaks correspond to: (2) BSA; (3) β-LG dimers; (4) α-LA monomers; (5) peptides.

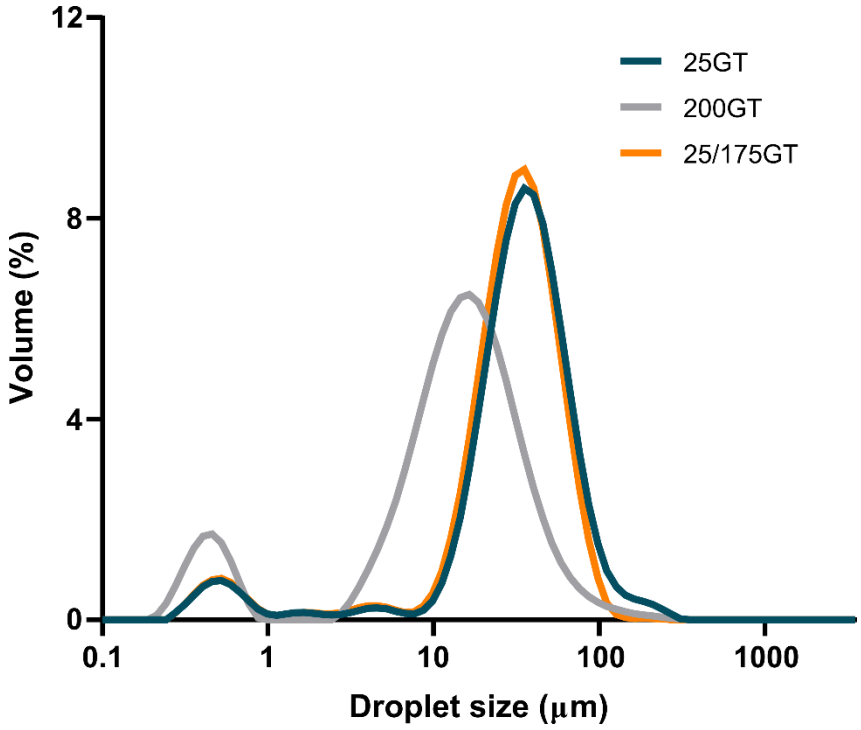

Figure 6.A2 – Droplet size distribution of emulsions produced by high pressure homogenization after 10 days of storage at 20 °C.

Supplementary Information: critical content of native WPI and microgels

The critical native WPI content was defined as the minimum amount of native WPI (g) after which a further decrease of droplet sizes was not observed. To experimentally determine the critical native WPI content, four oil-in-water emulsions (10% w/w) varying in native WPI content were prepared in colloidal mill (IKA MagicLab, Germany). The added mass of native WPI (M_{WPI}, mg) was estimated to result in a surface coverage (Γ, mg/m^2) of 0.5, 1.0, 2.0 and 4.0, respectively, as calculated by Equation 1.

$$M_{WPI} = \Gamma\, A_{interfacial} = \Gamma\, 4\pi R^2 \left(\frac{M_{oil}/\rho_{oil}}{4/3\,\pi R^3} \right) \quad (1)$$

in which $A_{interfacial}$ is the total interfacial area formed during the homogenization procedure. The droplet radius (R) was assumed to be 1.75 µm and 0.50 µm, for emulsions produced using colloidal mill and microfluidizer, respectively. These values represent the minimum droplet radius based on preliminary trials with emulsions produced using an excess of WPI. M_{oil} and ρ_{oil} were the mass and the density of oil phase (0.015 kg and 773 kg/m^3, respectively). The mean droplets size ($D_{3,2}$) of each emulsion was measured directly after preparation by static light scattering (Mastersizer 3000, Malvern Instruments, Worcestershire, UK).

The results are shown in Figure S1. Since no further decrease in droplet size was observed from Γ = 2 mg/m^2, the mass of native WPI added to attain a surface coverage of 2 mg/m^2 was set as the critical native WPI content. Assuming that this critical content is proportional to the stabilizer size and taking into account the radius of microgel particles (42,5 nm) and β-LG (≈ 3 nm) (Aymard et al., 1996), we estimated that the critical content of WPI microgels is 14 times higher than the critical content of WPI. Note that this is a roughly estimation, in which we considered that all microgels adsorb at the interface in their spherical shape (deformation at the interface was disregarded).

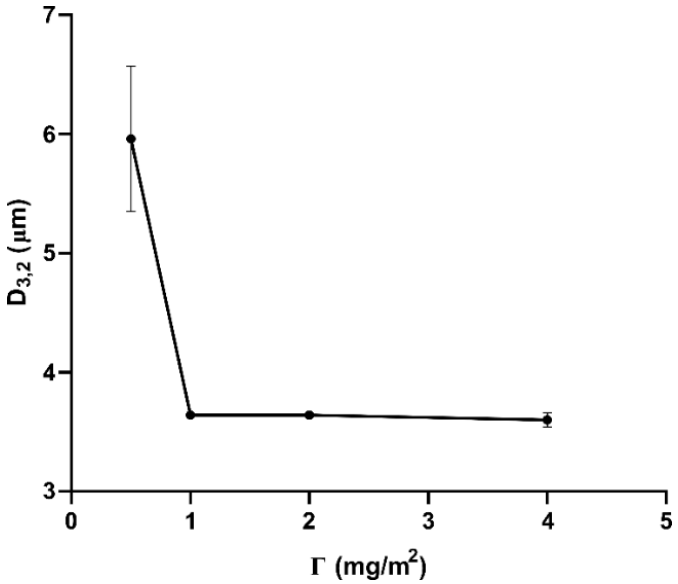

Figure 6.S1 – Emulsion droplet size (D3,2) as a function of the assumed surface coverage (Γ). Data is expressed as mean ± standard deviation of three replicates.

7 GENERAL DISCUSSION

The high physical stability provided by Pickering emulsions is a matter of great interest for researchers and an opportunity to improve the shelf life of emulsion-based products. Specially for the food industry, such systems could replace the use of low molecular weight surfactants that are associated with health hazard, contributing to the formulation of “clean label” products, an increasing demand among consumers. The attributes presented by a determined Pickering emulsion are intimately related to the properties of the stabilizer particles. The design of Pickering particles is primordial to guarantee the obtention of adequate emulsion for a target application.

Designing particles from food materials aiming an application into Pickering emulsion is not an easy task. This is because food materials are complex raw materials, which may generate non-homogeneous particles to which stabilization behaviour is hard to predict. Furthermore, a complete purification of materials from food source is almost infeasible, as the generated particles are often accompanied by trace elements that can affect emulsion stabilization. The interactions between particles and surface-active molecules during the adsorption process have been described either as competitive or synergistic and it is dependent on several parameters (concentration of each component, nature of both particles and molecules, mixing protocol, and polarity of disperse phase). Each system is unique, and it is of utmost importance to understand it well in order to ensure an adequate product formulation.

Although the individuality of each system is very important to consider, little is known about the fundamental concepts involved on food-grade Pickering emulsions. Many food researchers support their findings based on the behaviour of well-defined inorganic particles and many others disregard possible additional effects of the presence of surface-active molecules on emulsion’s stability. In this way, it is necessary to acquire more knowledge about the role of food-grade Pickering particles in emulsion droplets formation and stability before addressing to successful technological opportunities for Pickering emulsions in food systems.

The present thesis aimed to propose a new food-grade particle to be applied as Pickering stabilizer. The attributes of these particles were deeply investigated, as well as their behaviour upon adsorption and their interaction with surface-active molecules. The process for obtaining such particles was described and the main parameters

required by them to successfully stabilize Pickering emulsion were demonstrated. Thus, a completely characterized system was obtained, contributing to a more substantiated future application.

Whey protein isolate (WPI) was selected as raw material due to its high availability and for being already well-accepted as stabilizer in food products. Next, we proposed the crosslinking reaction of WPI with organic acids, plus a heat treatment at 80 °C during 15 min to promote protein molecules aggregation, giving rise to microgel particles. The selected acids were tannic acid and citric acid, both from natural sources, enabling to move away from conventional protein crosslinkers, such as formaldehyde and glutaraldehyde, that have been classified as toxic for humans. At first, we were interested on study the characteristics of food-grade Pickering emulsions stabilized by these microgels. However, throughout our investigation, we were interested in acquiring fundamental knowledge about such particle's organization at the interface and the most important parameters concerning their ability to stabilize emulsion droplets. In order to address all our question, we divided this thesis into three blocks that are presented as chapters 4, 5, and 6, respectively.

Initially, WPI microgels were produced in the presence and absence of crosslinker (tannic and citric acids) and their ability in stabilizing food emulsions was presented in Chapter 4. Roasted coffee oil was selected as disperse phase in an attempt to demonstrate a more straightforward application of Pickering emulsions in food systems. The results showed that, in fact, the crosslinking reaction has a great impact on the physical structure of WPI microgels, namely on particle size distribution and contact angle. By adding a crosslinking step, microgel particles had more homogeneous size (less polydispersity) and their mean diameter reduced around 8 to 10-fold compared to their non-crosslinked counterpart. In addition, the crosslinked microgels presented considerably higher contact angles than their non-crosslinked counterparts. This is attributed to the polarity change via chemical bonding between crosslinkers and carboxyl groups or amines in the protein structure, consequently reducing the number of polar side groups available to interact with water molecules. These features brought to microgels through organic acids resulted in the formation of more stable emulsions: droplets were smaller and less intense gravitational separation was observed in emulsions stabilized by crosslinked microgels compared to the one stabilized by conventional microgels.

Specially for emulsions stabilized by tannic acid-crosslinked WPI microgels, no gravitational separation at all was observed after 7 days of storage. This represented a major contrast to emulsions stabilized by native WPI or conventional WPI microgels, in which droplet flocculation and coalescence were observed within a few minutes after emulsification. The great performance of tannic acid-crosslinked WPI microgels (TA-WPI microgels) on stabilizing Pickering emulsions attracted our attention to deeper investigating their role as Pickering particles. Thus, from that point on, the experiments presented in this thesis were focused on exploring solely the TA-WPI microgels, since the results in Chapter 4 pointed to their improved performance as Pickering stabilizer.

In Chapter 5, we aimed to a more fundamental investigation about the organization of TA-WPI microgels at interfaces and their ability to stabilize emulsion droplets. For that reason, it was more convenient to work with a “clean” system, so hexadecane was selected as oil phase and the TA-WPI microgel dispersion was purified by a 7-step washing procedure using an ultrafiltration cell (0.03 μm membrane pore) to remove possible residual free proteins. Firstly, the compression behaviour of TA-WPI microgels at a model interface was investigated using a Langmuir trough. This enabled to verify their soft nature that allows them to spread at the interface, at which their loosely packed shell flatten out and their dense core remains like a bump. The similarities found between the surface pressure isotherms of native WPI and TA-WPI microgels indicated that microgel’s dangling chains are responsible for their surface activeness.

The dilatational modulus of monolayers formed by either native WPI and TA-WPI microgels presents a first maximum at similar surface pressure (9 – 10 mN/M), however, at surface coverages of 1.6 mg/m² and 11.6 mg/m² for native WPI and TA-WPI microgels, respectively. This difference in surface coverage may be due to some reasons: (1) the dense core of the microgels adds a substantial amount of material at the interface, (2) the denatured dangling chains of microgels present fewer hydrophilic parts to collapse at the subphase, and (3) microgels’ dangling chains are less mobile than native molecules because they are attached to microgels core. The first maximum in dilatational modulus indicates the onset of a conformational change in the monolayer, particularly associated with the collapse of hydrophilic parts of the molecules, forming loops and tails into the subphase. In another words, it is the point at which different molecules are in close proximity in the monolayer and they start to compress each other. Since similar conformational changes at flat interfaces are

expected upon adsorption to the O/W interfaces in emulsions, we assumed 1.6 mg/m² and 11.6 mg/m² as calibration values for monolayer coverage of native WPI and TA-WPI microgels, respectively.

The calescence stability of emulsion droplets produced into microfluidics device was accessed. Two parameters were evaluated: continuous phase concentration and adsorption time. As expected, the coalescence frequency of droplets increases with decreasing the continuous phase concentration. This is because the stabilizer content available to cover the formed interface is reduced, and thus droplets merge until achieving a completely covered interface. Interestingly, we found out that adsorption time also plays a role on the coalescence of microgel-stabilized droplets, contrasting to classic hard Pickering particles, in which only the applied shear force influence on droplets stabilization. Possibly, the surface-active character of microgels makes spontaneous adsorption possible throughout the channel. Additionally, longer adsorption times may also allow for further spreading of their polymeric shell at droplets interface. Both phenomena contribute to the formation of a more covered interface, which impacts on droplets stability against coalescence. When comparing emulsions stabilized by either native WPI or TA-WPI microgels, it was found that the microgels supress droplets coalescence trough bridging flocculation, a phenomenon very common for Pickering emulsions produced at particles-poor regime. Those bridging were transient and completely disrupted at the end of collision channel, probably due to rearrangements of microgel particles at the interface over time. In this way, emulsions stabilized by TA-WPI microgels showed an improved stability against coalescence than conventional emulsions (stabilized by native WPI).

The results provided in Chapter 5 regarding the characterization of TA-WPI microgels showed that the complete removal of non-reacted free proteins from the dispersion was impossible. Thus, some native WPI must be deal with when using TA-WPI microgels to stabilize emulsions. In view of that, we decided to evaluate the effect of native WPI on the physical characteristics of emulsions stabilized by TA-WPI microgels (Chapter 6). For these experiments, the microgel content in the continuous phase remained the same for all produced emulsions, while the native WPI varied from two limits: low limit (25% of WPI critical concentration) and high limit (200% ow WPI critical concentration). The mixing protocol and homogenization technique were also considered, in which native WPI was added either before or after homogenization, and

emulsions were prepared using two different equipment: rotor-stator (low shear) and high-pressure homogenizer (high shear).

The results presented on Chapter 6 demonstrated that bridging flocculation took place in emulsions produced in the presence of low native WPI content (25%), which was attributed to the emulsifier poor regime. However, after 14 days of storage, the flocs present in these samples were disrupted, indicating that interfacial organization took place over time, and native WPI molecules were able to replace part of the bridged TA-WPI microgels by reducing their desorption energy. In contrast, emulsions produced with high protein content did not present flocculation and remained stable over 14 days of storage, meaning that native WPI assisted droplets interfacial coverage. The presence of high content of native WPI prior to homogenization could guarantee enough stabilizer content to cover the interfacial area formed during homogenization, preventing bridging flocculation.

Some differences were observed when high shear was applied to prepare emulsions with the same composition as before. Emulsions produced by high-pressure homogenization appeared to have an increased viscosity than those produced by rotor-stator treatment, and size distribution measurements together with microscopic observations demonstrated a higher flocculation behaviour for all samples. The softness of TA-WPI microgels makes them prone to deformation at high shear rates. In this way, particles had achieved the droplets interface in a deformed form, occupying a bigger interfacial area than when in its regular shape. After a relaxation time, microgels may have shrunken and consequently exposed part of uncovered interface, which made droplets propense to suffer bridging flocculation.

By disrupting the flocs using SDS solution, it was observed that emulsion produced in the presence of high amount of native WPI had smaller droplet size than the ones produced with low WPI content. This may be a result of the ability of native WPI molecules to reduce the interfacial tension, facilitating droplet breakage during homogenization. The droplet size distribution of emulsions produced under high shear did not change over time. Probably, the diffusion of native molecules to the interface was hindered due to the high viscosity of these emulsions and by the fact that droplets were entrapped into networks of bridged droplets. Also, native WPI molecules were not able to promote significant microgel desorption over time, as showed by microscopic images. Combining the results presented on Chapter 6, we suggest a synergistic effect of WPI microgels and native WPI molecules to form emulsions: native

WPI assisted droplets' breakage, without impairing the adsorption of microgels nor promoting their complete desorption over time.

8 GENERAL CONCLUSIONS

In the present thesis, we demonstrated that the crosslinking of WPI microgels by organic acids is a feasible strategy to tune their physical properties. Such approach enabled the formation of particles more suitable for Pickering stabilization, besides being food-grade and complying with the “clean label” classification of food products. An improved performance was observed for tannic acid-crosslinked WPI microgels, in which emulsions stabilized by them showed neither creaming nor sedimentation after 7 days of storage.

A deeper investigation about the adsorption behaviour of tannic acid-crosslinked WPI microgels enabled us to verify their soft and surface-active nature. At the interface, the soft core of microgels flatten, covering a larger interfacial area than non-deformable particles. Experiments on microfluidics device revealed that the adsorption time has an important role on the stability of emulsions produced by these microgels. This contrasts with the former knowledge about Pickering particles, in which only the shear force is told to have a role on emulsion stability. This different behaviour is related to the surface-activeness of microgel particles and their ability to deform, which allow them to reach/reorganize at the interface over time. Also, we identified that microgel particles supress droplet coalescence by bridging flocculation, providing emulsions with enhanced stability when compared to their conventional counterparts (stabilized by native WPI).

Despite our efforts, the 10 step-ultrafiltration procedure was not able to remove all the non-reacted native WPI from the microgel dispersion, which means that a pure Pickering system could not be achieved in our work. However, by evaluating emulsions stabilized by blends of tannic acid-crosslinked WPI microgels and native WPI, we verified that native protein molecules assisted on disrupting flocs over time or in the formation of smaller droplets during homogenization, besides not being able to promote the desorption of microgels from the interface. This points to a synergistic mechanism of stabilization rather than competition for adsorption.

To conclude, a new food-grade particle with increased ability to stabilize Pickering emulsions is proposed in the present thesis, in addition to explanations on the mechanisms by which they adsorb at the interfaces and confer improved stability to emulsions. Even though the production of these microgel particles is accompanied by remaining non-reacted native proteins, we demonstrated that the presence of such

molecules does not impair either microgel adsorption or emulsion physical stability, which shows that tannic-acid crosslinked WPI microgels can be successfully applied to the production of food-grade Pickering emulsions.

9 SUGGESTIONS FOR FUTURE STUDIES

Investigate the long-term stability of emulsions stabilized by tannic-acid crosslinked WPI microgels, including microbiological growth over time.

Verify the performance of tannic-acid crosslinked WPI microgels on protecting bioactive compounds from stress conditions (i.e., exposure to light, heating, and presence of enzymes).

Study the impact of different crosslinking mechanisms (chemical, physical, and enzymatic) on microgels' physical properties.

Investigate the adsorption behaviour of WPI microgels with different crosslinking densities and evaluate the morphological aspect of the formed monolayers by using atomic force microscopy.

Propose a new methodology to purify the WPI microgel dispersion and produce/characterize a pure Pickering system – emulsions stabilized solely by microgel particles.

Propose a methodology to determine the interfacial composition of droplets stabilized by blends of WPI microgels and native WPI that enables to accompany the interfacial composition of droplets over storage time.

Compare hard particles obtained from proteins with protein microgels regarding to their performance as Pickering stabilizers.

REFERENCES

ARAIZA-CALAHORRA, A. et al. Conjugate microgel-stabilized Pickering emulsions: Role in delaying gastric digestion. **Food Hydrocolloids**, v. 105, n. February, p. 105794, 2020.

AZEREDO, H. M. C.; WALDRON, K. W. Crosslinking in polysaccharide and protein films and coatings for food contact - A review. **Trends in Food Science & Technology**, v. 52, p. 109–122, 2016.

BENETTI, J. V. M.; SILVA, J. T. DO P.; NICOLETTI, V. R. SPI microgels applied to Pickering stabilization of O/W emulsions by ultrasound and high-pressure homogenization: rheology and spray drying. **Food Research International**, v. 122, p. 383–391, 2019.

BERTON-CARABIN, C. C.; SAGIS, L.; SCHROËN, K. Formation, Structure, and Functionality of Interfacial Layers in Food Emulsions. **Annual Review of Food Science and Technology**, v. 9, p. 551–587, 2018.

BERTON-CARABIN, C. C.; SCHROËN, K. Pickering Emulsions for Food Applications: Background, Trends, and Challenges. **Annual Review of Food Science and Technology**, v. 6, n. 1, p. 263–297, 2015.

BERTON-CARABIN, C.; SCHROËN, K. Towards new food emulsions: designing the interface and beyond. **Current Opinion in Food Science**, v. 27, p. 74–81, 2019.

CALABRESE, V. et al. Pickering emulsions stabilized by naturally derived or biodegradable particles. **Current Opinion in Green and Sustainable Chemistry**, v. 12, n. Figure 1, p. 83–90, 2018.

CHEN, L. et al. Food-grade pickering emulsions: Preparation, stabilization and applications. **Molecules**, v. 25, n. 14, 2020.

CHEN, S.; ZHANG, L. M. Casein nanogels as effective stabilizers for Pickering high internal phase emulsions. **Colloids and Surfaces A: Physicochemical and Engineering Aspects**, v. 579, p. 123662, 2019.

CHEVALIER, Y.; BOLZINGER, M. Emulsions stabilized with solid nanoparticles : Pickering emulsions. **Colloids and Surfaces A: Physicochemical and Engineering Aspects**, v. 439, p. 23–34, 2013.

DESHMUKH, O. S. et al. Hard and soft colloids at fluid interfaces: Adsorption, interactions, assembly & rheology. **Advances in Colloid and Interface Science**, v. 222, p. 215–227, 2015.

DESTRIBATS, M. et al. Soft microgels as Pickering emulsion stabilisers: Role of particle deformability. **Soft Matter**, v. 7, n. 17, p. 7689–7698, 2011.

DESTRIBATS, M. et al. Pickering emulsions stabilized by soft microgels: Influence of the emulsification process on particle interfacial organization and emulsion properties. **Langmuir**, v. 29, n. 40, p. 12367–12374, 2013.

DESTRIBATS, M. et al. Impact of pNIPAM microgel size on its ability to stabilize pickering emulsions. **Langmuir**, v. 30, n. 7, p. 1768–1777, 2014a.

DESTRIBATS, M. et al. Emulsions stabilised by whey protein microgel particles: Towards food-grade Pickering emulsions. **Soft Matter**, v. 10, n. 36, p. 6941–6954, 2014b.

DICKINSON, E. Food emulsions and foams: Stabilization by particles. **Current Opinion in Colloid and Interface Science**, v. 15, n. 1–2, p. 40–49, 2010.

DICKINSON, E. Biopolymer-based particles as stabilizing agents for emulsions and foams. **Food Hydrocolloids**, v. 68, p. 219–231, 2017.

DICKINSON, E. **Strategies to control and inhibit the flocculation of protein-stabilized oil-in-water emulsionsFood Hydrocolloids**, 2019.

FARJAMI, T.; MADADLOU, A.; LABBA, M. Characteristics of the bulk hydrogels made of the citric acid cross-linked whey protein microgels. **Food Hydrocolloids**, v. 50, p. 159–165, 2015.

FERNANDEZ-RODRIGUEZ, M. A.; MARTÍN-MOLINA, A.; MALDONADO-VALDERRAMA, J. Microgels at interfaces, from mickering emulsions to flat interfaces and back. **Advances in Colloid and Interface Science**, v. 288, p. 102350, fev. 2021.

FRENCH, D. J. et al. Making and breaking bridges in a Pickering emulsion. **Journal of Colloid and Interface Science**, v. 441, p. 30–38, mar. 2015.

GANJU, S.; GOGATE, P. R. A review on approaches for efficient recovery of whey proteins from dairy industry effluents. **Journal of Food Engineering**, v. 215, p. 84–96, 2017.

GEISEL, K.; ISA, L.; RICHTERING, W. The Compressibility of pH-Sensitive Microgels at the Oil-Water Interface: Higher Charge Leads to Less Repulsion. **Angewandte Chemie**, v. 126, n. 19, p. 5005–5009, 2014.

GONSALVES, A. DE A. et al. Diferentes estretégias para a reticulação de quitosana. **Química Nova**, v. 34, n. 7, p. 1215–1223, 2011.

GONZALEZ ORTIZ, D. et al. Current Trends in Pickering Emulsions: Particle Morphology and Applications. **Engineering**, v. 6, n. 4, p. 468–482, 2020.

GOULD, J.; GARCIA-GARCIA, G.; WOLF, B. Pickering particles prepared from food waste. **Materials**, v. 9, p. 1–14, 2016.

GUO, J. et al. Preparation of soy protein-based microgel particles using a hydrogel homogenizing strategy and their interfacial properties. **Food Hydrocolloids**, v. 58, p. 324–334, 2016.

HU, S. et al. Development of tannic acid cross-linked hollow zein nanoparticles as potential oral delivery vehicles for curcumin. **Food Hydrocolloids**, v. 61, p. 821–831, 2016a.

HU, Y. T. et al. Techniques and methods to study functional characteristics of emulsion systems. **Journal of Food and Drug Analysis**, v. 25, n. 1, p. 16–26, 2017.

HU, Z. et al. Dried and Redispersible Cellulose Nanocrystal Pickering Emulsions. **ACS Macro Letters**, v. 5, n. 2, p. 185–189, 2016b.

HUNTER, T. N. et al. The role of particles in stabilising foams and emulsions. **Advances in Colloid and Interface Science**, v. 137, p. 57–81, 2008.

KARBASI, M.; ASKARI, G.; MADADLOU, A. Effects of acetyl grafting on the structural and functional properties of whey protein microgels. **Food Hydrocolloids**, v. 112, n. July 2020, p. 106443, 2021.

LI, D. et al. Impact of whey protein isolates and concentrates on the formation of protein nanoparticles-stabilised Pickering emulsions. **International Journal of Food Science and Technology**, v. 53, n. 3, p. 644–653, 2018.

LI, X. et al. Combination of egg white protein and microgels to stabilize foams: Impact of processing treatments. **Journal of Food Engineering**, v. 275, n. November 2019, p. 1–11, 2020.

LINKE, C.; DRUSCH, S. Pickering emulsions in foods - opportunities and limitations. **Critical reviews in food science and nutrition**, v. 58, n. 12, p. 1971–1985, 2018.

LIU, T. et al. Non-coalescence of oppositely charged droplets in pH-sensitive emulsions. **Proceedings of the National Academy of Sciences of the United States of America**, v. 109, n. 2, p. 384–389, 2012.

MAREFATI, A. et al. Fabrication of encapsulated oil powders from starch granule stabilized W/O/W Pickering emulsions by freeze-drying. **Food Hydrocolloids**, v. 51, p. 261–271, 2015.

MONTGOMERY, Lucy M. **Anne de Green Gables**. Jandira, SP: Ciranda Cultural, 2019.

MURPHY, R. W.; FARKAS, B. E.; JONES, O. G. Dynamic and viscoelastic interfacial behavior of β-lactoglobulin microgels of varying sizes at fluid interfaces. **Journal of Colloid and Interface Science**, v. 466, p. 12–19, 2016.

MURPHY, R. W.; FARKAS, B. E.; JONES, O. G. Effect of crosslinking on the physical and chemical properties of b - lactoglobulin (Blg) microgels. **Journal of Colloid and Interface Science**, v. 505, p. 736–744, 2017.

MURRAY, B. S. Microgels at fluid-fluid interfaces for food and drinks. **Advances in Colloid and Interface Science**, v. 271, p. 1–7, 2019.

MURRAY, B. S. et al. The perfect hydrocolloid stabilizer: Imagination versus reality. **Food Hydrocolloids**, v. 117, n. February, p. 106696, 2021.

NICOLAI, T.; BRITTEN, M.; SCHMITT, C. β-Lactoglobulin and WPI aggregates: Formation, structure and applications. **Food Hydrocolloids**, v. 25, n. 8, p. 1945–1962, 2011.

NIROULA, A. et al. Biomolecule-based pickering food emulsions: Intrinsic components of food matrix, recent trends and prospects. **Food Hydrocolloids**, v. 112, n. August 2020, p. 106303, 2021.

PICARD, C. et al. Organization of Microgels at the Air-Water Interface under Compression: Role of Electrostatics and Cross-Linking Density. **Langmuir**, v. 33, n. 32, p. 7968–7981, 2017.

PICKERING, S. U. Emulsions. **Journal of the Chemical Society**, v. 91, p. 2001–2021, 1907.

REY, M. et al. Poly- N-isopropylacrylamide Nanogels and Microgels at Fluid Interfaces. **Accounts of Chemical Research**, v. 53, p. 414–424, 2020.

RIBEIRO, E. F. et al. Chitosan and crosslinked chitosan nanoparticles: synthesis, characterization and their role as Pickering emulsifiers. **Carbohydrate Polymers**, v. 250, p. 116878, ago. 2020.

SAN-MIGUEL, A.; BEHRENS, S. H. Influence of nanoscale particle roughness on the stability of pickering emulsions. **Langmuir**, v. 28, n. 33, p. 12038–12043, 2012.

SCHMIDT, S. et al. Influence of microgel architecture and oil polarity on stabilization of emulsions by stimuli-sensitive core-shell poly(N -isopropylacrylamide- co - methacrylic acid) microgels: Mickering versus pickering behavior? **Langmuir**, v. 27, n. 16, p. 9801–9806, 2011.

SCHRÖDER, A. et al. Can we prevent lipid oxidation in emulsions by using fat-based Pickering particles? **Food Research International**, v. 120, p. 352–363, 2019.

TAN, H. et al. Gelatin particle-stabilized high internal phase emulsions as nutraceutical containers. **ACS Applied Materials and Interfaces**, v. 6, n. 16, p. 13977–13984, 2014.

TANG, C.-H. Globular proteins as soft particles for stabilizing emulsions: Concepts and strategies. **Food Hydrocolloids**, v. 103, n. January, 2020.

TATRY, M.-C. et al. Pickering emulsions stabilized by thermoresponsive oligo(ethylene glycol)-based microgels: Effect of temperature-sensitivity on emulsion stability. **Journal of Colloid and Interface Science**, v. 589, p. 96–109, maio 2021.

TATRY, M. C. et al. Kinetics of spontaneous microgels adsorption and stabilization of emulsions produced using microfluidics. **Journal of Colloid and Interface Science**, v. 548, p. 1–11, 2019.

TAVASSOLI-KAFRANI, E.; GOLI, S. A. H.; FATHI, M. Fabrication and characterization of electrospun gelatin nanofibers crosslinked with oxidized phenolic compounds. **International Journal of Biological Macromolecules**, v. 103, p. 1062–1068, 2017.

TAVERNIER, I. et al. Food-grade particles for emulsion stabilization. **Trends in Food Science & Technology**, v. 50, n. February, p. 159–174, 2016.

WALSTRA, P.; WOUTERS, J. T. M.; GEURTS, T. J. **Dairy Science and Technology**. 2. ed. Boca Raton: Taylor & Francis, 2006.

WANG, D. et al. Facile preparation of zein nanoparticles with tunable surface hydrophobicity and excellent colloidal stability. **Colloids and Surfaces A: Physicochemical and Engineering Aspects**, v. 591, p. 124554, 2020a.

WANG, L. J. et al. Fabrication and characterization of Pickering emulsions and oil gels stabilized by highly charged zein/chitosan complex particles (ZCCPs). **Food Chemistry**, v. 213, p. 462–469, 2016a.

WANG, T. et al. Development of tannic acid cross-linked hollow zein nanoparticles as potential oral delivery vehicles for curcumin potential oral delivery vehicles for curcumin. **Food hydrocolloids**, v. 61, p. 821–831, 2016b.

WANG, Z. et al. Rapeseed Protein Nanogels As Novel Pickering Stabilizers for Oil-in-Water Emulsions. **Journal of Agricultural and Food Chemistry**, v. 68, n. 11, p. 3607–3614, 2020b.

WEI, Z. et al. Genipin-crosslinked ovotransferrin particle-stabilized Pickering emulsions as delivery vehicles for hesperidin. **Food Hydrocolloids**, v. 94, p. 561–573, 2019.

WHITBY, C. P.; SCARBOROUGH, H.; NGOTHAI, Y. Drying oil-in-water Pickering emulsions to make redispersible powders. **Advanced Powder Technology**, v. 28, n. 11, p. 2940–2946, 2017.

XIAO, J.; LI, Y.; HUANG, Q. Recent advances on food-grade particles stabilized Pickering emulsions:fabrication,characterization and research trends. **Trends in Food Science and Technology**, v. 55, p. 48–60, 2016.

XIAO, J.; LU, X.; HUANG, Q. Double emulsion derived from kafirin nanoparticles stabilized Pickering emulsion: Fabrication, microstructure, stability and in??vitro digestion profile. **Food Hydrocolloids**, v. 62, p. S29–S38, 2017.

YANG, Y. et al. An overview of pickering emulsions: Solid-particle materials, classification, morphology, and applications. **Frontiers in Pharmacology**, v. 8, n. MAY, p. 1–20, 2017.

ZAMANI, S. et al. Formation of shelf stable Pickering high internal phase emulsions (HIPE) through the inclusion of whey protein microgels. **Food and Function**, v. 9, n. 2, p. 982–990, 2018.

ZANINI, M. et al. Universal emulsion stabilization from the arrested adsorption of rough particles at liquid-liquid interfaces. **Nature Communications**, v. 8, p. 1–9, 2017.

ZENG, T. et al. Development of antioxidant Pickering high internal phase emulsions (HIPEs) stabilized by protein/polysaccharide hybrid particles as potential alternative for PHOs. **Food Chemistry**, v. 231, p. 122–130, 2017.

ZHANG, J. et al. Study on β-lactoglobulin microgels adsorption onto a hydrophobic solid surface by QCM-D. **Food Hydrocolloids**, v. 98, p. 105320, 2020a.

ZHANG, S. et al. Pea protein microgel particles as Pickering stabilisers of oil-in-water emulsions: Responsiveness to pH and ionic strength. **Food Hydrocolloids**, v. 102, p. 105583, 2020b.

ZHANG, Y. et al. Influence of thermal treatment on oil-water interfacial properties and emulsion stabilization prepared by sono-assembled soy peptide nanoparticles. **Food Hydrocolloids**, v. 103, p. 105646, 2020c.

APPENDIX

Appendix A. Supplementary material

Table A1. Effect of crosslinker ratio on microgels mean particle size.

Molar ratio crosslinker:WPI	Mean particle size (nm)	
	Tannic acid-crosslinked microgels	Citric acid-crosslinked microgels
1:1	653.4 ± 40.9[a]	3,695.7 ± 19.2[a]
3:1	185.2 ± 2.2[b]	257.6 ± 4.2[b]
5:1	-*	245.2 ± 1.0[b]

WPI source: CL 3987, Alibra Ingredients.
Different letters in the same row indicate significant difference ($p < 0.05$) according to Tukey's mean test.
Data expressed as mean (n = 3) ± standard deviation.
* This sample formed a very compact structure due to the high crosslinking extension.

Figure A1 –Tannic acid-crosslinked WPI microgels prepared at 5:1 crosslinker:WPI molar ratio.

Figure A2 – Surface pressure curves of native WPI solutions used to estimate the concentration of native WPI in the filtrates obtained from microgels washing procedure.

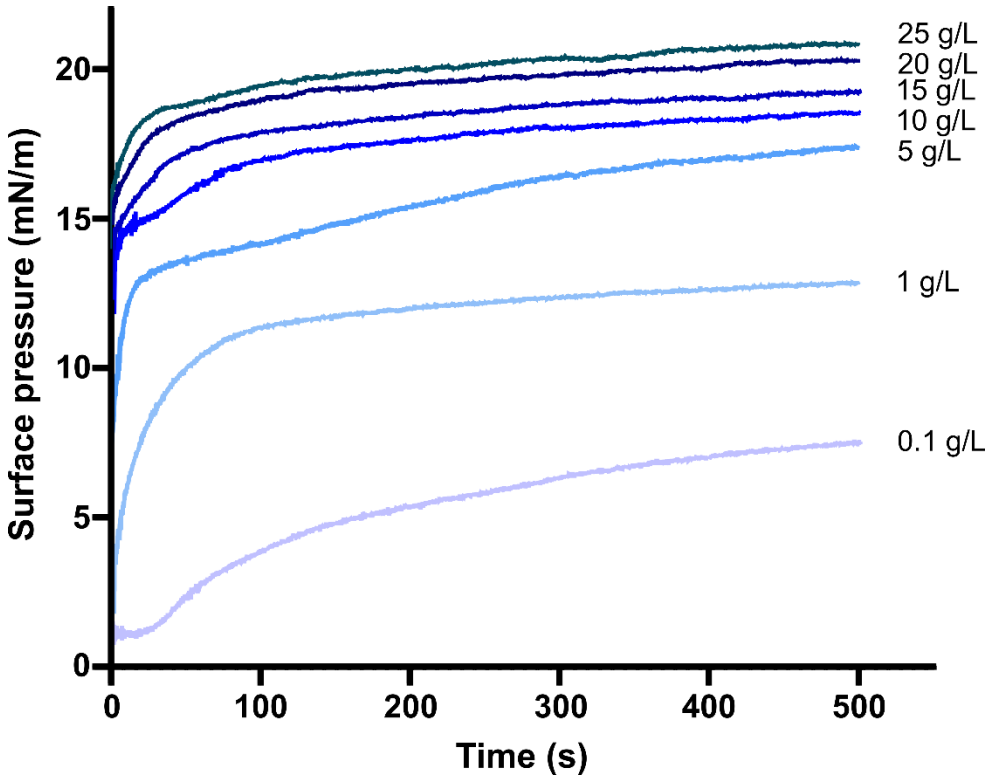

Table A2 – Composition of continuous phases used to prepare emulsions into microfluidics device.

Tannic acid-crosslinked WPI microgel dispersion		Native WPI solution	
*F**	Microgels (mg/L)	*F**	WPI (mg/L)
302.9	14275.0	73.2	500
151.5	7137.5	29.3	200
20.2	951.7	14.6	100
10.1	475.8	11.7	80
7.6	356.9	8.8	60
6.1	285.5	2.9	20
4.7	219.6		

F^* is the ratio between maximum surface coverage (considering that all stabilizers available in the continuous phase adsorbed at the interface) and the surface coverage Γ^* (obtained from dilatational modulus curves).

Figure A3 – CLSM images of microgel-stabilized droplets produced at 94 ms adsorption time with different microgel content in the continuous phase: *F** = 302.9 (A) and *F** = 6.1 (B). Microgels appears in green and hexadecane appears in red. Images highlight the excess of microgels in the continuous phase at higher microgel content. Scale bars represent 20 µm.

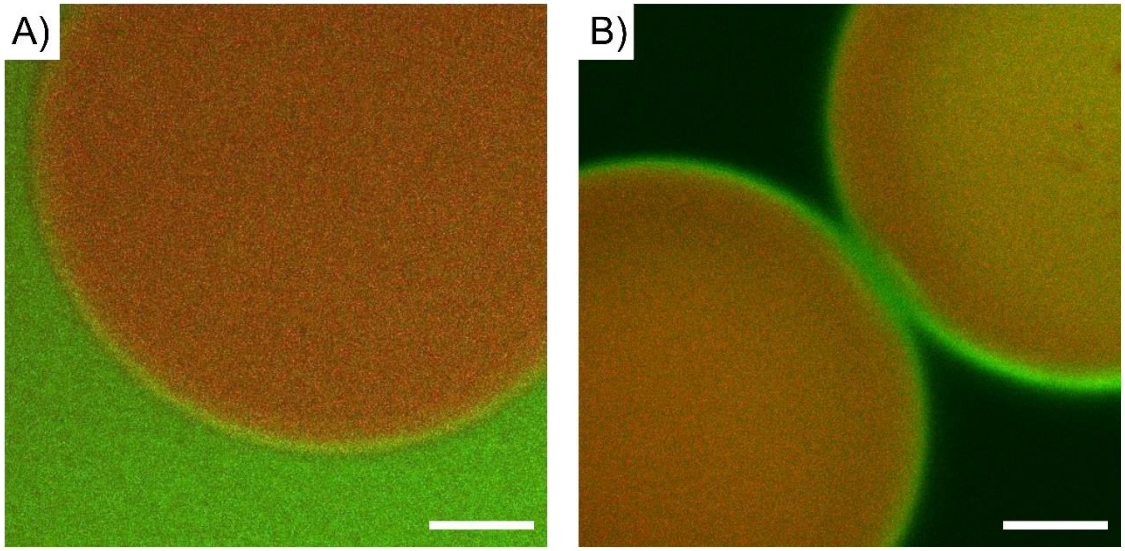

Appendix B. Characterization of additional emulsion samples stabilized either by native WPI or blends of TA-WPI microgels and native WPI.

The continuous phases used for stabilizing emulsions were composed by 33% microgels critical concentration and 50% (50G) or 100% (100G) native WPI critical concentration. Blank samples were composed only by native WPI at 50% (50B) and 100% (100B) WPI critical concentration. All emulsions were produced using rotor-stator homogenizer.

Figure B1 – Droplet size distributions in emulsions produced by rotor-stator homogenization on days 0 (A and C) and 14 (B and D).

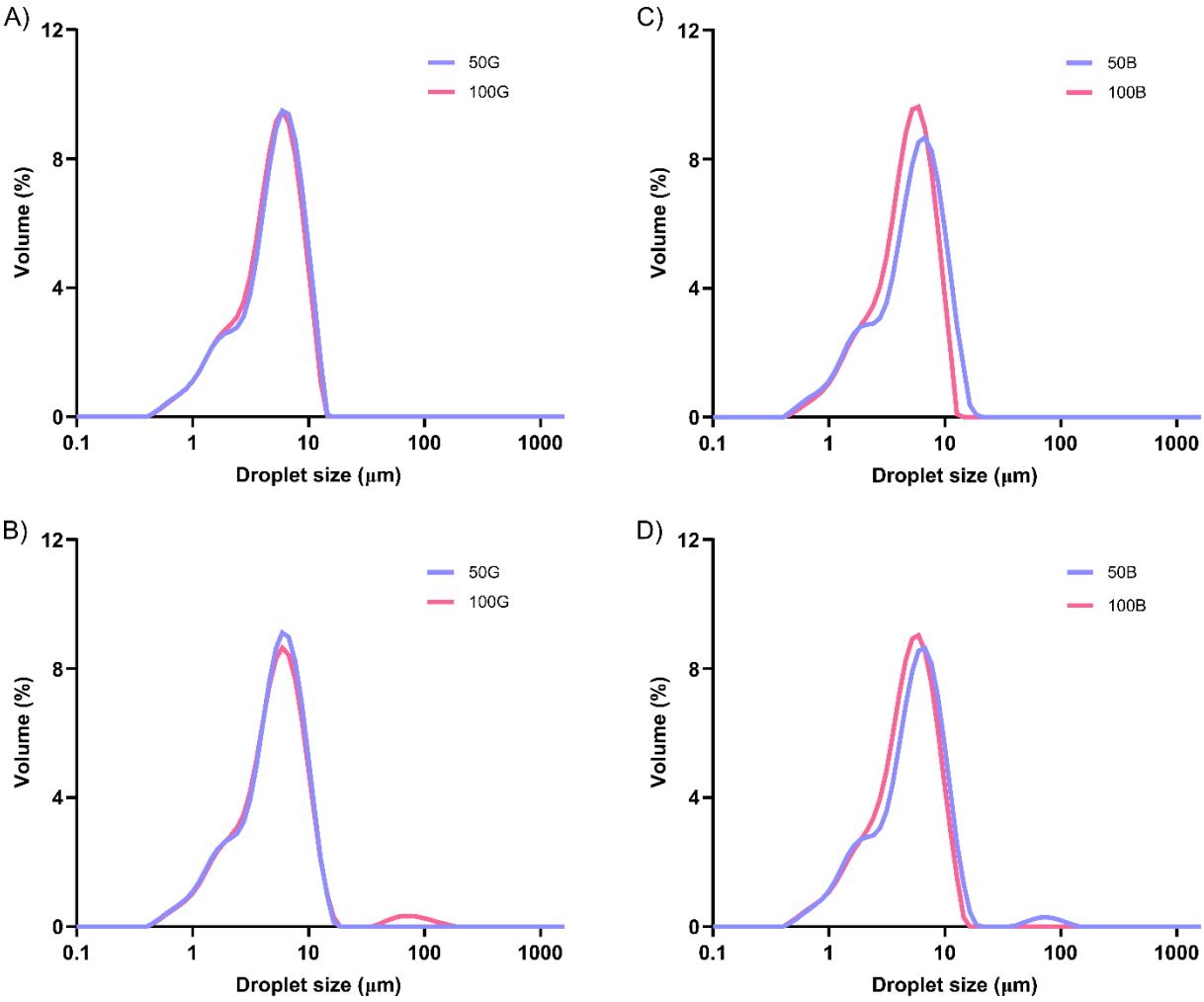

Figure B2 – Light microscope images of freshly prepared emulsions: (A) 50G; (B) 100G; (C) 50B; (D) 100B. Scale bars represent 50 µm.

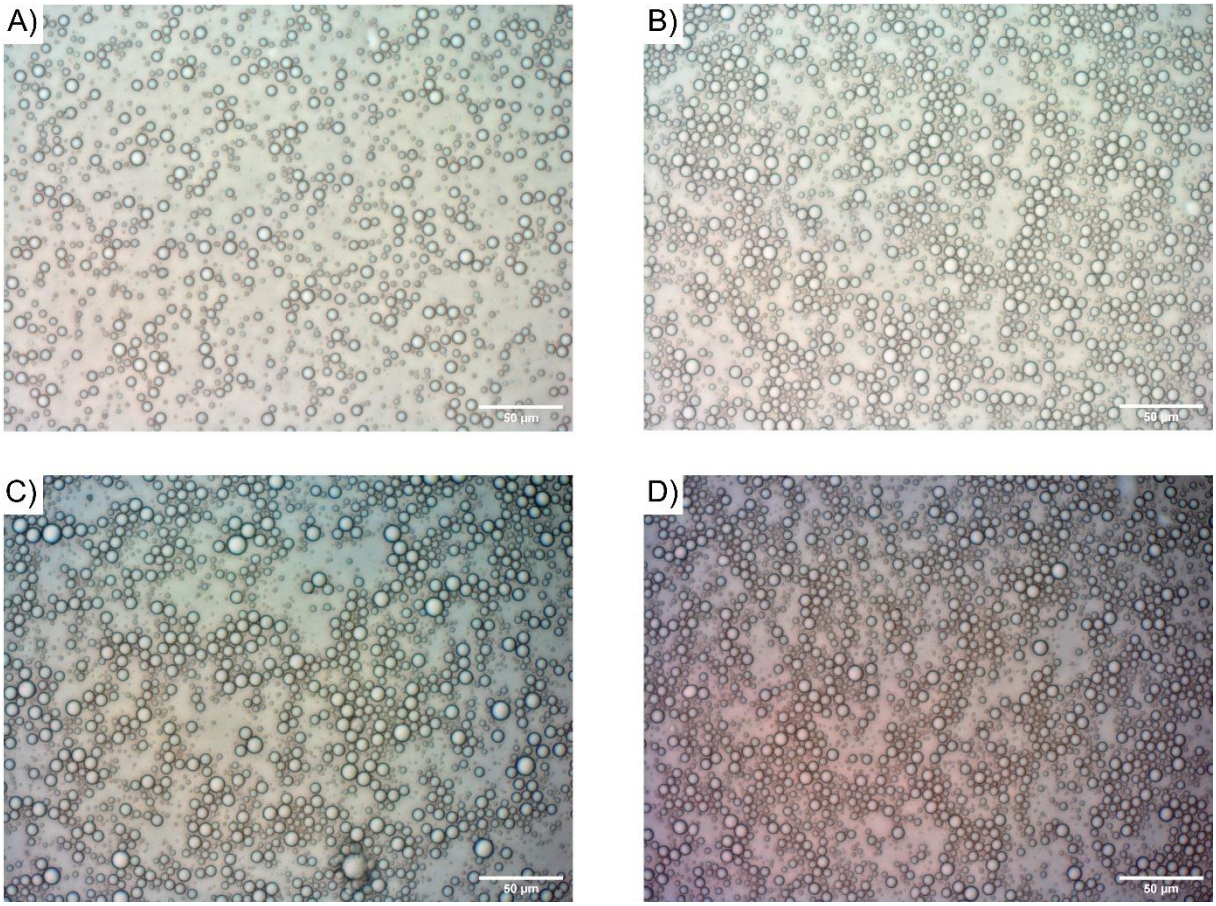

Figure B3 – CLSM images of: (A-B) blank emulsions on day 0, and (C-D) emulsions stabilized by blends of TA-WPI microgels and native WPI on day 0 and 14. Native WPI and microgels appear in green and hexadecane appears in red. (A) 50B; (B) 100B; (C) 50G; (D) 100G. Scale bars represent 20 µm.